Delay-Based Controllers Design for Dynamical Systems

José-Enrique Hernández-Díez

Thèse de doctorat

NNT: 2021UPASG018

Delay-Based Controllers Design for Dynamical Systems

Conception de Contrôleurs à retards pour Systèmes Dynamiques

Thèse de doctorat de l'université Paris-Saclay et de la Universidad Autónoma de San Luis Potosí

École doctorale n°580 Sciences et technologies de l'information et de la communication (STIC)

Spécialité de doctorat: Automatique

Unité de recherche: Université Paris-Saclay, CNRS, CentraleSupélec, Laboratoire des Signaux et Systèmes (L2S), 91190, Gif-sur-Yvette, France

Référent: Faculté de sciences d'Orsay

Thèse présentée et soutenue à Paris-Saclay, le 22 mars 2021, par

José-Enrique HERNÁNDEZ-DÍEZ

Composition du jury:

Säid MAMMAR Pr., Université d'Evry Val-d'Essone	Président
Hitay ÖZBAY Pr., Bilkent University	Rapporteur & Examinateur
Olivier SENAME Pr., Institut Polytechnique de Grenoble	Rapporteur & Examinateur
Woihida AGGOUNE MC, École Nationale Supérieure de l'Electronique et de ses Applications	Examinatrice
Emilio GONZALEZ-GALVAN Pr., Universidad Autónoma de San Luis Potosí	Examinateur
Tomas VYHLIDAL Pr., Czech Technical University in Prague	Examinateur

Direction de la thèse:

Cesar Fernando MÉNDEZ BARRIOS Pr., Universidad Autónoma de San Luis Potosí	Directeur de thèse
Silviu-Iulian NICULESCU DR, Centre National de la Recherche Scientifique	Directeur de thèse

Résumé Étendu

Le travail de recherche développé dans cette thèse explore l'utilisation du comportement retardé dans les schémas de contrôle par rétroaction comme élément interne du contrôleur. Profondément inspiré par les contrôleurs proportionnels-dérivés-intégraux bien connus, cette thèse propose une structure similaire avec l'ajout d'une action retardée. La première et la plus importante tâche étant de concevoir un contrôleur qui atteint la stabilité asymptotique du système en boucle fermée. La thèse présente une variété de cas d'étude pour ces schémas de contrôle basés sur le retard, une variété présente dans les deux éléments, les contrôleurs et les systèmes à contrôler. Différentes configurations de contrôleurs utilisant des processus proportionnels, intégraux, retardés et même d'intégration retardée sont proposées et testées. De plus, on étudie son potentiel de contrôle dans différents scénarios en considérant des classes générales de systèmes dynamiques linéaires, et une variété d'applications en mécanique, électronique de puissance, robotique et systèmes photovoltaïques.

Il est important de souligner que toutes les analyses effectuées dans ce travail sont des analyses linéaires. Plus précisément, nous supposons que les équations décrivant le schéma de contrôle complet (en considérant le contrôleur et le système à contrôler) sont des équations différentielles linéaires. Ceci est formellement argumenté en considérant les techniques de linéarisation, les modèles linéarisés ou par hypothèse directe. Nous exploitons ces structures linéaires pour développer une interprétation basée sur les fréquences, utile pour comprendre ces systèmes dynamiques de manière élégante et intuitive. En général, il est bien connu que les solutions des équations différentielles linéaires peuvent être décrites par une analyse de l'emplacement des racines de ses équations caractéristiques. Plus précisément, ces racines algébriques indiquent la décroissance exponentielle et la fréquence de vibration de ces solutions, et plus important encore, l'emplacement de ces racines est directement lié à la stabilité des solutions.

Cette thèse étudie en détail ces fonctions et ses racines dans le cas où un comportement retardé est présent. Dans un tel cas, ces fonctions sont des quasi-polynômes, ou des polynômes à coefficients exponentiels. Pour étudier ces racines, nous nous basons sur le fait que leur emplacement sur le plan complexe change continuellement au moyen de variations continues des paramètres des contrôleurs. Nous cherchons à caractériser ce comportement, à le concevoir, et par conséquent, à pouvoir concevoir la nature de ces solutions. Dans ce sens, nous utilisons la méthodologie dite de stabilité par croisement de racines. Enfin, cette thèse développe des observations analytiques et des méthodes numériques pour choisir les paramètres de ces contrôleurs à base de retard de telle sorte

que le système en boucle fermée soit stable. En particulier, nous visons à étudier la commande de systèmes linéaires invariants dans le temps à une seule entrée et une seule sortie. Aussi, son implémentation sur quelques applications : convertisseur de puissance buck et le pendule inversé rotatif. Une application d'ingénierie réelle avec des résultats expérimentaux : un système photovoltaïque avec suivi du point de puissance. Et enfin, le problème classique de la stabilisation d'une chaîne d'un nombre quelconque d'oscillateurs en utilisant un seul bloc de retard.

Extended Abstract

The research work developed in this thesis explores the use of delaying behavior in feedback control schemes as an inner element of the controller. Deeply inspired by the well-known proportional-derivative-integral controllers, this thesis proposes a similar structure with the addition of a delayed action. Being the first and most important task to design a controller that achieves asymptotic stability of the closed-loop system. The thesis presents a variety of cases of study for these delay-based control schemes, a variety present in both elements, controllers and systems to control. Different controllers' configurations using proportional, integral, delaying and even delayed integration processes are proposed and tested. Also, one studies its control potential in different scenarios by considering general classes of linear dynamic systems, and a variety of applications from mechanics, power electronics, robotics and photo-voltaic systems.

It is important to highlight that all analysis carried-out in this work are linear analysis. More precisely, we assume that the equations describing the full control scheme (considering controller and system to control) are linear differential equations. This is formally argued by considering linearization techniques, linearized models or by direct assumption. We exploit such linear structures to develop a frequency-based interpretation useful to understand these dynamic systems in an elegant and intuitive way. In general, it is well-known that the solutions of linear differential equations can be described by an analysis of the location of the roots of its characteristic equations. More precisely, these algebraic roots denote exponential decay and vibrations frequency of these solutions, and more importantly, the location of these roots is directly linked to the solutions' stability.

This thesis studies in detail these functions and its roots in the case in which delayed behavior is present. In such a case these functions are quasi-polynomials, or polynomials with exponential coefficients. To study such roots we rely on the fact that its location on the complex plane changes continuously by means of continuous variations of the controllers' parameters. We aim to characterize this behavior, to design on it, and in consequence, to be able to design these solution's nature. In this sense, we use the so-called crossing roots stability methodology. Ultimately, this thesis develops analytical observations and numeric methods to chose the parameters of these delay-based controllers such that the closed-loop system is stable. In particular, we aim to study the control of single-input single-output linear time invariant systems. Also, its implementation on some applications: buck power converter and the rotatory inverted pendulum. A real engineering application with experimental results: a match power point tracking photo-voltaic system. And finally, the classical problem of stabilizing a chain of any number of oscillators by using a single delay block.

Resumen Extendido

El trabajo de investigación desarrollado en esta tesis explora el uso del comportamiento retardado como un elemento para diseñar sistemas de control retroalimentados. Es decir, como un elemento interno del controlador. Inspirado en los controladores proporcionales-derivativos-integrales, ampliamente conocidos y usados en la actualidad. Esta tesis propone una estructura conceptual similar añadiendo la acción de tipo retardada. Para este fin, el primer objetivo y el más importante, es diseñar un controlador que asegure la estabilidad asintótica del sistema de lazo cerrado. Esta tesis presenta una variedad de casos de estudio para estos esquemas de control basados en retardos, una variedad presente en ambos elementos, los controladores y los sistemas a controlar. Se proponen y prueban diferentes configuraciones de controladores utilizando procesos proporcionales, de integración, de retardo e incluso de integración retardada. Además, se estudia su potencial de control en diferentes escenarios considerando clases generales de sistemas dinámicos lineales, y una variedad de aplicaciones desde la mecánica, la electrónica de potencia, la robótica y los sistemas fotovoltaicos.

Es importante destacar que todos los análisis realizados en este trabajo son análisis lineales. Más concretamente, se asume que las ecuaciones que describen el esquema de control completo (considerando el controlador y el sistema a controlar) son ecuaciones diferenciales lineales. Esto es argumentado formalmente considerando técnicas de linealización, modelos linealizados alrededor de puntos de operación, o por suposición directa. De hecho, estas estructuras lineales se aprovechan para desarrollar una interpretación basada en un enfoque frecuencia, útil para entender estos sistemas dinámicos de una manera elegante e intuitiva. Es bien sabido que las soluciones de las ecuaciones diferenciales lineales pueden ser descritas cualitativamente por la localización de las raíces de sus ecuaciones características. Estas raíces algebraicas indican el decaimiento exponencial y la frecuencia de vibración de estas soluciones. Y lo que es más importante, la ubicación de estas raíces está directamente relacionada con su estabilidad.

En esta tesis se estudian con detalle estas funciones y sus raíces, y debido al carácter retardado en las ecuaciones diferenciales lineales, se estudian las raíces de las funciones cuasi-polinómicas. Para esto, se sabe que la ubicación de estas raíces en el plano complejo cambia continuamente mediante variaciones continuas de los parámetros del controlador. Y se pretende caracterizar este comportamiento para manipularlo, y en consecuencia, manipular también la naturaleza de estas soluciones. En otras palabras, diseñar el comportamiento dinámico global, es decir, para controlarlo. Este proceso es más conocido en la literatura como teoría de estabilidad de cruce por frontera. En general, esta tesis desar-

rolla observaciones analíticas y métodos numéricos para elegir los parámetros de control de estos controladores basados en el retardo para que el sistema de lazo cerrado sea estable. En particular, se estudia el control de sistemas lineales invariantes en el tiempo con una sola entrada y una sola salida. Su implementación en algunas aplicaciones: convertidor de potencia buck cd/cd y el péndulo invertido giratorio. Una aplicación real de ingeniería con resultados experimentales: un sistema fotovoltaico con seguimiento del punto de potencia. Y por último, el problema clásico de estabilizar una cadena de cualquier número de osciladores utilizando un único bloque de retardo.

Contents

List of Figures

List of Tables

Symbols

$\mathbb{N}$	Set of natural numbers
$\mathbb{Z}$	Set of integer numbers
$\mathbb{Z}_+$	Set of positive integer Numbers
$\mathbb{Q}$	Set of rational numbers
$\mathbb{R}$	Set of real numbers
$\mathbb{R}_+$	Set of positive real numbers
$\mathbb{C}$	Set of complex numbers
$\Re$	Real part of a complex numbers
$\Im$	Imaginary part of a complex numbers
i	Imaginary unit
RHP	Right-Half Plane of the complex plane
LHP	Left-Half Plane of the complex plane
$< x, y >$	Scalar product of x and y
$\lceil \cdot \rceil$	Ceiling function
$\lfloor \cdot \rfloor$	Floor function
DDE	Delay Differential Equations
LTI	Linear Time Invariant
SISO	Single-Input Single Output
DC	Direct Current
PV	Photo-Voltaic
PWM	Pulse Width-Modulation
MPP	Match Power Point
MPPT	Match Power Point Tracking
LQR	Linear Quadratic Regulator
PID	Proportional-Integral-Derivative
$P\delta$	Proportional-Delayed
$PI\delta$	Proportional-Integral-Delayed

$P\delta I$	Proportional-Delayed Integral
PD^{δ}	Proportional-Delay-based Integral

Chapter 1

Introduction

Roughly speaking, we may interpret control schemes design as a conversation between controller and system, one in which language is nothing but dynamical behavior. In this sense, we interpret physical systems as differential-integral equations, and use the same elements for constructing a control scheme. We could easily mention the well-known PID (Proportional-Integral-Derivative) type controllers, in which one finds these precise elements. Considering only these three as means to design a control scheme is proved to be a useful and simple idea. In fact, the impact of each one of them on the overall closed-loop system has been studied deeply in the literature (see, for instance, [8, 55]). However, it is important to notice that this simplicity, found then consequently in its dynamics analysis and design, trades-off with the fact that they may not be sufficiently enough complex to control some systems, or to to do it at its full potential.

In any other case, one can interact directly with the closed-loop dynamics by varying the parameters of the system, physical ones or even the controller's ones. Plenty of literature has been developed in order to better understand this and to use it for control design (see, for instance, [2]). For example, consider the derivative action of a PID controller, usually one regards it as an enabler for damping manipulation. This can be easily explained by looking at the classical example of a mass-spring-damper system, in which this relationship between damping and the first derivative related term is found explicitly. It is interesting to notice that in such a classical example we could interact with the overall damping of the system in two different ways. One, by varying the proportional gain of the derivative action, and a second one by directly using different physical dampers, or its equivalent damping system according to the application. Interestingly enough, sometimes even parts of the model equations are built in the control law, this is made usually with the purpose of neglecting some non-desired dynamical behavior, or to take it into account directly. A common scenario of these is the well-known input/output linearization technique, in which we assume perfect understanding of the physical system's non-linearities using them in the control algorithm to neglect them. We address an illustrative example of this technique in this thesis document.

Whatever the case, one could argue that the main control design tool is knowledge. More precisely, a model which presumably contains all the dynamics information of the

system to be controlled, and one which even could forecast its behavior. This is partially correct, since reality appears to be more granulated than our tools to describe it. And even if one allows oneself to try it, our best efforts bring up a level of complexity in the models' equations not suitable for easy analytical handling. It is worthy to note that these can be used for complicated and accurate computer simulations. However, through all control theory literature, it has been shown that a good "trade of" between model and controller complexities is a success. In general, there is a saying: "all models are wrong but some are useful". In fact, even though it is not always the case, usually one is more interested in depicting the qualitative behavior of the physical system, rather than to get a perfect description out of it. A really accurate model, may be one so complex that the tools to analyzing it from a control perspective won't be enough, or they won't be able to do something interesting out of it. Also, and equally important, a sensing system capable of capturing information as rich in dynamics as possible is desired.

In this regard, this thesis embraces completely the idea of using linear differential interpretations of already existing models. It is mandatory to enhance that such a choice has nothing to do with a simplification of the needed analysis, or as a way to make those easier, as owe could assume. Rather, we exploit its stretch relationship with a really intuitive and elegant frequency-based interpretation. More precisely, and better explained in the sequel, the relationship between the characteristic roots location and the overall dynamic system response. In general, this thesis explores concepts as stability and closed-loop response manipulation through a detailed study of these roots and its equations. One statement that is repeatedly mentioned through the whole thesis is that a linear system is asymptotically stable, if and only if, all of its characteristic roots are located in the left-half plane of the complex plane. In other words, if and only if, all of them have negative real part. This is the main reason for this thesis to be basically a deep study of the behavior of these roots with respect to controllers parameters variations.

For the scope of this thesis, and in fact, as its particular objective, these ideas are used to study delay-based control schemes. In other words, the use of time-delays as means to develop a control system. The easiest way of understanding such an idea would be thinking of it as an extension of the PID type controllers. One in which a time-delayed action becomes an option in their design, one as valid as the integral or derivative one. As mentioned before, the general idea of these has always been using dynamical behavior for shaping dynamical behavior. Such ideas are explained in detail in the following lines, and deeply throughout this thesis document.

1.1 Time-Delay and Delay-Based Control

Time-delays can be found in almost any field, biology, chemistry, engineering or social sciences, to mention a few (as discussed in [56]). Either, this can be inherent to the system's nature and/or as a part of an inner communication system. Regarding dynamical systems, this time delay behavior can be mathematically described for further analysis through a variety of different interpretations. FDE's (Functional differential equations), abstract equations and DDE's (delay differential equations), to mention a few (see, for

instance, [66]). In this thesis we focus on the use of DDE's, these are a class of equations where the evolution of its solution depends not only on its actual value, but also on all the information from this instant to a particular moment in the past. As mentioned in [16], delays may occur due to finite velocities of signal propagation or processing delays leading to memory effects and, in general, infinite-dimensional systems.

One can think in the time a fluid takes to travel a pipeline, or that one that a remote control system takes to obtain information (sensing variables) and to send back adjusting commands to a remote location. Evidently, particularly important for teleoperation systems (see for instance, [3], [20] and [57]). Either the case, not taking it into account in the control design may be disadvantageous if happens to play a big role on the qualitative behavior of the system. It is well known that adverse effects as oscillations, instability and bandwidth sensitivity, among others, are the consequence of the presence of delay in the control loop (see, for instance, [52, 49]). However, it is worth mentioning that there exist some situations when the delay may improve the system's stability as discussed in the classical example [1, 68], where an oscillator is controlled by one gain-delay "block" with positive gains and small delay values (a detailed analysis of such an approach can be found in [54]). This thesis studies exactly this last idea, more precisely, a variety of delay-based control schemes is presented and discussed. In other words, we study the implications of adding a delayed nature as a control tool. Moreover, as mentioned before, we have to state that even though some non-linear formulations are used in the content of this thesis as means for describing physical systems, this work focuses ultimately on linear analysis. In this regard, and before discussing particular applications problematics, we have first to discuss two fundamental linear delay-based control problems: the stabilization of chains of integrators and oscilators.

One may argue that these problematics serve as theoretical observations for understanding the place of linear delay-based control in comparison to other PID alike control strategies. One main observation of this thesis, as discussed in chapters 4 and 5, it is that both problematics appear to be suitable to be solved using the purest forms of linear delay-based control. That is, using only delay "blocks" (gain, delay) without any additional integral-derivative process usually found in PID controllers. First, as deeply studied in [53], a chain of integrators can be stabilized only using delay blocks. This result states that a chain of any number of integrators can be stabilized by a classical control scheme based on a linear combination of delayed error signals with corresponding proportional gains (delay "blocks"). Second, the idea of stabilizing oscilators using delays is first introduced in the illustrative example reported in [1], and later on better understood in [54]. Such works study the stabilization of one oscillator by using only one delay "block". Along these lines, it is worthy to recall an interesting observation first introduced in [38], that one delay block may stabilize not only one but a chain of any number of oscillators. In general, the idea is that these open (in terms of the possible degree of the system) problematics can be solved by using relatively simple delay-based control schemes, and also, that it is the delayed nature the one enabling such capacity. As a first thought, these should not only be considered for its direct application, that is, stabilizing systems having such particular dynamics. And neither by doing it using only delay blocks (PID related terms may be easily added). But in fact, these are important puzzle pieces to understand

what can one get from using delay-based control, or at what extent using a delayed term may be advantageous.

Bearing such arguments in mind, the extension of these delay "blocks" to more complex forms using proportional-integral-derivative elements is evident. In this thesis we refer to the use of a delayed term using the Greek letter δ. In this way, one may have $P\delta$ (proportional-delayed) or $PI\delta$ (proportional-integral-delayed) controllers, as examples. Different forms of these delay-based controllers are already been studied theoretically and experimentally in the literature. In [61] the $PI\delta$ controller design is studied for its application to second-order LTI (Linear Time Invariant) systems. The $P\delta$ controller has being implemented experimentally in [32] for a haptic-virtual systems, to mention some cases. To this end and most importantly, in almost every study the main goal is first to develop a stability analysis to properly design such controllers. That is, to compute the proper gains and delay values such that the closed-loop system is at least stable. This thesis studies these time-delay control systems through the use of linear ordinary differential equations as a means to work with a frequency-based interpretation (similarly to [21]). In this regard, the most important feature to highlight in comparison to linear non-delayed systems is directly related to its characteristic equation. More precisely, the fact that the characteristic equation of a linear non-delayed system has a finite number of roots (characteristic roots). Being these zeros of the so-called characteristic polynomial. In contrast, a time-delay system has an infinite number of characteristic roots. Being these, zeros of the exponential-polynomial transcendentals function better known as quasi-polynomial. Also known as polynomial with exponential coefficients.

All chapters of this thesis aim to study time-delay systems, some in pure theory, and some through applications, simulations and experimentation. Nevertheless, they can be also easily interpreted as detailed studies of different and particular classes of these quasi-polynomials and its roots. In fact, all results derived related to time-delay systems in this thesis belong in the same way to quasi-polynomial complex analysis. To better understand the above mentioned insights, one can study the roots of the simplest quasi-polynomial, as explicatively depicted in the following proposition.

Proposition 1. *Consider the function:*

$$f(s) = 1 + ae^{-\tau s}, \quad a \in \mathbb{R}, \tau > 0.$$

The roots of $f(s)$ behaves as:

$$s = \begin{cases} \frac{1}{\tau}\left\{-\log\{\frac{1}{a}\} + i(2n+1)\pi\right\}, & \text{if } a > 0, \\ \frac{1}{\tau}\left\{-\log\{-\frac{1}{a}\} + i2n\pi\right\}, & \text{if } a < 0, \end{cases} \tag{1.1}$$

for all $n \in \mathbb{N}$. Additionally, the following can be stated:

$$\begin{aligned} \text{if} \quad |a| > 1, \quad &\rightarrow \quad \Re\{s\} > 0, \\ \text{if} \quad |a| < 1, \quad &\rightarrow \quad \Re\{s\} < 0. \end{aligned}$$

Proof. Assume that there is a root of $f(s) = 0$ on the complex plane in $s = \sigma + i\omega$, where $(\sigma, \omega) \in \mathbb{R}^2$. One can rewrite this equation as:

$$\left\{1 + ae^{-\tau\sigma}\cos(\tau\omega)\right\} - i\left\{ae^{-\tau\sigma}\sin(\tau\omega)\right\} = 0.$$

Given this equation, in order to solve the imaginary part, if $a \neq 0$ then $\omega = \frac{\pi}{\tau}n$ where $n \in \mathbb{N}$. Now, substituting this in the real part leads us to:

$$1 + ae^{-\tau\sigma}(-1)^n = 0.$$

Subsequently, solving for σ gives the following:

$$\sigma = -\frac{1}{\tau}\log\left\{\frac{(-1)^{n+1}}{\alpha}\right\}.$$

Having found σ and ω one can then explicitly describe s as in (1.1). □

From this proposition, one can notice that even this simple case has an infinite number of complex roots. Interestingly enough, all of them can be located in one half-plane at the same time. In general, it is important to notice that the distribution of them on the complex plane is governed by its parameters (coefficient and delay). If possible, the ideal case would always be to have as much information as the one presented in Proposition 1. However, deriving analytical observations for higher-order examples becomes extremely difficult. In fact, there are entire research communities dedicated to develop numeric methods to understand the location of the zeros of these special functions (see for instance, [73, 74]). Some of these strategies, and the ones developed in this thesis, are based in the so-called crossing roots analysis. In the following, we introduce in detail the basis of it.

1.2 Parameter Based Stability Analysis

As mentioned before, and as it is repeatedly done throughout this thesis: all time-delay systems studied in this thesis are asymptotically stable, if and only if, all the roots of its characteristic quasi-polynomial are located in the LHP (left-half plane) of the complex plane. Or that strictly none of them are located in the RHP (right-half plane). Straightforwardly, this is the main reason to study the behavior of these roots in relation with its parameters (time delay values, coefficients).

In this sense, it is important to highlight that the enabling idea behind every result presented in this thesis is the quasi-polynomials roots continuity property. More precisely, the fact that the location of such roots vary continuously on the complex plane as the quasi-polynomial parameters are varied in the same way. To illustrate such property, consider the polynomial case in the following theorem.

Theorem 1. *As discussed in [45]. Let:*

$$P_0(z) = a_n z^n + a_{n-1} z^{n-1} + \cdots + a_0 = a_n \prod_{j=1}^{p} (z - z_j)^{m_j}, \quad a_n \neq 0,$$

$$P_\epsilon(z) = a_n z^n + (a_{n-1} + \epsilon_{n-1}) z^{n-1} + \cdots + (a_0 + \epsilon_0),$$

polynomials with real coefficients and let D_k be a disk centered at z_k with radius r_k such that:

$$0 < r_k < \min |z_k - z_j|, \quad j = 1, 2, \ldots, k-1, k+1, \ldots, p.$$

There exists a positive number ϵ such that, if $|\epsilon_i| \leq \epsilon$ for $i = 0, 1, \cdots, n-1$, then $P_\epsilon(z)$ has precisely m_k roots in the disk D_k.

Roughly speaking, $P_\epsilon(z)$ may be interpreted as a slightly different version of polynomial $P_0(z)$. One with perturbed coefficients (through the addition operation). This proposition states that for every different root of $P_0(z)$, considering its multiplicity, there always exists a disk (region) centered at this root in which $P_\epsilon(z)$ has the same number of roots. In general, for sufficiently small perturbations this describes a continuous behavior. As its coefficients are varied, the locations at which polynomials banishes on the complex plane vary in a continuous way. A similar result regarding quasi-polynomial functions can be found in [48].

As an implication of this strong argument concerning continuity, the main line of thought chosen in this thesis scope is the so-called *crossing roots* analysis. Roughly speaking, this consists in understanding as clear as possible the behavior of the characteristic roots when for a proper choice of parameters these are located exactly on the imaginary axis, in other words, crossing it. A single choice of parameters with such properties is usually refereed as a *crossing point* on the *parameters space* (parameters vectorial space domain). Moreover, a continuous set of crossing points on the parameters space is called a *stability crossing curve*. Consider the following: a point of a stability crossing curve on the parameters space implies roots crossing. Then, a continuous parameters variation crossing through such curve implies the movement of at least a single characteristic root from one semi-plane to the other (LHP to RHP, or RHP to LHP). For which the crossing point is the enabler of such a situation.

This particular roots exchange between semi-planes impacts directly on the number of roots on the RHP of the complex plane. Usually depicted as the *stability index*. Again, all time-delay systems studied in this thesis are asymptotically stable, if and only if, all of its roots are located on the LHP of the complex plane. The same is true if no roots are located on the RHP, or in other words, if the stability index (or number of unstable roots) is equal to zero. This argument is the one that puts the term "stability" in all the above mentioned concepts related to crossing roots analysis. Now, consider a set of contiguous parameters choices delimited by stability crossing curves. Therefore, a continuous parameters variation inside such a set implies no root crossing. Consequently, such set has the property of having a fixed number of unstable roots or stability index. With such in mind, such sets are refereed to *stability crossing regions* which according to

its fixed stability index may be stable (index equal to zero) or unstable (index strictly greater than zero). A set with a stability index equal to zero is understood in this thesis document as a *stability region* and it is nothing else than the so-called stability or stabilizing conditions looked upon from the control theory point of view.

It is interestingly enough to highlight that the position on the imaginary axis at which roots crossing takes place is related, and consequently, usually refereed to a frequency value. This due to its direct relationship with the oscillations frequency of the corresponding ordinary differential equations solutions. In fact, if one choses a crossing point as the system parameters, and this implies a simple root crossing outside of the origin (no multiplicity in the roots and imaginary part different than zero). Then, these solutions will contain a sustained oscillation at a frequency value equal to the imaginary part at which the roots crossing takes place. This is partially why crossing roots analysis is understood as a frequential or frequency-based methodology. And also why throughout this thesis document such a terminology is used repeatedly. For the sake of clarity, some of the concepts introduced in this section are better defined in the following lines. As a simple illustrative example consider the following retarded quasi-polynomial:

$$\Delta(s) = P(s) + Q(s)e^{-\tau s},$$

where $P(s)$ and $Q(s)$ are polynomials with real coefficients such that $\deg\{P\} > \deg\{Q\}$ and τ is a positive delay value.

Remark 1. *An important property of the quasi-polynomial $\Delta(s)$ is that its zeros are continuous functions with respect to their parameters (see, for instance, [49, 15] and references therein). In this vein, the number of roots in the RHP can change only when some zeros cross the imaginary axis.*

Definition 1 (Frequency Crossing Set)**.** *The* frequency crossing set $\Omega \in \mathbb{R}$ *is the set of all ω such that:*

$$\Delta(i\omega) = P(i\omega) + Q(i\omega)e^{-i\omega} = 0.$$

Remark 2. *It is clear that if one takes the complex conjugate of $\Delta(i\omega)$, the following equality holds:*

$$P(-i\omega) + Q(-i\omega)e^{i\omega} = \overline{P(i\omega) + Q(i\omega)e^{-i\omega}}.$$

Therefore, in the rest of the document one considers only nonnegative frequencies, i.e., $\Omega \subset \mathbb{R}_+ \cup \{0\}$.

Definition 2 (Stability Crossing Boundaries)**.** *The stability crossing boundaries $\mathcal{T}$ is the set of all parameters for which there exists at least one $\omega \in \mathbb{R}_+ \cup \{0\}$ such that $\Delta(i\omega) = 0$. Moreover, for a fixed delay value $\tau \in \mathbb{R}_+$, any element $k \in \mathcal{T}$ is known as a* crossing point*.*

Remark 3. *Notice that if the number of parameters is two or three, these boundaries become curves or surfaces, respectively. This thesis focuses almost entirely in the first ones, the stability crossing curves.*

Finally, we present a proposition using all concepts introduced above to develop a crossing roots analysis. The function studied in this result can be obtained from considering a single integrator as open-loop system and a single delay block as controller.

Proposition 2. *Consider the pair of open-loop system and controller:*

$$G(s) = \frac{1}{s}, \qquad C(s) = Ke^{-\tau s},$$

respectively. Let $K > 0$, then, the closed-loop system is asymptotically stable if:

$$\tau \in [0, \tau^*), \quad \textit{where} \quad \tau^* = \frac{\pi}{2K}. \tag{1.4}$$

Proof. The characteristic equation of the closed-loop system can be computed directly from $G(s)C(s) + 1 = 0$ as follows:

$$\Delta(s) = s + Ke^{-\tau s} = 0. \tag{1.5}$$

Consider first the delay-free scenario $\tau = 0$, then:

$$\Delta(s) = s + K = 0,$$

it is clear that one achieves asymptotic stability iff $K > 0$, since this single real root has negative real part. Assume such selection of a gain and recall the roots continuity property. One can conclude then, that there must exist a τ interval containing $\tau = 0$ for which no root exchange planes (no root crossing is achieved) and therefore, stability is maintained. Let us investigate the existence of crossing roots.

First, it is clear that if $s = 0$ in (1.5) then $K = 0$ which by assumption is not possible. therefore, there is no crossing through the real axis. Second, consider now $s = i\omega$:

$$Ke^{-i\tau\omega} = -i\omega, \quad \rightarrow \quad K\left[\cos(\tau\omega) - i\sin(\tau\omega)\right] = -i\omega,$$

since $\omega \in \mathbb{R}$ a solution exists iff $\omega = n\frac{\pi}{2\tau}$, where $n \in \mathbb{N}$. That is, in order to both sides of the equation to be purely imaginary. Considering such ω, and comparing their imaginary parts of both sides one can derive that:

$$\tau = (-1)^{n+1} n \frac{\pi}{2K},$$

where since $\tau > 0$ by assumption of being the value of an amount of time delayed. Then, more precisely:

$$\tau = n\frac{\pi}{2K}, \text{ for } n \text{ odd}.$$

These are the before mentioned crossing points. It is clear finally that the nearest crossing point to $\tau = 0$ is the case for $n = 1$, implying directly the stabilizing interval depicted in

(1.4).

Additionally and for the sake of clarity let us investigate the so-called crossing directions. To this end, consider the following derivative using the *implicit function* theorem:

$$\frac{ds}{d\tau} = -\frac{\frac{\partial \Delta}{\partial \tau}}{\frac{\partial \Delta}{\partial s}} = \frac{sKe^{-\tau s}}{1 - \tau K e^{-\tau s}},$$

now consider the crossing frequencies $\omega = n\frac{\pi}{2\tau}$.

$$\left.\frac{ds}{d\tau}\right|_{s=in\frac{\pi}{2\tau}} = \frac{nK(-1)^{n+1}}{1 - i\tau K(-1)^{n+1}} = \frac{nK}{1 - i\tau K},$$

since n is odd. Finally, in order to investigate the crossing deviation with respect to the real part σ of the complex variable s we compute:

$$\operatorname{sgn}\left\{\frac{d\sigma}{d\tau}\right\} = \operatorname{sgn}\left\{\Re\left\{\left[\left.\frac{ds}{d\tau}\right|_{s=in\frac{\pi}{2\tau}}\right]^{-1}\right\}\right\} = \operatorname{sgn}\left\{\frac{1}{K}\right\} = 1.$$

Therefore, for any increasing variation of τ around any crossing point, the real part of the crossing root tends to augment, i.e, to traverse to the RHP of the complex plane. Implying instability for any interval of $\tau > \tau^* = \frac{\pi}{2K}$. □

1.3 Motivational Examples

It is well recognized that low-order controllers are one of the most widely applied strategies to control industrial processes (see, e.g., [8, 55]). Such a "popularity" is mainly due to their particular distinct features: simplicity and ease of implementation. Among these controllers, those of PID-type are known to be able to cope with uncertainties, disturbances, elimination of steady-state errors and transient response improvement (see, for instance, [7, 46, 61]). However, the one of the main drawbacks of PID controllers, as reported in [7], lie in the tuning of the derivative term, which may amplify high-frequency measurement noise. In fact, as mentioned in [8, 55] the above arguments advise to avoid the derivative action in most applications. In order to circumvent such a problem, the Euler approximation of the derivative:

$$y'(t) \approx \frac{y(t) - y(t - \epsilon)}{\epsilon}, \tag{1.6}$$

for small $\epsilon > 0$, seems to be the simplest way to replace the derivative action by using its delay-difference approximation counterpart ([53]). In the sequel, one presents two controllers alternatives using *delays* as *design parameters* to the classical PD and PI control schemes. These are studied in detail In Chapter 2. But now, they serve as

potential examples for the spirit of this thesis. In the sequel one develops three different illustrative examples regarding these in comparison with its PID counterparts.

On one hand, we study the PD^{δ} controller, which consists in substituting directly the derivative part of a PD controller by the above mentioned Euler approximation:

$$C(s) = k_p + k_\delta \frac{1 - e^{-\tau s}}{\tau}, \tag{1.7}$$

One of the main benefits in considering such an approximation is that most control schemes are implemented digitally. As a consequence, a numerical method needs to be considered in order to achieve a derivative action. In this vein, one of the main features of the PD^{δ} controller is that is easier to implement on such platforms and its model approximates more accurately to a derivative action for small delay values.

On the other hand, based on a PI controller, we consider a delay in the error signal only in the integral action:

$$C(s) = k_p + k_i \frac{e^{-\tau s}}{s}, \tag{1.8}$$

This provides an extra degree of freedom in the tuning of this controller maintaining the most important feature of the PI controller, which is the null steady state error in the regulation of zero type systems (open-loop systems with no poles at the origin). We depict some motivating examples on the use these of delay-based controllers. The main purpose of these is to enhance some advantages regarding the stability of the closed-loop system with respect to their low-order controllers counterparts (PD and PI). It is worth noticing that both examples consider the classical control scheme shown in Fig. 2.1 with a unitary step as reference input $r(t)$.

First, we consider an example in which a PD does not have the enough impact to stabilize the system. And this shows numerical results in which its delay-based counterpart, the PD^{δ} controller stabilizes it and can be also interpreted as a derivative-alike action.

Example 1. *Consider the following open-loop transfer function:*

$$G(s) = \frac{1}{s^3 - s^2 + 4s - 6},$$

with two stable poles $s_{1,2} = 0.17 \pm 2.1i$ and a real unstable one $s_3 = 1.34$. Considering the use of the well known PD controller, such a case leads to the following characteristic equation:

$$\Delta(s) = s^3 - s^2 + (k_d + 4)s + (k_p - 6) = 0.$$

Using the Routh-Hurwitz stability criterion is easy to prove that a necessary condition for closed-loop stability lies in having a positive second-order term. Notice that in this case, the PD controller does not have the necessary impact on the characteristic equation to achieve it. In fact, it is only possible to design the zero and first-order terms through this control scheme. In contrast, in Fig. 1.1, we present some simulation results considering now the PD^{δ} controller with parameters $[k_p, k_\delta]^T = [6.4, -3.4]^T$ with a fixed delay $\tau = 1s$. As can be seen in this results, this scheme allows us to have closed-loop stability maintaining this

derivation alike process for this set of parameters. Nevertheless, it is important to point out that a desired performance is not achieved since the steady state value of the output is clearly far from the unitary step.

Second, a similar example than the first one but now regarding the PI and $PI\delta$ controller is presented. In this one, the addition of the delay to the PI controller enables closed-loop stabilization.

Example 2. *Consider the following open-loop transfer function:*

$$G(s) = \frac{1}{s^2 - s + 3},$$

with unstable poles $s_{1,2} = 0.5 \pm 1.65i$. *Considering the use of the* PI *controller, such a case leads to the following characteristic equation:*

$$\Delta(s) = s^3 - s^2 + (k_p + 3)s + k_i = 0.$$

In a similar fashion that the first example, using the Routh-Hurwitz stability criterion it arises the necessary condition of having only positive terms in this polynomial in order to achieve closed-loop stability. Also for this example, the use of the PI *controller it is not enough for this purpose due to its null impact on the second-order negative term of the characteristic equation. In contrast, in Fig. 1.1, are also presented some simulation results considering now the* $P\delta I$ *controller with parameters* $[k_p, k_i]^T = [48.38, 106.6.4]^T$ *with a fixed delay* $\tau = 0.5s$. *From this results, it is shown how the addition of the delayed action presented in this controller gives the possibility of achieving stability and even null steady state error as expected.*

Finally, we present the following comparisons. On of the most common applications of purely PD alike controllers is trajectory tracking, such as the well known control problem in industrial robots. However, as mentioned in the Introduction, it is in this kind of implementations in which non-desired high frequency sensors noise can potentially be amplified by the use of a classical PD controller. Even some filtered schemes have been proposed in the literature (see, for instance [55]) to circumvent such a scenario. Probably the most direct example of this is the PD_f controller (PD controller with filtered derivative) shown below:

$$C_f(s) := K_c \left[1 + \frac{T_d}{1 + \frac{T_d}{N} s} \right],$$

where K_c, T_d and N are real parameters and can be described as a PD controller with a low-pas filter in the derivative action with break frequency $w_o = \frac{N}{T_d}$. We show an example in which we compare three different schemes using the PD, PD_f and PD^δ controllers applied to the open-loop system shown in (2.29). Also, we evaluate these considering a tracking problem under high-frequency noise disturbances due to sensors noise.

Example 3. *Consider a low frequency reference signal* $r(t) = sin(2\pi f_R)$ *with* $f_R = 1Hz$ *and a high frequency noise signal in the error as* $e(t) = r(t) - [y(t) + n(t)]$, *where* $n(t) =$

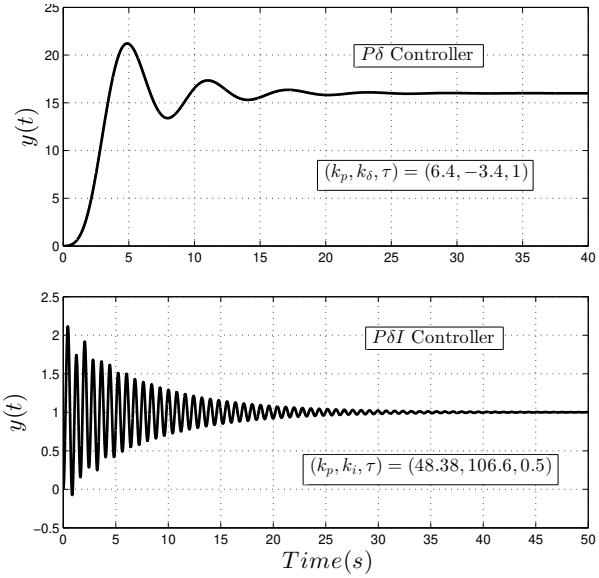

Figure 1.1: Motivating Examples – Closed-Loop System Responses.

$sin(2\pi f_n)$ with $f_n = 50Hz$. Furthermore, in order to make an equivalent comparison regarding controllers tuning, we focus on the proportional and derivative gains analogies inside each topology. That is, using the PD^δ controller gains $c_7 = (700, 80)$ with $\tau = 0.04s$, this translates as $(k_p, k_d) = (k_p, k_\delta)$ for the PD controller and $(K_c, T_d) = (k_p, \frac{k_\delta}{k_p})$ for the PD_f controller. Finally, for this last one chooses $N = T_d\omega_0$ for achieving a break frequency of $w_o = 2\pi f_o$ with $f_o = 40Hz$ (below the noise signal frequency). The results of this tests are shown in Fig 1.2a.

Now, with the purpose of making a quantitative comparison we propose the following performance indicators:

- *e_A-Amplitude of the ripple in the error signal in steady state due to noisy behavior.*
- *e_M-Maximum peak of the absolute value of the error signal.*
- *t_s-Settling time (Transitory period of time before achieving steady state).*

All of these indicators values are shown in Tab. 1.1. Using this information we show in Fig. 1.2b a radar chart normalized with respect to the worst case for a given indicator. In other words, if a controller indicator reach the unitary circle this controller has the worst performance of all. Also, another interesting indicator of this figure is the areas A of the polygons depicted in this figure for each controller. It is easy to observe that the ideal scenario concerns to the case in which this area is zero, that is basically no error signal. In other words, as this area is minimized, a controller fulfills more suitably the ideal indicators.

From the analysis depicted in Fig. 1.2b and Tab 1.1 one can notice that the controller better fulfilling this indicators is the PD_f controller. However, even thou the correspondent area of the PD^δ controller is larger in this radar chart, it is worth noticing that is the one

Table 1.1: Performance Indicators Values

Controller	e_A	e_M	t_s	A
PD	0.44	0.802	0.1	0.225
PD_f	0.35	0.870	0.1	0.129
PD^δ	0.38	2.137	0.95	0.507

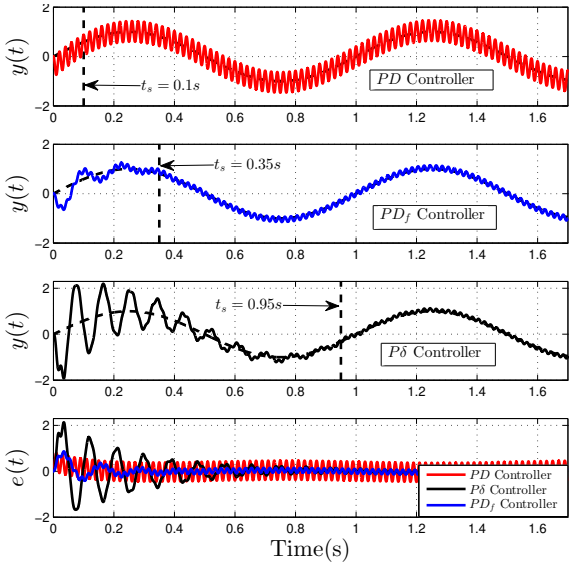

(a) Tracking Performance and Noise Rejection.

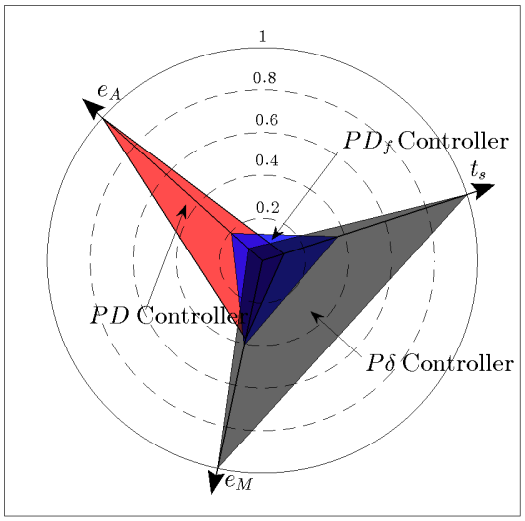

(b) Radar Chart.

Figure 1.2: Comparison Between the PD, PD_f and PD^δ Controllers.

that achieves the better high frequency noise rejection without implementing any additional behavior such as the filtered version of the PD controller. This indicates that this it is worth further studying for achieving an advantageous frequency response.

Finally, we discuss that implementing a continuous derivative action is by itself an interesting problematic. One can achieve continuous derivation using analogue electronics (for example, operational amplifiers). However, digital processes tend to be more common nowadays. And the way these solve the derivation problem may be similar and in some cases exactly the same as the Euler approximation and/or which inspires the $PD\delta$ controller. Evidently, a discrete analysis brings up its own interpretation of these dynamics. But from the continuous analysis point of view, it is not an absurd idea that one could be studying a continuous finite dimensional system with a derivative process in which the implementation of it could cause to turn it into a infinite-dimensional one. In this case, even applying a filter will not change such property. And a delay-based representation of it may bring useful information regarding its stability.

1.4 Thesis Content Overview

This thesis studies linear delay-based control schemes inspired by PID control strategies through well-known crossing roots analysis mentioned above. On one hand, we study the implementation of these delay-based control schemes through a variety of applications. Among others, we consider power electronic devices and the Furuta pendulum, real engineering problems and experimental results: one PV (photo-voltaic) application and a haptic-virtual system. On the other hand, we are interested in using delay-based controllers in engineering and to understand their possible advantages. To this end, we focus on some theoretical examples and some classic problems. On one hand, we develop numerical methodologies for tunning three different delay-based controllers inspired in PID controllers: proportional + delay ($P\delta$), proportional + delayed integral ($P\delta I$), and proportional + delay-based derivative (PD^{δ}) controllers. Interesting examples and discussions comparing them with their non-delayed counterparts are also addressed. On the other hand, we aim to solve the classical problem of stabilizing a chain of any number of oscillators using one-delay block. To be precise, the content of each chapters of this thesis is described in the following lines. Also, the academic publications resulted from this work are explicitly highlighted in relationship with each chapter.

Chapter 2: Crossing Roots Analysis: Alternative "PID Inspired" Delay-Based Controllers. The application of three delay-based controllers to LTI-SISO (Single-Input Single Output) systems is studied. These are: the $P\delta$, PD^{δ} and $P\delta I$ controllers. Particularly, we derive two different methodologies for computing proper gains stabilizing the closed-loop system (the controllers' tunning) using crossing roots analysis. On one hand, for the $P\delta$, we construct an algorithm capable of computing the closed-loop system stability index. On the other hand, for the PD^{δ} and $P\delta I$ controllers, we propose a rapid and practical method to find possible stability regions using the concept of σ-instability curves. This last idea is one of the main products of the thesis and was published in the conference paper [29]:

J.-E. Hernández-Diez, C.-F. Méndez-Barrios and S.-I. Niculescu.
Practical Guidelines for Tuning PD and PI Delay-Based Controllers.
In 15th IFAC Workshop on Time Delay Systems. Sinaia, Rumania, 2019

Chapter 3: Delay-Based Control Design: Some Applications. Three different illustrative applications of delay-based controllers are studied and discussed. First, a bilateral control scheme using a $P\delta$ controller in two different applications of haptic devices:haptic-virtual system and master-slave teleoperation system. The ideas studied in this chapter can also be found in the following five conference papers: [32] and [27] being previous to this thesis work[1]. Experimental results are addressed and discussed as practical examples of the use of delay-based control schemes. Second, a DC/DC buck converter using the $P\delta$ and $P\delta I$ controllers. These results presented in the following conferences, [34] and [29]:

[1], It is important to mention that these ideas are partially presented in Hernández-DÍez master's thesis [31].

J.-E. Hernández-Diez, C.-F. Méndez-Barrios, S.-I. Niculescu, E.-J González-Galván, G. Mejia-RodrÍguez and V. Ramirez-Rivera.
Closed-Loop Stability Analysis of Voltage Mode Buck Using a Proportional-Delayed Controller.
In 25th Mediterranean Conference on Control and Automation (MED). Valletta, 2017

J.-E. Hernández-Diez, C.-F. Méndez-Barrios, S.-I. Niculescu and V. RamÍrez-Rivera.
Closed-Loop Stability Analysis of Voltage Mode Buck Using a Proportional-Delayed-Integral Controller.
In 14th IEEE Conference on Industrial Electronics and Applications (ICIEA). Xi'an, China, 2019

And third, the analysis of the Furuta pendulum considering a delay in the control input. The results obtained in this work are depicted in the conference [33]:

J.-E. Hernández-Diez, C.-F. Méndez-Barrios, S.-I. Niculescu, E.-J González-Galván and A. Loredo.
Delay Margin in Controlling a Furuta Pendulum.
XIX Congreso Mexicano de Robótica. Mazatlán, México, 2017

Chapter 4: Stabilizing Integrators: Photo-voltaic Application. The control scheme design of a MPPT (Match Power Point Tracking) algorithm for a PV application is studied by considering a delay-based control strategy. An input-output linearization technique is used to cope with the system's non-linearities. Then, the resulted linear system is a chain of oscillators whose closed-loop stabilization is achieved using a $P\delta$ controller. A deep analysis of the roots of the characteristic quasi-polynomial is presented, also the zero dynamics of the system is studied. Several experimental results concerning set-point changes and solar irradiation disturbances are presented and discussed in detail. The ideas studied in this chapter can also be found in the following journal paper [36]:

J.-E. Hernández-Diez, C.-F. Méndez-Barrios, S.-I. Niculescu and E. Bárcenas-Bárcenas.
A Current Sensorless Delay–Based Control Scheme for MPPT–Boost Converters in Photo-voltaic Systems.
In IEEE Access, vol. 8, pp. 174449-174462, 2020.

Chapter 5: Stabilizing Oscillators: Remarks on the Solution of the General Case. The classical problematic of stabilizing a chain of any number of oscillators using only one delay block is studied. Explicit stabilizing conditions for the pair gain,delay are derived. Well-known crossing roots analysis as well the Mikhailov criterion are used to obtain the main results of the chapter. Lastly, the case in which the oscillators natural frequencies are equally spaced between one an other is studied and solved in detail. In the author's personal opinion, at the moment this document iswritten these are the most interesting ideas of his research and in this document. The ideas studied in this chapter can also be found in the following conference paper [35]:

J.-E. Hernández-Diez, C.-F. Méndez-Barrios and S.-I. Niculescu.
Some Insights on the Asymptotic Stabilization of a Class of SISO Marginally Stable Systems Using One Delay Block.
IFAC World Congress. Berlin, Germany, 2020.

Chapter 6: Concluding Remarks. Final thoughts on the overall content of the thesis are addressed. Also, some future work and interesting expanding ideas are exposed.

Chapter 2

Crossing Roots Analysis: Alternative "PID Inspired" Delay-Based Controllers

The content of this chapter studies the application of delay-based controllers using a classical feedback control scheme for controlling LTI-SISO systems. In general, the stability of some "PID inspired" delay-based controllers is studied through well-known crossing roots stability theory. To such an end, this chapter introduces a variety of analytical observations regarding the location of the closed-loop characteristic roots. Such results are later on used to generate algorithms and to propose methods to compute de so-called "stability index" (i.e number of unstable roots) or to find stability regions in the controllers parameters space. For each case study, illustrative numerical examples of the application of such methods are carried-out to clarify its reliability. Concluding remarks regarding the proper situations in which this variety of delay-based control schemes may be advantageous with respect to their counterparts are addressed.

This chapter is divided in two main sections, each of these studying different delay-based controllers and design methodologies. However, it is worth to recall that the core of both sections is based in a similar conceptual background (crossing roots theory and continuity). Three different controllers configurations are considered:

- $P\delta$ controller (Proportional-Delayed).
- $P\delta I$ controller (Proportional Delayed-Integral).
- PD^{δ} controller (Proportional Delay-Based Derivative).

First, the $P\delta$ controller is straightforwardly a low-order controller having proportional and proportional/delayed parts, each with its tunable gain, and one tunable delay. Second,

the $P\delta I$ is a direct variation of the PI controller, in which the integral part is also delayed, one could say that the PI is a particular case with delay value set to zero. Third, the PD^{δ} is understood as a PD controller by substituting the derivative part with its delay-based counterpart. That is, the Euler's approximation of the derivative, which is the simplest version of it (change rate computation between two non-contiguous points).

In general, the main difference between these sections appears in the crossing roots theory interpretations used in each. On one hand, section 2.1 studies uniquely the $P\delta$ controller, however, this is the most detailed section in terms of the obtainable information using the results derived in it. All of these, regarding the characteristic roots behavior with respect to the controller's parameters regarding different classes of open-loop systems and how to handle them. Nevertheless, the main contribution of this chapter is an easily programmable method for computing not only the stability property but also the stability index of a particular region in the controllers parameters space. On the other hand, section 2.2, studies two controllers configurations ($P\delta I$ and PD^{δ} controllers) and aims to compute closed-loop stabilizing conditions for both of them. More precisely, introduces a practical "quick and easy" method to compute possible necessary and sufficient conditions without assuring its reliability. However, from a practical sense it is interestingly enough to be used, numerical examples are depicted and discussed in this regard. The core of such a method is the use of the so-called σ-stability analysis, not in a usual way, but by considering positive unstable σ values in order to discriminate stability crossing regions. Before fully diving into detail, one describes the open-loop system taken into account in both sections.

Through the overall chapter, consider the class of proper SISO open-loop systems given by the transfer function:

$$G(s) := \frac{P(s)}{Q(s)} = \boldsymbol{c}^T(s\boldsymbol{I} - \boldsymbol{A})^{-1}\boldsymbol{b}, \tag{2.1}$$

where $(\boldsymbol{A}, \boldsymbol{b}, \boldsymbol{c}^T)$ is a state-space representation of the open-loop system. P and Q are polynomials defined as:

$$\begin{aligned} P(s) &:= \ p_m s^m + p_{m-1}s^{m-1} + \ldots + p_1 s + p_0, \\ Q(s) &:= \ q_n s^n + q_{n-1}s^{n-1} + \ldots + q_1 s + q_0, \end{aligned}$$

where $p_m \neq 0$ and $q_n \neq 0$, that are assumed to satisfy the following:

Assumption 1. *Polynomials P and Q satisfy the following conditions:*

(i) $\deg Q > \deg P$.

(ii) *$P(s)$ and $Q(s)$ are co-prime polynomials.*

(iii) $|P(i\omega)| > 0$, $\forall \omega \in \mathbb{R}$.

(iv) *If $Q(i\omega^*) = 0$, then $|Q'(i\omega^*)| > 0$, $\omega^* \in \mathbb{R}$.*

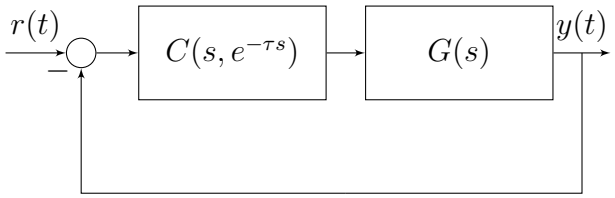

Figure 2.1: Classical Delay-Based Control Scheme

It is clear that Assumption 1-(i) states that the system is causal. If Assumption 1-(ii) is not fulfilled, this implies that there exist a non constant common factor $c(s)$, such that $P(s) = c(s)\tilde{P}(s)$ and $Q(s) = c(s)\tilde{Q}(s)$. In such a case, choosing $c(s)$ to be of the highest possible degree, the analysis can be pursued if $c(s)$ is a Hurwitz polynomial, otherwise, the system will remain unstable independently of the control action. Finally, in order to simplify the presentation, (iii) and (iv) are made to avoid having multiple roots on the imaginary axis in P and Q, respectively.

2.1 Stability Index Algorithm: $P\delta$ Controller

Before discussing the technical content of this chapter, it is important to notice that these ideas were first explored in the author's master's thesis [31]. The main reason to considered them in this chapter is that it exemplifies perfectly the crossing roots theory spirit used in this thesis for the design of delay-based control schemes. Also, for its contrast with the complementary σ-instability methodology depicted in the following section. Both methods are used in the following chapters.

This section develops a methodology for designing a $P\delta$ controller for a LTI systems. To be more precisely, this is stated in the following problem definition:

Problem 1. *Consider the transfer function* (2.1) *and the* $P\delta$ *controller:*

$$C(s) = k_p + k_\delta e^{-\tau s}. \tag{2.4}$$

. The $P\delta$ *controller stabilization problem is defined as the task of finding a proper set of parameters choice* (k_p, k_δ, τ) *such that the closed-loop system is asymptotically stable. In other words, such a choice of parameters implies that all roots of the closed-loop characteristic equation:*

$$\Delta\left(s; k_p, k_\delta, \tau\right) := P(s)\left(k_p + k_\delta e^{-\tau s}\right) + Q(s) = 0, \tag{2.5}$$

are located in the LHP of the complex plane. Moreover, and in the spirit of this chapter, the main goal is to find stability regions in the PD^δ *controller parameters space.*

The following remark may be evident, however, it is introduced for the sake of clarity.

Remark 4. *The* $P\delta$ *controller shown in* (2.4) *is its transfer function representation. Considering a classical control scheme as the one shown in Fig. 2.1 this implies that the*

control law in continuous time is computed as:

$$u(t) = k_p e(t) + k_\delta e(t-\tau),$$

where $e(t)$ is an error signal.

As mentioned before, all results developed in this chapter have at its core the spirit of well-known crossing roots theory. In this regard, through the following lines, first, the controller's parameters crossing roots conditions are characterized (several cases are studied). Second, the crossing tendency of these roots is studied (for each particular case). Third, using these observations (and the propositions developed in the first two sections) one derives and explains in detail an algorithm for the stability index computation. Forth and finally, illustrative examples are shown.

2.1.1 $P\delta$ Controller: Crossing Roots Existence

It is mandatory to notice in advance that a special situation arises when the open-loop transfer function G is even [1]. In order to treat properly this case, such is distinguished in the phrasing of the following results, having one in particular that treats it in detail. Similarly, the so-called *neutral case* is also treated separately.

Proposition 3 ([31, 28]-Purely imaginary crossing curves)**.** *Assume that G is not an even function such that* $\deg Q > \deg P$*, and let $\tau \in \mathbb{R}_+$ be a fixed delay value with $\Omega := \bigcup_\ell \Omega_\ell$ for $\ell \in \mathbb{N}$, where the subsets Ω_ℓ are defined as:*

$$\Omega_\ell := \left\{ \omega \in \mathbb{R}_+ \,\middle|\, \omega \in \left(\tfrac{\pi}{\tau}(\ell-1), \tfrac{\pi}{\tau}\ell\right) \right\}.$$

Then, $\omega \in \Omega$ is a crossing frequency*, if and only if, $\boldsymbol{k}(\omega) := [k_p(\omega), k_\delta(\omega)]^T$, where:*

$$\begin{aligned} k_p(\omega) &= -\,\Re\left[\frac{Q(i\omega)}{P(i\omega)}\right] - \cot(\tau\omega)\Im\left[\frac{Q(i\omega)}{P(i\omega)}\right], \\ k_\delta(\omega) &= \csc(\tau\omega)\,\Im\left[\frac{Q(i\omega)}{P(i\omega)}\right], \end{aligned}$$

defines a crossing point $\boldsymbol{k}(\omega) \in \mathcal{T}$.

In the previous result one assumes that G is not an even function. The following result covers such a case:

Proposition 4 ([31, 28]-Even function special case)**.** *Let $\tau \in \mathbb{R}_+$ be a fixed value and $G(s)$ an* even function*. Then, the set of all stability crossing curves is composed by the following set of lines:*

[1] Although G is a complex function, one considers the even functions definition for the real domain, i.e., $G(x) = G(-x),\ \forall x \in \mathbb{R}$.

(i)

$$\begin{aligned} k_p &= -G^{-1}(i\omega), \quad \omega \in \mathbb{R}_+ \cup \{0\}, \\ k_\delta &= 0. \end{aligned}$$

(ii)

$$k_p + (-1)^\ell k_\delta = -G^{-1}(i\omega), \quad \omega = \frac{\ell\pi}{\tau},\ \ell \in \mathbb{N}.$$

Proposition 5 ([31, 28]-Purely real crossing)**.** *Let $\tau \in \mathbb{R}_+$ be a fixed value. Then, the line:*

$$k_\delta = -k_p - \frac{q_0}{p_0}, \tag{2.7}$$

represents a stability crossing curve. Furthermore, this corresponds to a crossing through the origin of the complex plane.

When $\deg Q = \deg P$ the system is of neutral-type. The behaviour of the neutral root chain far from the origin (see for instance, [41, 25]) imposes necessary stability conditions on k_p and k_d.

Proposition 6 ([31, 28]-Neutral-type condition)**.** *Assume that* $\deg Q = \deg P$*. Then, if $\boldsymbol{k} \in \mathbb{R}^2$ is a stabilizing controller, the following condition holds:*

$$|k_\delta| < \left| k_p + \frac{q_n}{p_n} \right|.$$

Furthermore, this inequality defines a stability crossing curve.

One presents next a summary of the results of this section. Given all stability crossing points $\boldsymbol{k}(\omega)$ and the frequency crossing set Ω, one can define each stability crossing curve through its continuity, as follows:

$$\begin{aligned} \mathcal{T}_0 &:= \left\{ \boldsymbol{k} \in \mathbb{R}^2 \,\middle|\, k_\delta = -k_p - \frac{q_0}{p_0} \right\}, \\ \mathcal{T}_i &:= \left\{ \boldsymbol{k}(\omega) \in \mathbb{R}^2 \,|\omega \in \Omega_i \text{ for } i \in \mathbb{N} \right\}. \end{aligned}$$

For the special case of even transfer functions the stability crossing curves also include:

$$\mathcal{T}_{p_\ell} := \left\{ \boldsymbol{k} \in \mathbb{R}^2 \,\middle|\, k_\delta = (-1)^{\ell+1} \left\{ k_p + \frac{Q(i\omega_\ell)}{P(i\omega_\ell)} \right\} \right\}, \qquad \text{for } \ell \in \mathbb{N}.$$

By defining $\mathcal{T}_{p_\ell} := \emptyset$ when G is not even, one can describe the set $\mathcal{T}$ as:

$$\mathcal{T} = \bigcup_i \mathcal{T}_i \bigcup_\ell \mathcal{T}_{p_\ell}, \quad i \in \mathbb{N} \cup \{0\}, \ell \in \mathbb{N}.$$

In addition to the crossing roots conditions discussed above, one presents a pair of results concerning multiple roots. The first one, concerns positive real roots while the second one gives a necessary condition to characterize multiple pure imaginary roots.

Proposition 7 ([31, 28]-Unstable curve)**.** *Let $\tau \in \mathbb{R}_+$ be a fixed value, and $\boldsymbol{k} \in \mathbb{R}^2$. Then, if $\boldsymbol{k}$ is a stabilizing controller the following condition holds:*

$$\boldsymbol{k} \neq \tilde{\boldsymbol{k}}(\tilde{s}) := \left[\tilde{k}_p(\tilde{s}), \tilde{k}_\delta(\tilde{s})\right]^T,$$

for all $\tilde{s} \in \mathbb{R}_+$ such that $P(\tilde{s}) \neq 0$, with $\tilde{k}_p(\tilde{s})$ and $\tilde{k}_\delta(\tilde{s})$ defined as follows:

$$\begin{aligned} \tilde{k}_p(\tilde{s}) : &= -\frac{Q(\tilde{s})}{P(\tilde{s})} - \frac{1}{\tau}\frac{P(\tilde{s})Q'(\tilde{s}) - P'(\tilde{s})Q(\tilde{s})}{P^2(\tilde{s})}, \\ \tilde{k}_\delta(\tilde{s}) : &= \frac{1}{\tau}\frac{P(\tilde{s})Q'(\tilde{s}) - P'(\tilde{s})Q(\tilde{s})}{P^2(\tilde{s})}e^{\tau\tilde{s}}, \end{aligned}$$

where P' and Q' denote the derivative of P and Q, respectively. Furthermore, if $\boldsymbol{k} = \tilde{\boldsymbol{k}}(\tilde{s})$ for some $\tilde{s} \in \mathbb{R}_+$, then the characteristic equation of the closed-loop system has at least two roots in the RHP of the complex plane at $s = \tilde{s}$.

Remark 5. *A direct consequence of the previous result is that regions intersecting the curve described in Proposition 7 are unstable ones. An illustration of this result can be found in Example 5.*

The next result deals with multiple pure imaginary roots characterization:

Proposition 8 ([31, 28]-Multiple pure imaginary roots)**.** *Let $\tau \in \mathbb{R}_+$ be a fixed value, $\boldsymbol{k} \in \mathbb{R}^2$ and let $\Omega_m \subset \Omega$ be the subset of crossing frequencies with multiplicity $m \geq 2$. Assume that there is no constant $a \in \mathbb{R}_+$ satisfying the following condition:*

$$\frac{\Im\{f(i\omega)\}}{\Re\{f'(i\omega)\}} = a, \quad \forall\omega \in \mathbb{R}, \tag{2.12}$$

where $f(i\omega) := G^{-1}(i\omega)$. Then, the cardinality of Ω_m, i.e., $|\Omega_m|$, is finite. Furthermore, if $\Omega_m \neq \emptyset$ and there exist some constant $a \in \mathbb{R}_+$ fulfilling (2.12), then the cardinality of Ω_m is infinite (but countable) for some $m \geq 2$.

2.1.2 $P\delta$ Controller: Crossing Roots Directions

The results presented through Propositions 3-4 allow us to determine the values of k_p and k_δ for which crossing roots exist, but do not give any information on their crossing direction. In order to characterize regions according their number of unstable roots, one must make a distinction between switches (crossing towards instability) and reversals (crossing towards stability), and carry out a careful accounting of the unstable roots in each region.

To determine the roots tendency as the vector $\boldsymbol{k}$ deviates from the curve $\mathcal{T}$, one starts by introducing some notions. A stability crossing curve $\mathcal{T}_i$ for $i \neq 0$ is generated by $\boldsymbol{k}(\omega)$ for all $\omega \in \Omega_i$, therefore one defines as *positive direction* of $\mathcal{T}_i$ the direction of the curve

$\boldsymbol{k}(\omega)$ that corresponds to increasing ω's. Fig. 2.2 illustrates a positive direction when ω increase from $\frac{\pi}{\tau}(i-1)$ to $\frac{\pi}{\tau}i$.

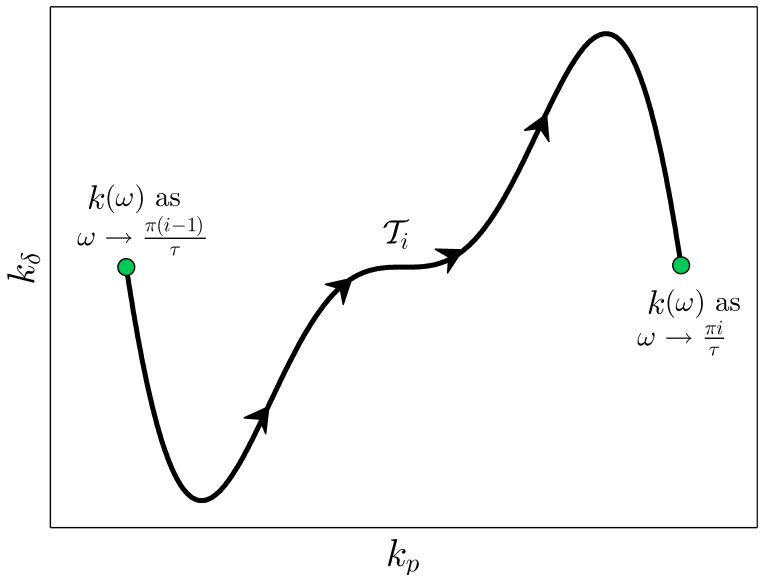

Figure 2.2: Positive Direction Convention of $\mathcal{T}_i$.

Remark 6. *Recall the geometric approach of the* basis orientation *in* $\mathbb{R}^2$ *from linear algebra (for further details, see [12]). Let* $\boldsymbol{u} := [u_1, u_2]^T$ *and* $\boldsymbol{v} := [v_1, v_2]^T$ *be vectors of* $\mathbb{R}^2$*, and* $\mathcal{B}$ *be a basis on* $\mathbb{R}^2$ *on the field* $\mathbb{R}$*, defined as:*

$$\mathcal{B} := \{\boldsymbol{u}, \boldsymbol{v}\} = \left\{[u_1, u_2]^T, [v_1, v_2]^T\right\}.$$

$\mathcal{B}$ *is said to be positively oriented if the shortest path from* $\boldsymbol{u}$ *to* $\boldsymbol{v}$ *is in the counterclockwise direction, and is said to be negatively oriented if the shortest path from* $\boldsymbol{u}$ *to* $\boldsymbol{v}$ *is in the clockwise direction. Then,* $\mathcal{B}$ *is positively oriented if and only if the following condition holds:*

$$\det[\boldsymbol{u}\ \boldsymbol{v}] = u_1 v_2 - u_2 v_1 > 0. \tag{2.13}$$

Furthermore, $\mathcal{B}$ *is negatively oriented if and only if the inequality* (2.13) *is reversed.*

Proposition 9. *[31, 28]-Let* $\tau \in \mathbb{R}_+$ *be a fixed delay, and consider the set of all stability crossing curves* $\mathcal{T}_i$*,* $\forall i \in \mathbb{N}$*. Then a pair of roots of* (2.5) *crosses from the LHP to the RHP of the complex plane as* $\boldsymbol{k}$ *traverses a stability crossing curve* $\mathcal{T}_i$ *from left to right with respect to the positive direction of* $\mathcal{T}_i$ *if* i *is even. Furthermore, the crossing is reversed if* i *is odd.*

Observe that Proposition 9 does not give any information about the crossing when $i = 0$. The following result fills this gap.

Proposition 10. *[31, 28]-Given a fixed delay* $\tau \in \mathbb{R}_+$*. Then, one root of* (2.5) *crosses from the LHP to the RHP of the complex plane through the origin as* $\boldsymbol{k}$ *crosses* $\mathcal{T}_0$ *from*

left to right if the intersection of $\boldsymbol{k}$ *and* $\mathcal{T}_0$ *is located at the left of the point* $\boldsymbol{k}_0 \in \mathcal{T}_0$*, defined by:*

$$\boldsymbol{k}_0 := [k_{p_0}, k_{\delta_0}]^T = \left[\frac{p_1 q_0 - (\tau q_0 + q_1)p_0}{\tau p_0^2}, \frac{p_0 q_1 - q_0 p_1}{\tau p_0^2}\right]^T.$$

Furthermore, the crossing of the root is from the RHP to the LHP if the intersection is located at the right of $\boldsymbol{k}_0$*.*

As in the case of stability crossing curves, additional considerations must be taken into account when G is an even function. Such a situation is considered below:

Proposition 11. *[31, 28]-Let* $\tau \in \mathbb{R}_+$ *be a fixed delay and* G *an even function. Then, as* $\boldsymbol{k}$ *crosses in any direction from the left side to the right side of* $\mathcal{T}_\ell$*,* $\ell \in \mathbb{N}$ *through the point* $\hat{\boldsymbol{k}} := [\hat{k}_p, \hat{k}_\delta]^T \in \mathcal{T}_\ell$*, a pair of roots of* (2.5) *crosses from the LHP to the RHP of the complex plane, if* $\hat{\boldsymbol{k}}$ *satisfies the following conditions:*

$$\hat{k}_\delta > 0 \text{ for } \ell \text{ even}, \qquad \hat{k}_\delta < 0 \text{ for } \ell \text{ odd}.$$

Furthermore, the crossing of the roots is from the RHP to the LHP if these inequalities are reversed.

2.1.3 Algorithm Construction

Based on the crossing directions obtained in the previous section, one presents first, a conceptual example explaining these results and secondly, a novel algorithm aiming at finding the invariant number of roots η (stability index) of a given region of the parameters space. As stated in Propositions 9-10, one refers to a *positive crossing* of $\boldsymbol{k}$ over $\mathcal{T}_i$, if the direction of $\boldsymbol{k}$ coincides with the positive direction. Otherwise, one says that one has a *negative crossing* of $\boldsymbol{k}$. Moreover, one defines the numbers $\eta, \eta_0 \in \mathbb{N}_+ \cup \{0\}$, as the number of roots in the RHP, of the closed-loop system and of the open-loop system, respectively.

Example 4 ([31, 28]-Conceptual example)**.** *Let* $\tau \in \mathbb{R}_+$ *be a fixed value, and consider the particular case where* $Q(i\omega) \neq 0$ *for all* $\omega \in \Omega \cup \{0\}$*. Fig. 2.3 shows a possible scenario for the problem of stabilization of the closed-loop system in the* k_p*-*k_δ *parameters plane, where, as mentioned above, the arrows of the stability crossing curves* $\mathcal{T}_i$ *indicate the positive direction of* $\mathcal{T}_i$*.*
In order to analyze the stability of each region in the k_p*-*k_δ *parameters plane, one computes first the number* η *of each region by analyzing the crossing directions as one varies the controller gains* $\boldsymbol{k}$ *continuously from* A *to* F*, as shown in Fig. 2.3. From* (2.5) *it can be seen that at the origin of the* k_p*-*k_δ *parameters plane, the roots of this function are the same as the roots of the open-loop system, that is, the roots of* $Q(s)$*. Therefore,* $\eta = \eta_0$ *for* $\boldsymbol{k} = [0, 0]^T$*, which corresponds to the point* A *as depicted in Fig. 2.3.*
The rest of the analysis concerns to describe how the characteristic roots behave by means of a continuous controller's parameters variation from A *to* F*. All controller's choices* $A - F$ *represent a crossing point, how the roots deviate to the LHP of the complex plane is summarized in Table 2.1, accordingly to Propositions 9 and 10. Each type of crossing*

through $\mathcal{T}_i$ is indicated according to the positive direction of $\mathcal{T}_i$ for $i \neq 0$, and to the point $\boldsymbol{k}_0$ of $\mathcal{T}_0$ for $i = 0$ (see, Proposition 10). Furthermore, η_- and η_+ denote the numbers of roots in the RHP of the complex plane in the previous and future region as $\boldsymbol{k}$ crosses $\mathcal{T}_i$. Observe also from Fig. 2.3, that the only plausible scenario corresponds to the case when

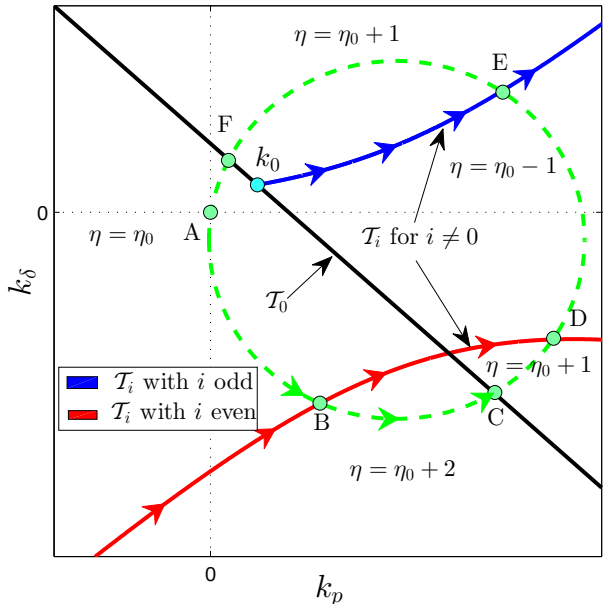

Figure 2.3: Conceptual Example of a Stability analysis Using Stability Crossing Curves.

Table 2.1: Crossing Directions Analysis of the Conceptual Example

Point	Type of crossing through $\mathcal{T}_i$	i	Position related to $\mathbf{k_0}$	$k-$direction	η_-	η_+
B	left to right	even		$+$	η_0	$\eta_0 + 2$
C	left to right	0	to the right	$-$	$\eta_0 + 2$	$\eta_0 + 1$
D	right to left	even		$-$	$\eta_0 + 1$	$\eta_0 - 1$
E	right to left	odd		$+$	$\eta_0 - 1$	$\eta_0 + 1$
F	right to left	0	to the left	$-$	$\eta_0 + 1$	η_0

$\eta_0 \geq 1$, since η cannot be a negative number. Moreover, the only scenario in which one could have a stability region in the section of the $k_p - k_\delta$ parameters plane, is the one in which $\eta_0 = 1$.

Let $\boldsymbol{k}^* := [k_p^*, k_\delta^*]^T$ denote a point on the k_p-k_δ parameters plane such that $\boldsymbol{k}^* \notin \mathcal{T}_i$ for $i \in \mathbb{N} \cup \{0\}$. One proposes a linear path for $\boldsymbol{k}$ from the origin (at which $\eta = \eta_0$) to $\boldsymbol{k}^*$. The set Ω_s denote all $\omega \in \Omega$ for which $\boldsymbol{k}(\omega)$ intersects the vector $\boldsymbol{k}^*$. This set corresponds to all $\omega \in \Omega$ such that the following equation holds:

$$k_p^* k_\delta(\omega) - k_\delta^* k_p(\omega) = 0,$$

and satisfies at least one of the following conditions:

$$0 < \frac{k_p(\omega)}{k_p^*} < 1, \qquad 0 < \frac{k_\delta(\omega)}{k_\delta^*} < 1.$$

Observe that there can only be one intersection between $\mathbf{k}^*$ and $\mathcal{T}_0$. This intersection exists if and only if (2.7) holds for $\boldsymbol{k} = \alpha \boldsymbol{k}^*$ where $\alpha \in (0, 1)$. This leads to the definition of the indicative function $\mathcal{I}_\alpha$ as follows:

$$\mathcal{I}_\alpha := \begin{cases} 1 \quad if \quad \alpha \in (0,1), \\ \\ 0 \quad if \quad \alpha \notin (0,1), \end{cases}$$

where α is computed as:

$$\alpha = -\frac{q_0}{p_0} \frac{1}{k_p^* + k_\delta^*}.$$

The indicative function $\mathcal{I}_\alpha$ establishes the existence of an intersection between $\boldsymbol{k}^*$ and $\mathcal{T}_0$ if and only if $\mathcal{I}_\alpha = 1$. Note that the stability crossing curve $\mathcal{T}_i$ for $i \in \mathbb{N} \cup \{0\}$ may cross at the origin of the parameters space. That situation is related to the possible roots on the imaginary axis of the open-loop characteristic equation. Such a case must be treated separately, and for that reason one defines the set Ω_t as the set of all $\omega \in \mathbb{R}_+ \cup \{0\}$ where $Q(i\omega) = 0$. Let $\mathcal{R}^* \subset \mathbb{R}^2$ denote the region where $\boldsymbol{k}^*$ is located. Finally, using Remark 6, one constructs the functions ∇ and ∇_0 defined as:

$$\nabla_0(\boldsymbol{k}^*) := \operatorname{sgn}\left\{k_{p_0} k_\delta^* - k_p^* k_{\delta_0}\right\}, \qquad \nabla(\boldsymbol{k}^*, \omega) := (-1)^{\left\lceil \frac{\tau}{\pi}\omega \right\rceil} \operatorname{sgn}\left\{k_p^* k_\delta'(\omega) - k_p'(\omega) k_\delta^*\right\},$$

where $k_p'(\omega)$ and $k_\delta'(\omega)$ stand for the derivatives of $k_p(\omega)$ and $k_\delta(\omega)$ with respect to ω, respectively. One has the following result:

Proposition 12 ([31, 28]-Stability index determination algorithm)**.** *Let G be a non even function with $\deg Q > \deg P$, $\tau \in \mathbb{R}_+$ be a fixed value and let $\boldsymbol{k}^* := [k_p^*, k_\delta^*]^T \in \mathcal{R}^* \subset \mathbb{R}^2$ such that $\boldsymbol{k}^* \notin \mathcal{T}_i, \forall i \in \mathbb{N} \cup \{0\}$. For $f(i\omega) := G^{-1}(i\omega)$ assume that the following condition holds:*

$$-\Im\left\{f\left(i\omega\right)\right\} + \frac{1}{\tau}\Re\left\{f'\left(i\omega\right)\right\} \neq 0, \quad \forall \omega \in \Omega_s.$$

If $\Omega_t = \emptyset$, then, $\forall \boldsymbol{k} \in \mathcal{R}^*$ the number of roots η on the RHP of the complex plane of (2.5) can be computed by:

$$\eta = \eta_0 + \mathcal{I}_\alpha \nabla_0\left(\boldsymbol{k}^*\right) + 2\sum_{\omega \in \Omega_s} \nabla(\boldsymbol{k}^*, \omega).$$

Furthermore, if $\Omega_t \neq \emptyset$, then $\forall \boldsymbol{k} \in \mathcal{R}^*$ the number of roots $\tilde{\eta}$ on the RHP of the complex

plane of (2.5) *is given by:*

$$\tilde{\eta} = \eta + \sum_{\omega\in\Omega_t}\left\{\frac{(1-\operatorname{sgn}(\omega))(\nabla_0(\boldsymbol{k}^*)+1)+2\operatorname{sgn}(\omega)(\nabla(\boldsymbol{k}^*,\omega)+1)}{2}\right\}.$$

Remark 7. *It is noteworthy that although Proposition 12 is restricted to non even open-loop systems and non neutral closed-loop systems, it can be easily extended using the ideas introduced in Section 2.1.2 and Proposition 6, respectively.*

2.1.4 Illustrative Examples

In order to illustrate the effectiveness of the proposed results, one considers several numerical examples.

Example 5 ([31, 28]-Marginally stable fourth-order system)**.** *Consider a system with the following transfer function:*

$$G(s) = \frac{0.038}{s^4 + 0.1276s^3 + 9.3364s^2 + 1.1484s + 3.0276},$$

subject to the P-δ controller $C(s) = k_p + k_\delta e^{-\tau s}$*. The open-loop poles of the system are located at* $s = -0.0638 \pm 0.5765j$ *and* $s = \pm 3j$*, which means that the system is* marginally stable. *In order to illustrate the proposed results, let consider a fixed delay* $\tau = 5$*. According to Proposition 3, one has:*

$$\begin{aligned} k_p(\omega) &= \left(3.35789\omega^2 - 30.2211\right)\omega\cot(\tau\omega) - 26.3158\omega^4 + 245.695\omega^2 - 79.6737, \\ k_\delta(\omega) &= \omega\left(30.2211 - 3.35789\omega^2\right)\csc(\tau\omega). \end{aligned}$$

Considering (2.14) *along with Propositions 3 and 5, one obtains the stability crossing curves depicted in Fig.2.4 (left). Now, as can be seen in figure 2.4 (right) with the purpose to discriminate unstable regions avoiding unnecessary computations, one plots the* $\mathcal{T}_u-$*curve by applying Proposition 7. Next, in order to find the stability regions, one applies Proposition 12, leading to the result illustrated in Fig. 2.4 (right). To illustrate how Proposition 12 is applied, let us consider three points* $\boldsymbol{k}_1^*$*,* $\boldsymbol{k}_2^*$ *and* $\boldsymbol{k}_3^*$ *on the parameters space. The results are summarized in table 2.2.*

Table 2.2: Stability Index Algorithm-Marginally Stable Fourth-Order System.

Point	k_p	k_δ	$\mathcal{I}_\alpha$	Ω_t	Ω_s	$\nabla, \omega \in \Omega_t, \Omega_s$	η_0	η
$\boldsymbol{k}_1^*$	400	200	0	$\{1.3278, 2.5451\}$	$\{3\}$	$\{1,1\}$,$\{-1\}$		4
$\boldsymbol{k}_2^*$	350	-25	0	$\{\emptyset\}$	$\{3\}$	$\{0\}$,$\{1\}$	0	2
$\boldsymbol{k}_3^*$	500	-200	0	$\{0.8395, 1.2150, 1.9358\}$	$\{3\}$	$\{1,-1,1\}$,$\{1\}$		4

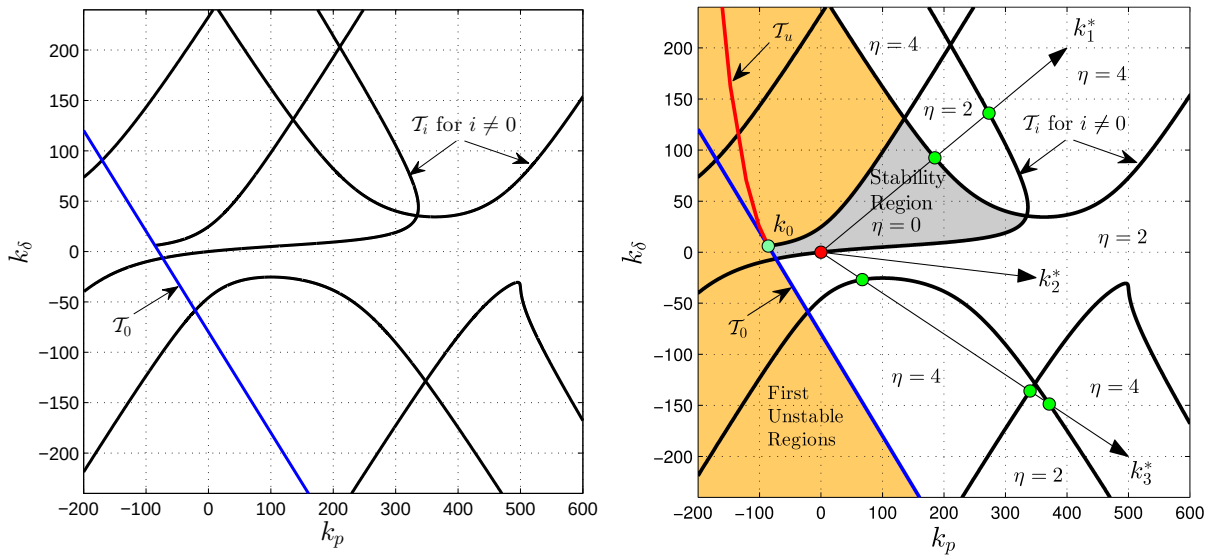

(a) Stability Crossing Curves

(b) Stability Regions.

Figure 2.4: Marginally Stable Fourth-Order System.

Example 6 ([31, 28]-Neutral-type system)**.** *Consider a system with the following transfer function:*

$$G(s) = \frac{s^6 - 5s^5 + 20s^4 - 10s^3 + 5s + 1}{s^6 + s^4 + 4s^3 + 7s^2 + 9s + 1}.$$

One proposes a fixed delay $\tau = 0.5$ for the stabilization of the closed-loop system using a P-δ controller. It is clear that this system is of neutral type since $\deg Q = \deg P$*. Therefore, in order to characterize all possible stability crossing curves, one must consider the result shown in Proposition 6 in addition to the Propositions 3 and 5. Notice that all the points of the k_p-k_δ parameters plane which do not satisfy the condition proposed in Proposition 6 implies that the closed-loop system is unstable. Fig. 2.5 shows the application of this result denoted as the neutral type condition.*

Finally, in order to characterize each region bounded by the stability crossing curves, one uses the stability analysis algorithm proposed in Proposition 12 for at least one point in each region which does not satisfy the neutral type condition. Fig. 2.5 illustrate the application of this proposition for three points $\boldsymbol{k}_i^*$, with $i \in \{1, 2, 3\}$. The results of each analysis are summarized in table 2.3 and illustrated in Fig 2.5.

Table 2.3: Stability Index Algorithm: *Neutral-Type* System.

Point	k_p	k_δ	$\mathcal{I}_\alpha$	Ω_t	Ω_s	∇_0	∇	η_0	η
$\tilde{\mathbf{k}}_1^*$	2	2	1		$\{0.9002, 3.1862\}$	-1	$\{-1, -1\}$		0
$\tilde{\mathbf{k}}_2^*$	2	0.5	1	$\{\emptyset\}$	$\{0.8357\}$	-1	$\{-1\}$	5	2
$\tilde{\mathbf{k}}_3^*$	1.5	-1.5	0		$\{0.4982\}$		$\{-1, -1\}$		3

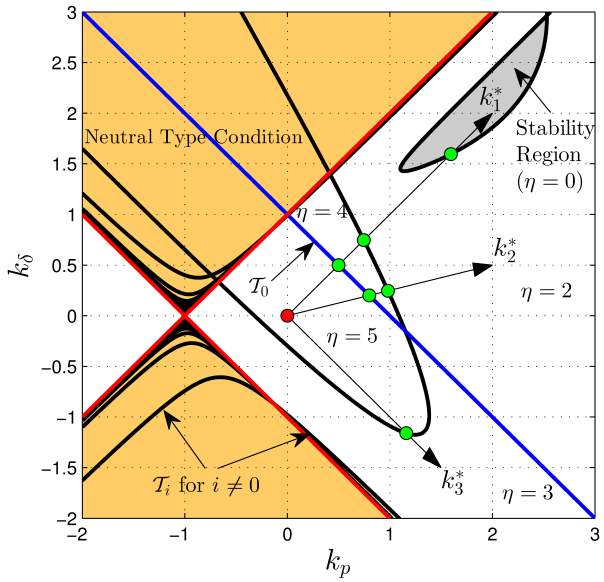

Figure 2.5: Algorithm Example - Neutral type system.

Example 7 ([31, 28]-Even-type system)**.** *Consider the following system presented in [52]:*

$$G(s) = \frac{1}{s^2 + 1}.$$

This system is an even-type *system, these can be easily verified by substituting $s = i\omega$ in the transfer function shown above. Therefore, it must be analyzed by using the results shown in section 2.1.1. One proposes a fixed delay $\tau = 1$ for the stabilization of the closed-loop system using a P-δ controller.*
The construction of the stability crossing curves *$\mathcal{T}_0$, $\mathcal{T}_{p_\ell}$ and $\mathcal{T}_i$ is obtained using Propositions 5 and 4 and the crossing directions analysis is computed by the Propositions 9 and 11. Fig. 2.6 illustrates the behavior of the roots when $\boldsymbol{k}$ varies continuously from the point A to the point F. Notice that the starting point A corresponds to the characteristic equation of the open loop system, and consequently, at this point this equation has two roots on the imaginary axis. The results of this analysis can be found in table 2.4.*

Table 2.4: Stability Analysis: Even Function Example.

Point	**Type of crossing through $\mathcal{T}_i$**	i	ℓ	**Position related to k_δ**	$k-$**direction**	η_-	η_+
A	left to right	odd			$-$		0
B	left to right		odd	< 0	$+$	0	2
C	right to left	even			$-$	2	0
D	left to right		even	> 0	$+$	0	2
E	right to left		odd	> 0	$+$	2	4
F	right to left		even	> 0	$-$	4	2

In order to study the stability of the closed-loop system along the k_p-k_δ parameters plane, this type of analysis can be easily extended as shown in Fig. 2.6. Furthermore, one studies three particular stability regions *by analyzing the explicitly the behavior of these regions as τ is varied from* 1 *to* 3.5 *as shown in Fig. 2.7. Bearing in mind Remark 1, all the points inside this geometric shape stabilize the closed-loop system for any fixed value τ in the interval* $[1, 3.5]$.

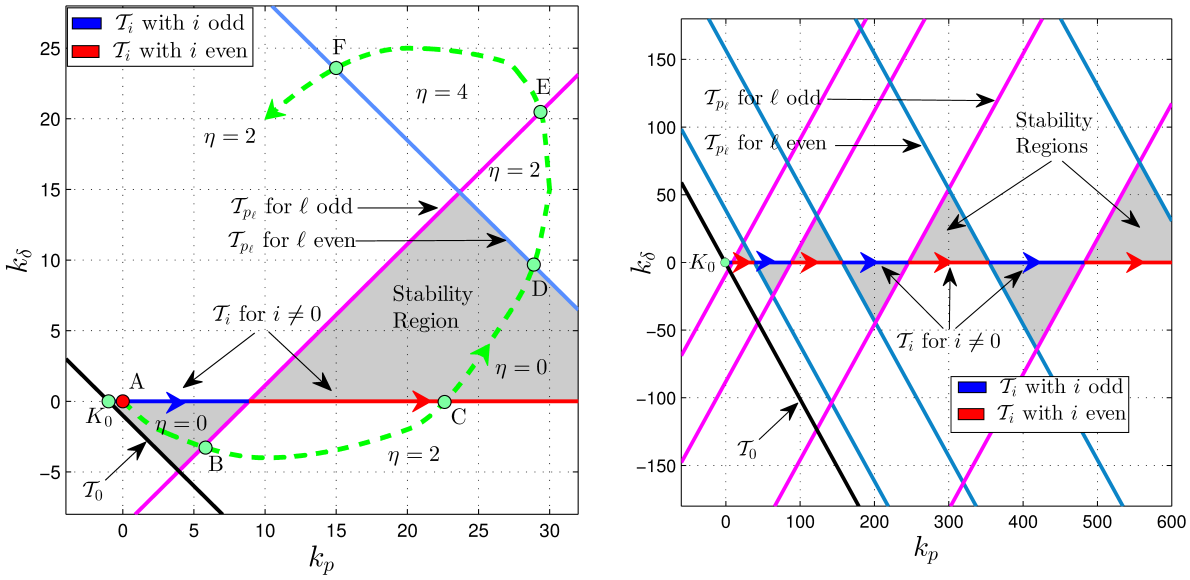

Figure 2.6: Stability Analysis - Even Function Example.

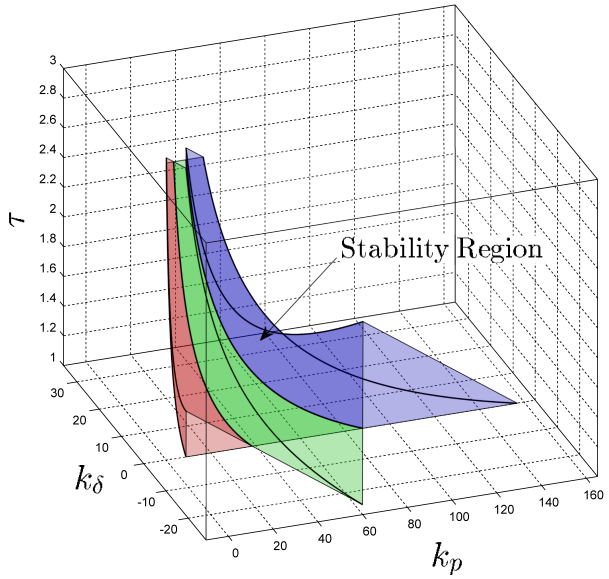

Figure 2.7: Stability Region Behavior Through the τ-Axis - Even Function Example.

Example 8 ([31, 28]-Unstable second-order system)**.** *In order to illustrate the case analyzed in Proposition 8, that is, the case where exists an infinite number of multiple crossing*

frequencies (for different gain parameters), let us consider the following second-order system:

$$G(s) = \frac{1}{-s^2 + s + 1}. \tag{2.15}$$

Now, since condition (2.12) *is fulfilled, i.e.,*

$$\frac{\Im\{f(i\omega)\}}{\Re\{f'(i\omega)\}} = \frac{1}{2} > 0,$$

according to Proposition 8, one has that system (2.15) *has an infinite but countable crossing frequencies of multiplicity $m \geq 2$, if one chooses $\tau = 2$. Then, in order to illustrate such a phenomenon, ne takes the linear path $\overrightarrow{\boldsymbol{k}}$ shown in figure 2.8 (left). The rightmost root-locus is depicted in figure 2.8 (right), where one can appreciate the multiplicity of the crossing frequency. Finally, others points corresponding to a multiple crossing frequencies are indicated by the "square points".*

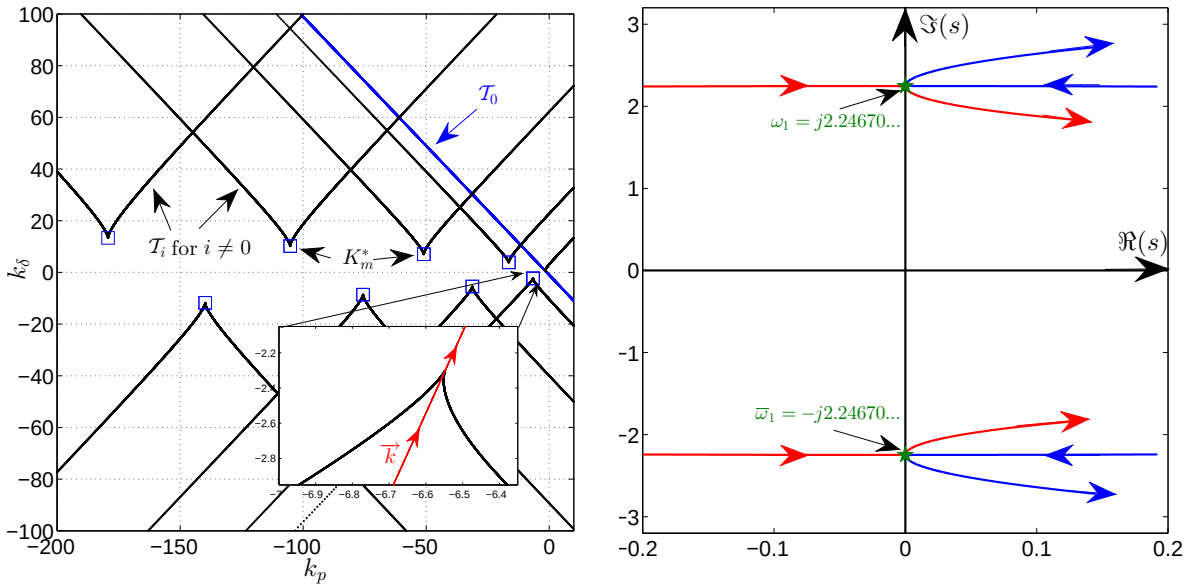

(a) Stability Crossing Curves

(b) Crossing Roots Deviation

Figure 2.8: Marginally Stable Fourth-Order System.

2.2 σ-Instability Methodology: PI and PD inspired Delay-Based Controllers

Consider the classical control scheme shown in Fig. 2.1, where the application of a delay-based controller $C(s, e^{-\tau s})$ is illustrated. Considering such scheme, one formulates the problematics listed below:

Problem 2. *Find explicit conditions on the parameters* $(\tau, k_p, k_\delta) \in \mathbb{R}_+ \times \mathbb{R}^2$*, such that the* PD^δ *controller*(1.7)*:*

$$C_\delta(s) = k_p + k_\delta \frac{1 - e^{-\tau s}}{\tau},$$

asymptotically stabilizes the closed-loop system.

Problem 3. *Find explicit conditions on the parameters* $(\tau, k_p, k_i) \in \mathbb{R}_+ \times \mathbb{R}^2$*, such that the* $P\delta I$ *controller* (1.8)*:*

$$C_i(s) = k_p + k_i \frac{e^{-\tau s}}{s},$$

asymptotically stabilizes the closed-loop system.

2.2.1 σ-Instability: Main Remarks

In this section one presents the spirit of the σ instability methodology. Without any loss of generality one considers both controllers ($C_\delta(s)$ and $C_i(s)$) as $C(s, e^{-\tau s})$ with its respective gains $\boldsymbol{k} \in \mathbb{R}^2$ ($\boldsymbol{k}_\delta$ and $\boldsymbol{k}_i$). Consider the classical control scheme shown in Fig. 2.1. The characteristic equation of this closed-loop scheme rewrites as follows:

$$\Delta_\tau(s) = C(s, e^{-\tau s}) + G^{-1}(s) = 0. \tag{2.16}$$

It is well known that, in order to achieve asymptotic stability, all the roots of (2.16) have to remain in the LHP of the complex plane.

Now, let $\tau \in \mathbb{R}_+$ and $\sigma \in \mathbb{R}_+ \cup \{0\}$ be fixed values, one introduces the following set:

$$\mathcal{T}(\sigma) := \left\{ \boldsymbol{k} \in \mathbb{R}^2 \,|\Delta_\tau(\sigma + i\omega) = 0, \forall \omega \in \Omega \right\},$$

with $\Omega \subset \mathbb{R}_+$, which is the set of all ω values such that $\Delta_\tau(\sigma + i\omega) = 0$ for a fixed pair (τ, σ). Such a set of frequencies is characterized in Propositions 13 and 14 considering the PD^δ and $P\delta I$ controller, respectively. Roughly speaking, the set $\mathcal{T}(\sigma)$ contains all gain vectors k such that the characteristic equation of the closed-loop system has at least one root on a vertical line in σ on the complex plane. In other words, Ω includes all the frequencies for which the gains $k \in \mathbb{R}^2$ define some crossing points, that is, points located in the complex plane on the line $\Re\{s\} = \sigma$.

With this notation, it is clear that all possible gain vectors k such that the system has at least one root in the RHP (right-half plane) or in the imaginary axis of the complex plane can be characterized by:

$$\bar{\mathcal{T}}^+ := \bigcup_{\sigma \in \mathbb{R}_+ \cup \{0\}} \mathcal{T}(\sigma).$$

Therefore, all stabilizing controllers k are contained in the following set:

$$\bar{\mathcal{T}}^- := \mathbb{R}^2 \setminus \bar{\mathcal{T}}^+.$$

It is worthy to notice that one focuses in a particular region of the parameters-space of k. This process is explained below.

First of all, it is necessary to enhance the importance of the set $\mathcal{T}(0)$. This set contains all possible gain vectors k such that the characteristic equation (2.16) has at least one root on the imaginary axis. That is the set of all crossing points, in other words, $\mathcal{T}(0)$ is nothing else that the so-called "stability crossing curves" (see, e.g. [52], for the definition). Bear in mind the fact that any continuous variation of k such that $k \notin \mathcal{T}(0)$ implies that no roots exchange through the imaginary axis can be achieved. It is easy to observe how these *stability crossing curves* partition the parameters-space in regions in which any choice of k implies that (2.16) has a finite number of roots on the RHP of the complex plane.

Second, notice that if some element of $\mathcal{T}(\sigma)$ with $\sigma > 0$ is located inside one of this regions implies that the characteristic equation (2.16) has at least one unstable root in the RHP of the complex plane. Therefore, this can be labeled as an *unstable region*. Finally, any region which is not unstable is a subset of $\bar{\mathcal{T}}^-$ and can be labeled as a *stability region*.

2.2.2 PD^δ Controller Design

Consider the control scheme shown in Fig. 2.1, using the PD^δ controller shown in (1.7). The corresponding control law to be applied can be described as:

$$u(t) = k_p e(t) + k_\delta \left(\frac{e(t) - e(t-\tau)}{\tau} \right).$$

Notice that the delayed action resembles the simplest approximation of a derivative given by the Euler approximation (1.6) previously discussed in the Introduction. Roughly speaking, for small values of τ this controller approximates to a classical PD controller as:

$$C_d(s) = k_p + k_\delta s \approx C_\delta(s).$$

In order to study its stability, the characteristic equation of the closed-loop system can be computed by:

$$C_\delta(s)G(s) + 1 = 0,$$

which straightforwardly lead us to:

$$\Delta_\delta(s) = k_p + k_\delta \left(\frac{1 - e^{-\tau s}}{\tau} \right) + G^{-1}(s) = 0. \tag{2.17}$$

The following result shown in this section works as a tool for describing the behavior of the roots of this equation.

Proposition 13. *Let $\tau \in \mathbb{R}_+$ and $\sigma \in \mathbb{R}$ be fixed values. Then, the characteristic equation*

(2.17) *has at least one root in* $s = \sigma + i\omega$*, iff:*

$$\begin{aligned} k_p &= \Re(\sigma,\omega) + \left(e^{-\tau\sigma}\csc(\tau\omega) - cot(\tau\omega)\right)\Im(\sigma,\omega), \\ k_\delta &= -\tau e^{\tau\sigma}\csc(\tau\omega)\Im(\sigma,\omega). \end{aligned}$$

with $\omega \in \Omega_\delta$ *where the set* Ω_δ *is defined by:*

$$\Omega_\delta := \left\{ \omega \in \mathbb{R} \,\middle|\, \omega \neq \frac{\pi}{\tau}n, \quad P(\sigma + i\omega) \neq 0 \right\},$$

where $n \in \mathbb{Z}$*. Furthermore, it has a single root in* $s = \sigma$ *iff* $P(\sigma) \neq 0$ *and:*

$$k_\delta = \frac{\tau}{e^{-\tau\sigma} - 1}\left(k_p + G^{-1}(\sigma)\right), \quad \textit{for} \quad \sigma \neq 0, \tag{2.20}$$

$$k_p = -\frac{q0}{p0}, \quad k_\delta \in \mathbb{R}, \quad \textit{for} \quad \sigma = 0. \tag{2.21}$$

Proof. Consider the characteristic equation (2.17) with $s = \sigma + i\omega$. Taking the real and imaginary parts gives the following:

$$\Re\left[\Delta_\delta(\sigma + i\omega)\right] = 0, \quad \Im\left[\Delta_\delta(\sigma + i\omega)\right] = 0,$$

which leads to the system of equations:

$$\frac{1}{\tau}\begin{bmatrix} \tau & 1 - e^{-\tau\sigma}\cos(\tau\omega) \\ 0 & 1 - e^{-\tau\sigma}\sin(\tau\omega) \end{bmatrix}\begin{bmatrix} k_p \\ k_\delta \end{bmatrix} = -\begin{bmatrix} \Re(\sigma,\omega) \\ \Im(\sigma,\omega) \end{bmatrix}.$$

By solving this system for k_p and k_δ one gets directly (2.18). Now, considering $s = \sigma \neq 0$ and $s = 0$ the conditions above lead directly to (2.20) and (2.21), respectively. Finally, the set Ω_δ is constructed to avoid discontinuities in the solutions of the studied equations. □

2.2.3 $P\delta I$ Controller Design

Consider the control scheme shown in Fig. 2.1 using the $P\delta I$ controller shown in (1.8). The control law corresponding to this scheme can be described by:

$$u(t) = k_p e(t) + k_i \int_0^t e(v - \tau)dv.$$

Notice that this is basically a classical PI controller in which the error signal is delayed a finite constant amount of time τ before integrating it. As mentioned before, the main reason for adding this delayed action to this controller is to study the behavior of the closed-loop response as τ is varied. In other words, to have an extra degree of freedom in the tuning of a PI-alike controller.

In order to study its stability, the characteristic equation of the closed-loop system rewrites as:

$$C_i(s)G(s) + 1 = 0,$$

which straightforwardly lead us to:

$$\Delta_i(s) = s\left(k_p + G^{-1}(s)\right) + k_i e^{-\tau s}. \tag{2.22}$$

The following result summarized in this section works as tools for describing the behavior of the roots of this equation.

Proposition 14. *Let $\tau \in \mathbb{R}_+$ and $\sigma \in \mathbb{R}$ be fixed values. Then, the characteristic equation* (2.22) *has at least one root in $s = \sigma + i\omega$, iff:*

$$\begin{aligned} k_p &= -\Re(\sigma,\omega) + \frac{\omega\sin(\tau\omega) - \sigma\cos(\tau\omega)}{\sigma\sin(\tau\omega) + \omega\cos(\tau\omega)}\Im(\sigma,\omega), \\ k_i &= \frac{\sigma^2 + \omega^2}{\sigma\sin(\tau\omega) + \omega\cos(\tau\omega)}\Im(\sigma,\omega)e^{\tau\sigma}, \end{aligned}$$

with $\omega \in \Omega_i$ where the set Ω_i is defined by:

$$\Omega_i := \{\omega \in \mathbb{R} \,|\omega\cot(\tau\omega) + \sigma \neq 0, \quad P(\sigma + i\omega) \neq 0\},$$

where $n \in \mathbb{Z}$. Furthermore, it has a single root in $s = \sigma$ iff $P(\sigma) \neq 0$ and:

$$k_i = -\sigma\left(k_p + G^{-1}(\sigma)\right)e^{\tau\sigma}.$$

Proof. The proof follows similar lines that the proof of Proposition 13 and, for the sake of brevity it is omitted. □

Furthermore, one presents an additional proposition for computing the stabilizing interval of the delay value given a stabilizing triplet (k_p, k_i, τ).

Proposition 15. *Let (k_p, k_i, τ^*) be a stabilizing triplet, then, the closed-loop system is asymptotically stable for any delay value $\tau \in [\tau^*, \tau_c)$, where:*

$$\tau_c = \min\{\tau \in \mathbb{R} \,|\tau(\omega^*) > 0, \omega^* \in \Omega_p\}, \tag{2.25}$$

in which $\tau(\omega^*)$ is computed as:

$$\tau(\omega^*) = \frac{1}{\omega^*}\left[\arg\left\{\frac{k_i P(i\omega^*)}{i\omega^*(k_p P(i\omega^*) + Q(i\omega^*))}\right\} + (2n+1)\pi\right], \tag{2.26}$$

for $n \in \mathbb{Z}$ and where the set Ω_p is defined as the set of all real roots of the following equation:

$$|k_i P(i\omega^*)|^2 - \omega^{*^2}|k_p P(i\omega^*) + Q(i\omega^*)|^2 = 0. \tag{2.27}$$

Proof. By taking into account the fact that the closed-loop system is stable for $\tau = \tau^*$ implies that for $\tau > \tau^*$ sufficiently small all the roots of (2.22) will remain on the LHP of the complex plane. Moreover, there exists a critical value τ such that (2.22) has at least one root on the imaginary axis and hence, such a value induces the instability of the closed-loop system if the delay value increases.

Now, notice that the characteristic equation (2.22) can be rewritten as:

$$\Delta_\tau(s) := s(k_p P(s) + Q(s)) + k_i P(s) e^{-\tau s}.$$

As it can be seen in [50], there exists some value τ such that the quasi-polynomial $\Delta_\tau(s)$ has at least one root on the imaginary axis at $s = i\omega^*$, if and only if, the following condition:

$$\left| \frac{k_i P(i\omega^*)}{i\omega^*(k_p P(i\omega^*) + Q(i\omega^*))} \right| = 1, \tag{2.28}$$

holds for some value $\omega^* \in \mathbb{R}_+$. Moreover, the correspondent time-delay value can be computed by (2.26). Furthermore, notice that condition (2.28) can be rewritten easily as (2.27), which is a polynomial, implying that it has a finite number of solutions. Finally, by defining Ω_p as the set of all real roots of (2.27), the critical delay value can be computed as in (2.25). □

2.2.4 Illustrative Examples

In this section, one describes in detail how the methodology explained in Section 2.2.1 can be applied for two different examples of second-order systems using the PD^δ and $P\delta I$ controllers, respectively. On one hand, one studies an open-loop unstable system which suggests the application of a derivative action for its stabilization in closed-loop. On the other hand, one shows how the addition of the delayed action to the PI controller can inject damping to the closed-loop response. All graphical and simulation results presented in this section were derived by using the software "MatLab" in the programmable environment "Simulink".

Example 9. *Unstable Second-Order System Consider the following transfer function:*

$$G(s) = \frac{1}{s^2 - 3s + 5}, \tag{2.29}$$

which two poles lie on $s = 1.5 \pm 1.65i$. Since it has one root on the RHP of the complex plane, it is an unstable system. Now, lets consider the application of a PD controller, the characteristic equation of the closed-loop system can be computed as:

$$s^2 + (kd - 3)s + k_p + 5 = 0.$$

By Hurwitz criterion, it is easy to observe that in order to achieve closed-loop stability the application of a derivative action is mandatory so every coefficient has the same sign.

This is the case of a simple PD controller with $k_p > -5$ and $k_d > 3$. To avoid such a derivative action one proposes the use of the PD^δ controller in the following lines.

Considering the open-loop transfer function (2.29) *and the PD^δ controller shown in* (1.7) *the characteristic equation of the closed-loop system can be computed as:*

$$\Delta_\delta(s) = s^2 - 3s + 5 + k_p + k_\delta \left(\frac{1 - e^{-\tau s}}{\tau} \right) = 0.$$

Using Proposition 13 with a fixed delay value $\tau = 0.04s$ one computes the stability crossing curves *($\mathcal{T}(0)$) as some curves from the set (σ) with $\sigma > 0$. These graphical results are shown in Fig. 2.9 on the $k_p - k_\delta$ parameters-space. Recall that the* stability crossing curves *partition the parameters-space in regions with a fixed number of unstable roots, that implies that one of these regions could be a* stability region *with zero unstable roots. As shown in Fig. 2.9 one uses the curves from the set $\mathcal{T}(\sigma)$ with $\sigma > 0$ for discriminating the unstable region to finally find the* stability region.

Finally, in order to test this result one chooses three different controllers, being c_1 and c_2 stable and c_3 unstable controllers as is depicted in Fig. 2.9. Some simulation results using these controller parameters are shown in Fig. 2.9 by considering some unitary step as input reference. Also in this figure, one shows the closed-loop response of a PD controller using the same gains as the PD^δ controller ($(k_p, k_d) = (k_p, k_\delta)$). As expected, these results corroborate the graphical results on figure 2.9.

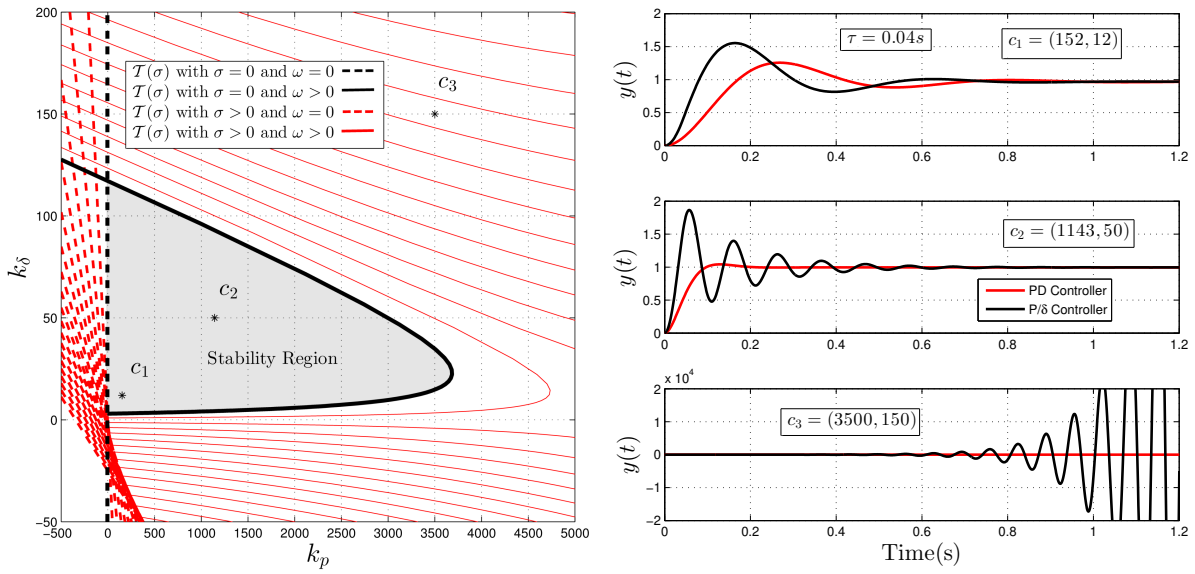

Figure 2.9: PD^δ Controller: Stability Analysis and Closed-Loop System Response Comparison

Example 10. *Closed-loop response manipulation through the delay value Consider the following open-loop transfer function:*

$$G(s) = \frac{1}{s^2 + 2s + 3}, \tag{2.30}$$

which poles has poles $s = -1 \pm 1.41i$. *In this stable open-loop system one is considering the problem of a controller design such that the steady state error is equal to zero. This can be easily achieved by a simple* PI *controller, however, as stated before one aims to use the delayed action to manipulate the closed-loop response.*

Considering the open loop transfer function (2.30) *and the* $PI\delta$ *controller shown in* (1.8) *the characteristic equation of the closed-loop system can be computed as:*

$$\Delta_\delta(s) = s^3 + 2s^2 + (3 + k_p)s + k_i e^{-\tau s} = 0.$$

Following the same methodology explained in the last example using a fixed delay $\tau = 0.5s$ *one finds a stability region as shown in Fig. 2.10. In a similar way, one tests its reliance with three different controllers,* c_4 *and* c_5 *stable controllers and* c_5 *a unstable one. Considering again a unitary step as reference input one shows some simulation results presented in Fig. 2.10 which corroborates this result in comparison to a simple* PI *controller* $\tau = 0$. *From this comparison, one can notice the damping added with controller* c_5 *relative to the controller* c_4 *and also to the simple* PI *controller. At last, one shows another way to tune the delayed action in the* $P\delta I$ *controller. Consider the* $P\delta I$ *gains* $(k_p, k_i) = (5, 5)$ *with* $\tau = 0$, *the roots of the characteristic equation are* $s_{1,2} = -0.64 \pm 2.58i$ *and* $s_3 = -0.7$. *Since this is a stable system, one considers Proposition 15 to compute the stabilizing delay interval* $\tau = (0, \tau_c)$, *obtaining* $\tau_c = 2.15s$. *Some simulation results depicting the continuous variation of the closed-loop response as* τ *is varied on this interval are presented in Fig. 2.11. In this figure, one can notice how from* $\tau = 0$ *to* $\tau = 0.2\tau_c$ *one is able to inject damping to the closed-loop response. Recall that this task is commonly achieved by the use of a derivative action which one is avoiding. Also in this figure, one shows the behavior of the closed-loop response as the other part of the interval is considered, leading as expected to instability.*

2.3 Concluding Remarks

In this chapter one studies three delay-based controllers ($P\delta$, $P\delta I$ and PD^δ controllers) and its application to LTI systems. Two different crossing roots based methodologies for computing stability regions on the parameters space are presented. A stability index computation algorithm based on computing crossing directions and the σ-instability method (first developed in this research) based on computing known unstable conditions. Illustrative examples on the application of these methods and also on the performance of these delay-based controllers are addressed. In the next chapter, one studies the design of a variety of control schemes for different applications making use of the these methods and its basic notions.

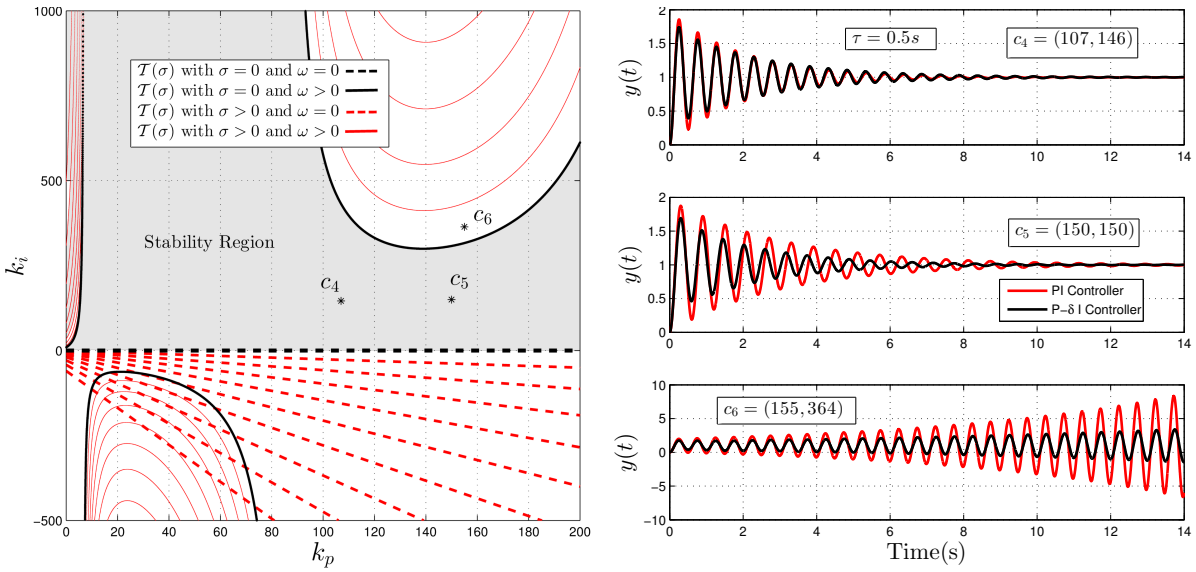

Figure 2.10: $PI\delta$ Controller: Stability Analysis and Closed-Loop System Response Comparison

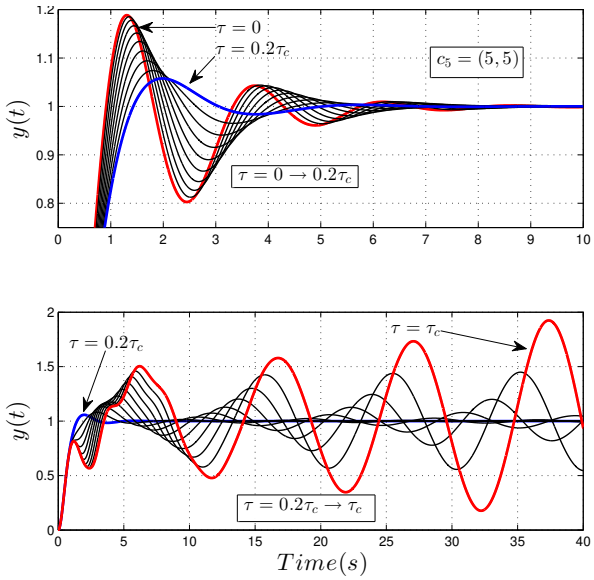

Figure 2.11: $P\delta I$ Controller: Closed-Loop System Response with $\tau \in (0, \tau_c)$

Chapter 3

Delay-Based Control Design: Applications

Three different delay-based control schemes are presented. First, we show a bilateral control scheme based on $P\delta$ controllers applied in two different setups: a haptic-virtual system and a haptic master-slave system. In a similar spirit to a teleoperated system these are designed to synchronize two robotic devices or a real/physical one and a virtual one. in order to create a feeling of virtual (or remote) interaction. Experimental results are shown and discussed. Second, one studies the application of the $P\delta I$ controller to a Buck DC/DC converter. This is straightforwardly an output regulation problem. Numerical results are depicted and interesting remarks concerning the role and impact of the time-delay value are addressed. Third and lastly, one studies the rotatory inverted pendulum better known as the Furuta pendulum by considering a time-delay in the control input. Such a delay is studied as inherent to the control scheme application and/or as an extra control parameter. Illustrative numerical results are presented.

In all studies found in this chapter one takes a look at the stability of the closed-loop system and its performance. To this end, one derives an understanding of the location pf the characteristic quasi-polynomial roots with respect to the controller's parameters and delays. All these analysis are developed In the same spirit of Chapter 2 by using crossing roots theory.

3.1 Haptic Systems: $P\delta$ Bilateral Control Scheme

In this section, one can find the experimental application of the $P\delta$ controller to two different mechanical applications. Particularly, one discusses some experimental results on the use of haptic devices (see Fig. 3.7) in two different settings: an haptic-virtual system and a master-slave teleoperation system. The design methodology used in both cases is directly related to the ideas shown in Section 2.1 but applied to a bilateral control scheme. Such a derivation is not shown in this section and for better understanding the details regarding this particular delay-based control scheme one can do it in [27] and [32].

In these studies one can find a careful analysis carried-out for tunning the parameters of the $P\delta$ controller in both scenarios, respectively. It is important to mention that similar bilateral control strategies have been studied in detail in the literature, for haptic devices applications (virtual and teleoperated) or teleoperation systems in general (see, for instance, [5, 6]). In the scope of this section, one uses these experimental results to illustrate the idea of using a delay-based controller instead of a derivative-based one. Both control schemes are designed to create a bilateral tracking control system. These kind of tasks are often realized by using a PD controller, avoiding the integral action. As mentioned in the Introduction, one can imitate this derivative alike effect using delays, a particular situation of this is the $P\delta$ controller. First, one explains the main ideas behind this control scheme. The dynamics of a haptic device as the one shown in Fig. 3.7 can be modeled by considering a Lagrangian formulation [70], as follows:

$$M\left(\theta\right)\ddot{\theta}+C\left(\theta,\dot{\theta}\right)\dot{\theta}+B=F_{\lambda},$$

where M is the inertia matrix, C is the Coriolis matrix, B is a vector associated to the effect of gravity, F_{λ} is the torque input vector and θ is the angular position vector. The derived model is clearly a non-linear one. Inspired by the contributions of [70, 43], a few assumptions can be taken into account in order to describe the dynamics of the system as a decoupled LTI model. This is formed by the three mechanical admittances of each joint in the following form:

$$P(s):=\frac{\Theta(s)}{\Lambda(s)}=\frac{1}{s(ms+b)},$$

where each mechanical admittance $P(s)$ is described by the transfer function from each torque input $\Lambda(s)$ to its respectively angular position $\Theta(s)$ and depicts the behavior of each mechanical joint.

3.1.1 Haptic Virtual System

As an experimental application of the P-δ controller, consider the haptic-virtual system developed in [32]. This experimental setup, shown in Fig. 3.1, consists in a haptic device working in a virtual environment with the main purpose of providing the human operator a perfect telepresence on the virtual environment, and a full sense feedback of it. In order to fulfill this objective, one uses a $P\delta$ controller to achieve a *kinematic correspondence* between the haptic and virtual devices, this last one simulated on the virtual environment. The stability of the closed-loop system is studied using the methodology introduced in Section 2.1. A fixed delay value $\tau=0.1$ is proposed for the controller design. The angular position of the haptic and virtual devices are normalized with respect to the mechanical stops of each joint and are defined as θ_h and θ_v, respectively. Fig. 3.2 shows the stability region of the closed loop system. In order to observe the qualitative behaviour of the system response for this particular joint, the system is tested for a fixed $k_p=10$ and three particular values of the delay term gain, $k_\delta=-1$, $k_\delta=2.6$ and $k_\delta=4$, corresponding to

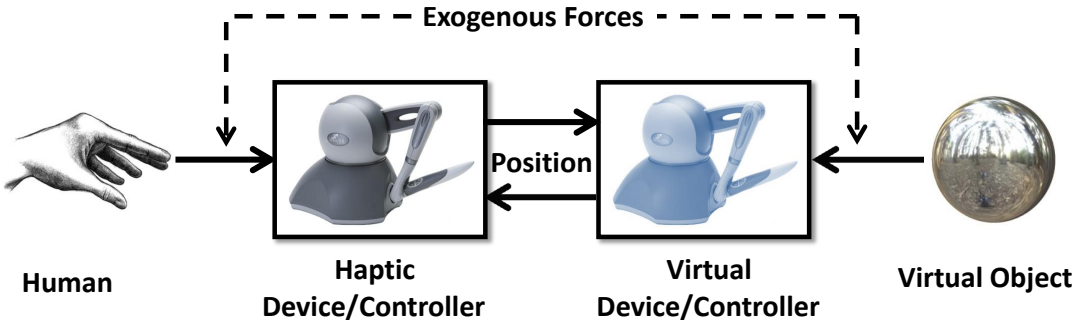

Figure 3.1: Bilateral control scheme.

a stable point, a stable point near some *stability crossing curve* and an unstable point, respectively. The results are illustrated in Fig. 3.2, where oscillations of greater amplitude appear as $\boldsymbol{k}$ approaches the *stability crossing curve*.

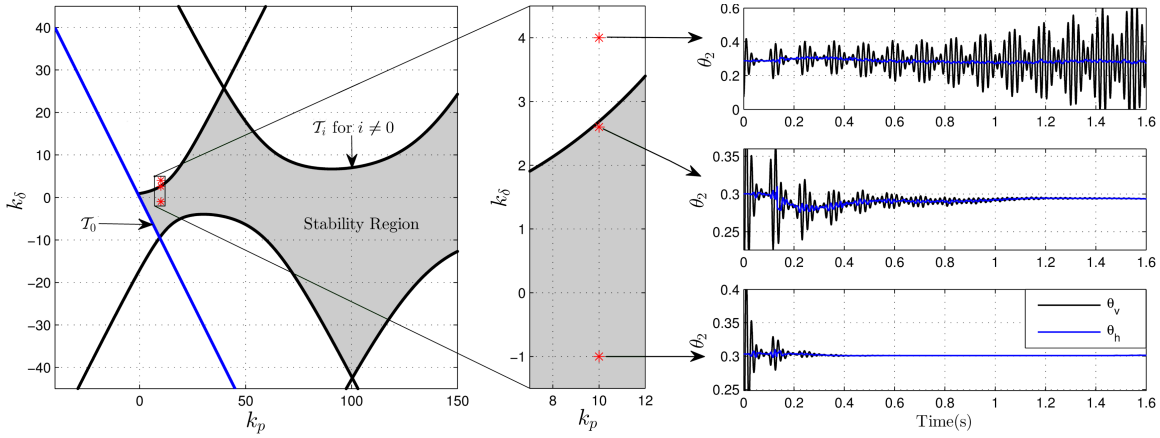

Figure 3.2: Stability regions vs Experimental Behaviour for the Second Joint

The three joints system is tested by choosing the controller gains either in stable and unstable regions (for further details see [32]). The system response is shown in Fig.3.3. On Fig.3.3a one observes that choosing the controller gains in the stability region leads to a stable response with a good bilateral position tracking between the haptic and the virtual device. Fig.3.3b shows that choosing the controller gains in an unstable region produces an unstable system response, thus no tracking between both devices is achieved.

Finally, a virtual wall was implemented in the X-Z plane applying a force F_y normal to the X-Z plane in the increasing direction of the Y axis. The behavior of the wall is modeled as a simple spring with a Hooke constant $\boldsymbol{k}_h$ using the error between the position of the final effector of the haptic device in the Y axis Y_f, and a fixed value Y_w, which is the location of the virtual wall on the Y axis. This implementation is described by the

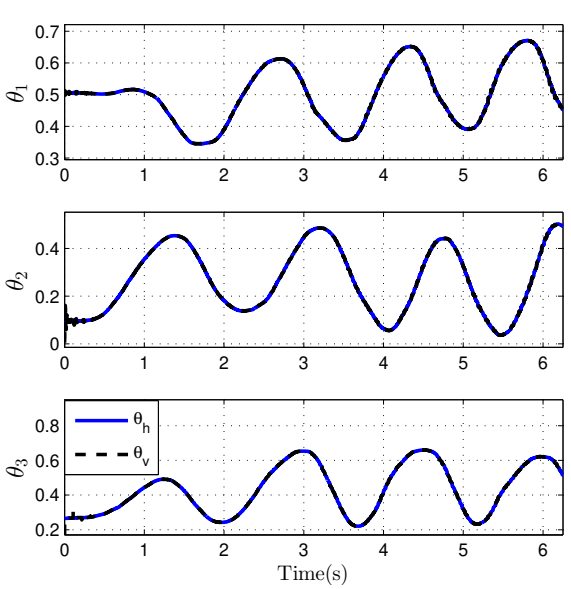

(a) Stable Response

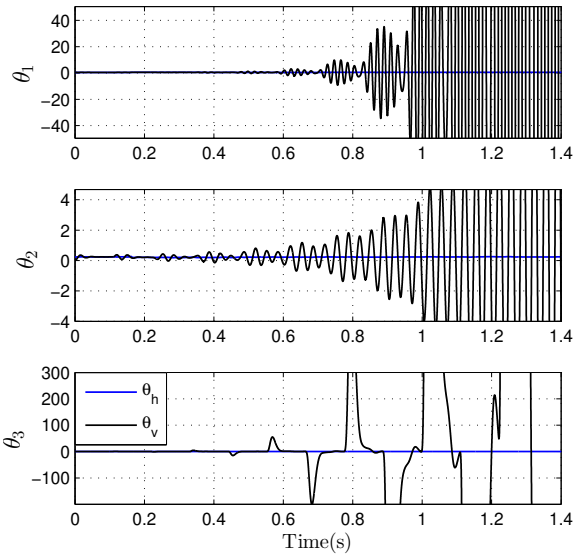

(b) Unstable Response

Figure 3.3: Total System Response

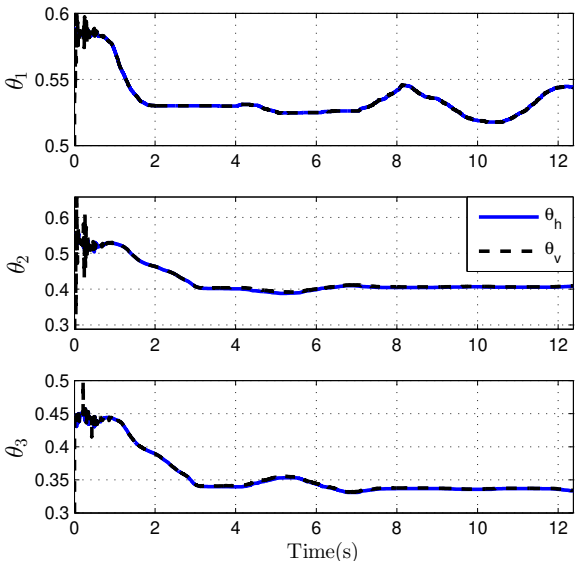

(a) Joints

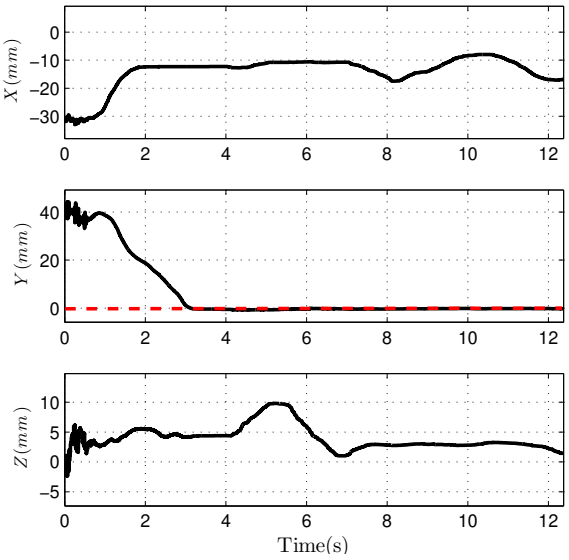

(b) Final effector position

Figure 3.4: Total System Response Perceiving a Wall

following equation:

$$F_y(Y_f) = \begin{cases} 0, & if \quad Y_f > Y_w, \\ \\ K_h(Y_w - Y_f), & if \quad Y_f \leqq Y_w. \end{cases}$$

In the implementation the correspondent torques perturbations T_e for each joint produced by the virtual environment are obtained by using the following equation:

$$T = J^T F,$$

where T contains each correspondent T_e for each joint, $F = (0, F_y, 0)^T$ represents the forces vector applied by the virtual environment modeled as a virtual wall and J is the jacobian matrix (see, for instance [69]), obtained directly from the direct kinematic model studied by [70]. The results using $\boldsymbol{k}_h = 1$ and $Y_w = 0$ are shown in Figs. 3.4a and 3.4b, where it is easy to observe how the haptic device moves freely until second three where the virtual wall restricts the movement along the Y axis producing the human operator perception of the virtual wall.

3.1.2 Haptic Teleoperated System

In this case, the main goal of the proposed control scheme is to achieve a *kinematic correspondence* between a master and a slave devices. As illustrated in Fig. 3.5, the main idea is to maintain a perfect bilateral position tracking under the interaction of the exogenous forces of the human and the remote environment on the master and the slave device, respectively. The ideal result is to have a complete perception of the remote environment to the human operator and a complete telepresence of the human operator on the remote environment (see, for instance, [26]). The bilateral control scheme proposed

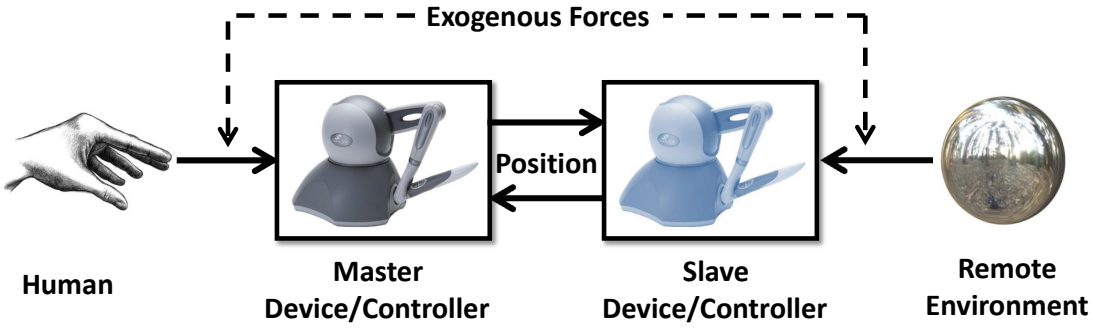

Figure 3.5: Bilateral Control Scheme (Conceptual).

in this section is shown in Fig. 3.6, where τ_p is considered as the delay due to signal processing, Λ_h and Λ_e are the exogenous torques related to the human operator and the remote environment, respectively, P_M and P_S are the mechanical admittances of the master and the slave device, respectively; furthermore, a similar notation is used for the controllers C_M and C_S and the angular positions Θ_M and Θ_S. This scheme is a variation of the one presented in [43] for haptic-virtual systems, however here, one has considered the

time delays due to signal processing and, instead of using a P-D controller, a $P\delta$ controller is proposed. In order to illustrate how the proposed controller works, one considers the

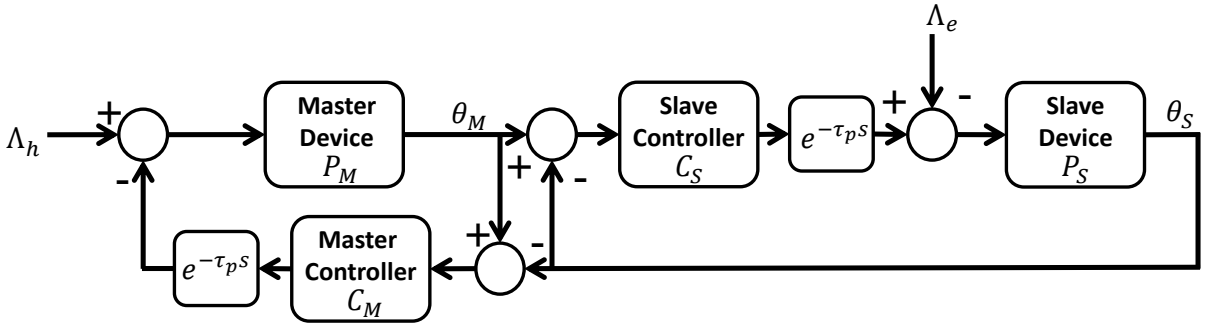

Figure 3.6: Bilateral Control Scheme.

experimental setup consisting in two Phantom Omni haptic devices as the one depicted in Fig.3.7 (in a master/slave configuration), implemented by means of the Matlab-Simulink toolkit Phansim. It is also worth mentioning that the angular positions were normalized with respect to the mechanical stops of each joint. To this end, in this experimental setup the delay is estimated to be $\tau_p = 0.001$ seconds. In all following examples, one proposes a fixed delay value $\tau_d = 0.1$ seconds in the design of the $P\delta$ controller. Now, using the stability analysis described in Chapter 2, one choses the controller's gains $K = [k_p, k_\delta]$ $K = [20, 2]^T$, $K = [20, 1]^T$ and $K = [10, 2]^T$ for the joint one, two and three, respectively. This process is documented in detail in [32].

Furthermore, one proposes an experimental test perceiving a plastic sphere as it is shown in figure 3.7. This consists in manipulating the master device in order to "feel" the plastic sphere in a remote environment, where the slave device is located (it is worth to mention, that it is not necessary that the master and slave are located "close" to each-other. However, for illustrative purposes only one has chosen the proposed physical configuration for the visualization of the experiment). The experimental results are illustrated in figures 3.8a, 3.8b and 3.9. Furthermore, Fig. 3.9 shows how the control scheme implemented drives the trajectory of the master device which is also guided by the human operator, following the path created by the human operator but restricted by the plastic sphere located in the remote environment, this creates the "feel" sensed by the human operator.

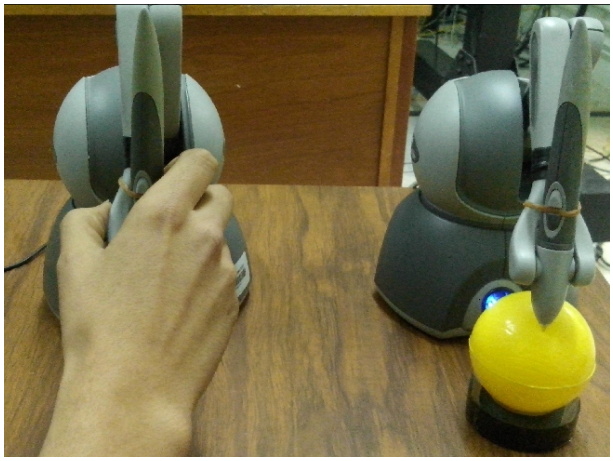

Figure 3.7: Experimental setup.

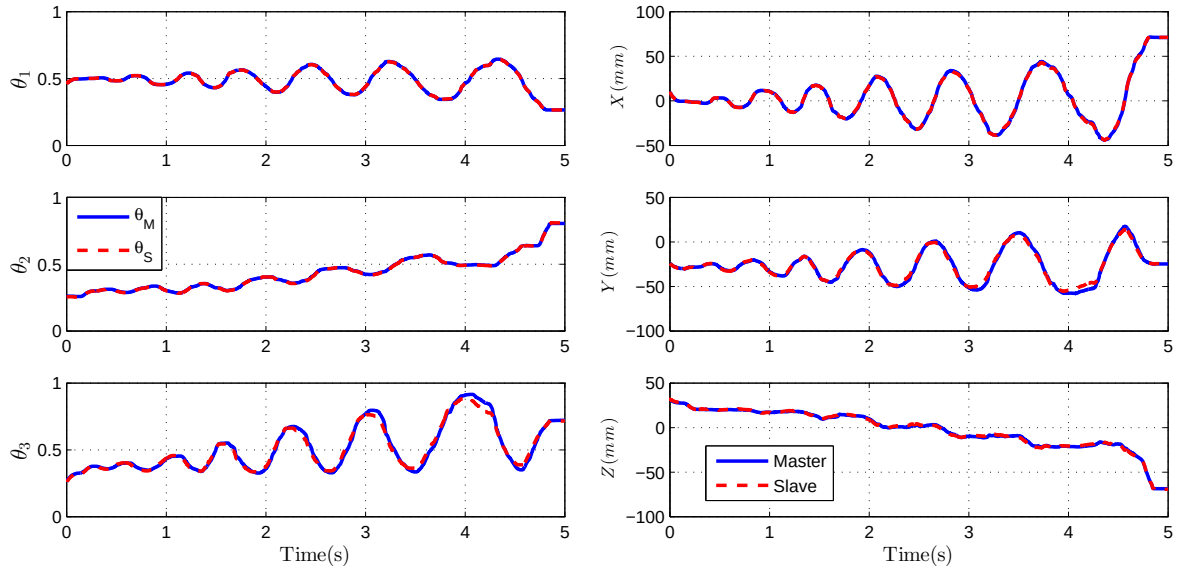

(a) Joints (b) Final Efector Position

Figure 3.8: Total System Response Perceiving a Sphere

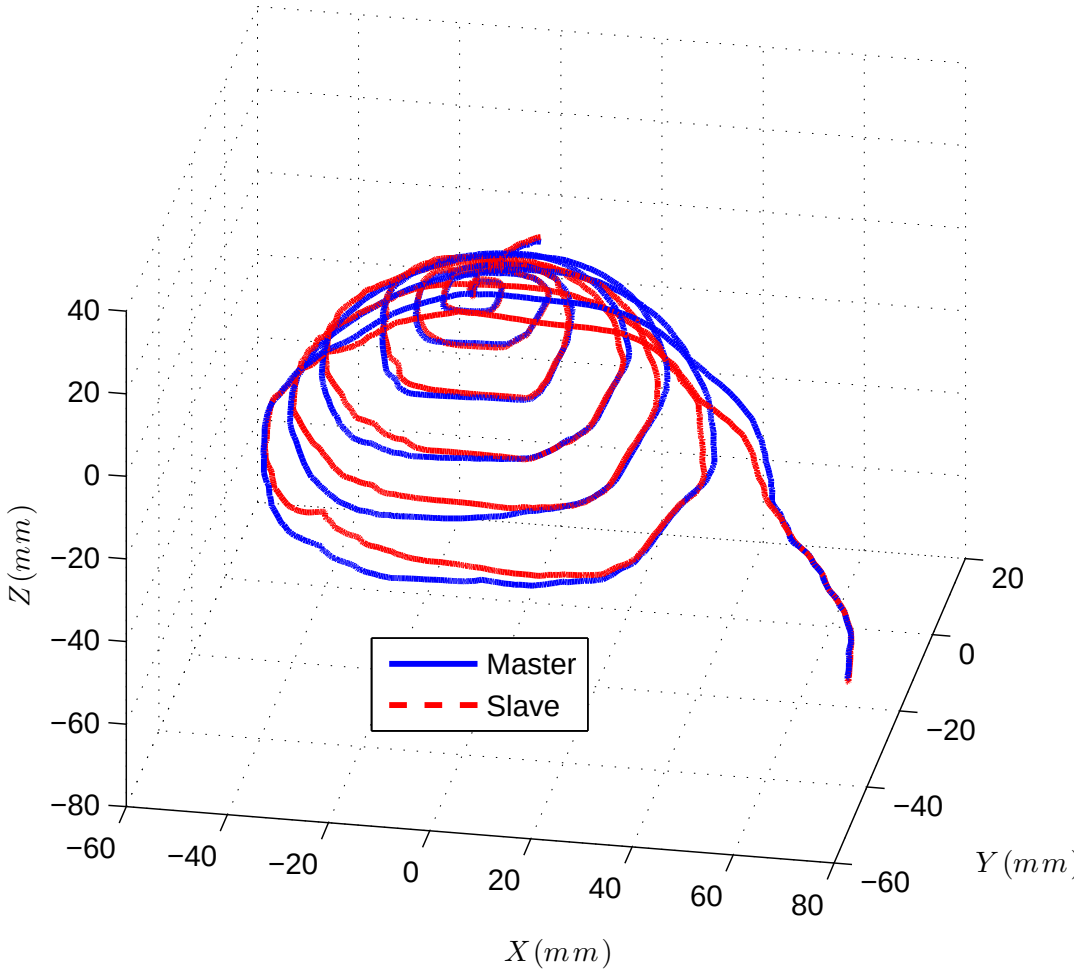

Figure 3.9: Trajectory of the System Under the Perception of a Sphere

3.2 Buck DC/DC Converter: $P\delta$ and $P\delta I$ Controllers

This section studies the application of two alternative PID inspired delay-based controller in a classical feedback control scheme to a switching power electronics device. Particularly, such a device being a standard dc/dc buck converter and as feedback compensator the $P\delta$ and $PI\delta$ controllers. On one hand, This consisting in a variation of the well-known PI controller by the addition of a delay in the integral process. The main idea is to study the potential of the delay nature for being an extra degree of freedom in the controllers tunning for closed-loop dynamics manipulation. The $P\delta I$ controller (1.8) is defined as:

$$C(s) := k_p + k_i \frac{e^{-\tau s}}{s},$$

where $k := [k_p, k_i]^T$ are the controller gains and τ is a fixed time-delay. The control law corresponding to this scheme is described by:

$$\tilde{u}(t) = k_p e(t) + k_i \int_0^t e(v - \tau) dv,$$

where $e(t)$ is an error signal. In other words, a PI controller in which the error signal is delayed a finite constant amount of time τ before integrating it.

3.2.1 DC/DC Buck Converter Dynamics

Figure 3.10 depicts the classical topology of a buck dc/dc converter, where v_s and v_o are the supply and output voltages, respectively. This configuration contains four basic elements: inductor (L), capacitor (C), diode (D) and a controlled switch (Q). A resistive load R is assumed. Considering a fixed DC voltage supply v_s, the main task of this topology is to adjust the output voltage v_o through the switching pattern applied to D . To such an end, probably the most widely used switching technique is the so-called PWM (Pulse-Width Modulation). This consists in creating a switching pattern at a fixed frequency f and being $T = \frac{1}{f} = t_{on} + t_{off}$ the full pattern time period, the switch has activated and non-activated periods t_{on} and t_{off}, respectively. Furthermore, the rate between the activation and the full pattern periods $U := \frac{t_{on}}{T}$ (better known as "duty cycle") is the crucial measure to handle in order to manipulate this switching power device. In the following lines one describes briefly the dynamical model derivation of this circuit. For a more detailed explanation of such ideas one encourages the reader to further investigate the didactic material found in [72]. Particularly, the continuous-conduction mode (CCM).

This process consists in the following steps:

- Obtain the equivalent circuit dynamics of the activated (Q: ON, $\mu = 1$) and non-activated (Q: OFF, $\mu = 0$) states using Kirchhoff's laws, separately.
- Integrate both in a single model through the variable μ, this is called switched model (it corresponds to Q: ON, if $\mu = 1$, and to Q: OFF, if $\mu = 0$).
- Assume that all variables have a constant (nominal) value and a fluctuating part

("small gain" analysis, see for instance, [62]), i.e.:

$$\begin{aligned} v_s(t) &= V_s + \tilde{v}_s(t), \\ v_o(t) &= V_o + \tilde{v}_o(t), \\ i_o(t) &= i_o + \tilde{i}_o(t), \\ u(t) &= U + \tilde{u}(t). \end{aligned}$$

- Consequently, by considering a PWM switching pattern, a so-called averaged state-space model is derived as:

$$\begin{aligned} \dot{x}_1 &= -\frac{x_2}{L} + \frac{V_s + \tilde{v}_s}{L} u, \\ \dot{x}_2 &= -\frac{x_1}{C} - \frac{x_2}{RC}. \end{aligned}$$

  These averaged states $[x_1, x_2] := [i_L, v_o]$ are defined as:

$$x_1 := \frac{1}{T} \int_{t-T}^{t} i_L(h)dh, \quad \text{and} \quad x_2 := \frac{1}{T} \int_{t-T}^{t} v_o(h)dh,$$

  and a new control variable:

$$u := \frac{1}{T} \int_{t-T}^{t} \mu(h)dh$$

  , is defined and it represents the duty cycle (Integrates the switch rate state μ over the commutation period T).
- The relations between the nominal values (V_s, V_o, I_o, U) are derived from (3.5) by

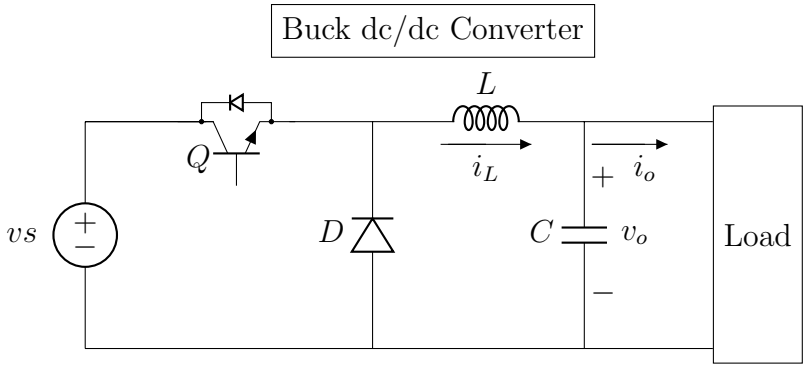

Figure 3.10: Topology of the Buck DC/DC Converter [72].

setting the derivatives equal to zero leading to:

$$I_L = \frac{V_o}{R}, \qquad V_o = UV_s. \tag{3.6}$$

- Finally, taking a linear approximation from (3.5) around the nominal conditions, two transfer functions with respect to the variations in the output voltage $\tilde{v}_o$ are defined as:

$$G_1(s) := \frac{\tilde{v}_o(s)}{\tilde{u}(s)} = V_s \frac{\frac{1}{LC}}{s^2 + \frac{1}{RC}s + \frac{1}{LC}}, \quad G_2(s) := \frac{\tilde{v}_o(s)}{\tilde{v}_s(s)} = U \frac{\frac{1}{LC}}{s^2 + \frac{1}{RC}s + \frac{1}{LC}}. \tag{3.7}$$

Remark 8. *It is worth mentioning that this averaged model can describe the nature of the system only if the commutation frequency f is sufficiently large. Also, notice that the transfer functions presented in* (3.7) *describe the dynamical behavior of the transient response of the circuit in relation with nominal conditions. That is, one needs to include in the control scheme design the nominal conditions presented in* (3.6)*. For a desired nominal condition V_o, the control scheme has the task of minimizing the fluctuating part $\tilde{v} - o(t) \to 0$. Directly, considering a classical feedback control scheme, the error signal is defined as:*

$$e(t) := 0 - \tilde{v}_o(t) = V_o - v_o(t).$$

In the following sections one develops two different stability analysis for delay-based controllers: $P\delta$ and $P\delta I$ controllers. Numerical results are addressed to illustrate the proposed methods, the parameters considered in such results are depicted in Tab. 3.1.

Table 3.1: Parameters of the System

Symbol	Value	Unit
R	3	Ω
L	180×10^{-5}	H
C	40×10^{-6}	F
V_s	40	V
f	20×10^3	Hz

3.2.2 $P\delta I$: σ-Instability

Consider the before stated dc/dc buck converter dynamics (3.7) and the $PI\delta$ controller (1.8) shown in the beginning of this section. One aims to study the systems stability through the closed-loop transfer function:

$$T(s) = \frac{C(s)G_1(s)}{C(s)G_1(s) + 1}.$$

Particularly, the task of computing stability conditions for the gains pair (k_p, k_i) considering a fixed delay-value τ. Equivalently, such that the characteristic equation of the closed-loop system computed as:

$$C(s)G_1(s) + 1 = 0,$$

has all of its roots on the LHP of the complex plane (see, [49]. This equation rewrites directly as:

$$\Delta(s) := \frac{LC}{V_s}s^3 + \frac{L}{V_sR}s^2 + \left(\frac{1}{V_s} + k_p\right)s + k_ie^{-\tau s} = 0.$$

In order to simplify the analysis, from now on consider the following notation:

$$a := \frac{LC}{V_s}, \qquad b := \frac{L}{RV_s}, \qquad c := \frac{1}{V_s}.$$

Finally, one obtains the characteristic quasi-polynomial:

$$\Delta(s) = as^3 + bs^2 + (c + k_p)\,s + k_ie^{-\tau s} = 0. \tag{3.8}$$

The following part of this section is dedicated to the deep study of the location of the roots of this equation. Before diving into full discussion, first consider the following notation. Let $\tau \in \mathbb{R}_+$ and $\sigma \in \mathbb{R}_+ \cup \{0\}$ be fixed values, one introduces the following set:

$$\mathcal{T}(\sigma) := \left\{\boldsymbol{k} \in \mathbb{R}^2 \,|\Delta(\sigma + i\omega) = 0, \forall\omega \in \Omega\right\},$$

with $\Omega \subset \mathbb{R}_+$, some appropriate set of frequencies characterized in Proposition 14. Roughly speaking, this set contains all gain vectors $k := [k_p, k_i]^T$ such that the characteristic equation of the closed-loop system (3.8) has at least one root on a vertical line in σ on the complex plane. In other words, Ω includes all the frequencies for which the gains $k \in \mathbb{R}^2$ define some σ-crossing points, that is, points located in the complex plane on the line $\Re\{s\} = \sigma$. Using this notation, it is clear that all possible gain vectors k such that the system has at least one root in the RHP or on the imaginary axis of the complex plane can be characterized by:

$$\bar{\mathcal{T}}^+ := \bigcup_{\sigma\in\mathbb{R}_+\cup\{0\}} \mathcal{T}(\sigma).$$

Therefore, all stabilizing controllers k are contained in the following set:

$$\bar{\mathcal{T}}^- := \mathbb{R}^2 \setminus \bar{\mathcal{T}}^+.$$

Considering this notation, it is mandatory to enhance the importance of the set $\mathcal{T}(0)$. This set contains all possible gain vectors k such that the characteristic equation (3.8) has at least one root on the imaginary axis. That is, the set of all *crossing points*, in other words, $\mathcal{T}(0)$ is nothing else that the so-called "stability crossing curves". Bear in

mind the fact that any continuous variation of k such that $k \notin \mathcal{T}(0)$ implies that no roots exchange through the imaginary axis can be achieved. It is easy to observe how these *stability crossing curves* partition the parameters-space in regions in which any choice of k implies that (3.8) has a finite number of roots on the RHP of the complex plane. Furthermore, notice that if some element of $\mathcal{T}(\sigma)$ with $\sigma > 0$ is located inside one of this regions implies that the characteristic equation (3.8) has at least one unstable root in the RHP of the complex plane. Therefore, this can be labeled as an *unstable region*. Finally, any region which is not unstable is a subset of $\mathcal{T}^-$ and can be labeled as a *stability region*.

The following results summarized in this section work as tools for describing the behavior of the roots of the characteristic equation of the closed-loop system. As mentioned above, the first result presented in this section characterize the pairs (k_p, k_i) such that the characteristic equation of the closed-loop system (3.8) has at least one root on a desired vertical line ($\Re\{s\} = \sigma$) of the complex plane. This is useful for two reasons, first, to construct an approximation of the set $\tilde{\mathcal{T}}^-$ by discriminating the regions of the parameters space partitioned by $\mathcal{T}(0)$ with some elements of the set $\tilde{\mathcal{T}}^+$. Second, assuming that one found an stability region, to develop a tracking of the rightmost root of the characteristic equation, as is shown in detail in Section 3.2.3.

Proposition 16. *Let $\tau \in \mathbb{R}_+$ and $\sigma \in \mathbb{R}$ be fixed values. Then, the characteristic equation* (3.8) *has at least one root in $s = \sigma + i\omega$, iff:*

$$\begin{aligned} k_p &= -\Re(\sigma,\omega) + \frac{\omega\sin(\tau\omega) - \sigma\cos(\tau\omega)}{\sigma\sin(\tau\omega) + \omega\cos(\tau\omega)}\Im(\sigma,\omega), \\ k_i &= \frac{\sigma^2+\omega^2}{\sigma\sin(\tau\omega) + \omega\cos(\tau\omega)}\Im(\sigma,\omega)e^{\tau\sigma}, \end{aligned}$$

where the functions $\Re$ and $\Im$ stands for the real and imaginary part of $G_1^{-1}(\sigma + i\omega)$:

$$\begin{aligned} \Re\left\{G_1^{-1}(\sigma+i\omega)\right\} &= a(\sigma^2-\omega^2) + b\sigma + c, \\ \Im\left\{G_1^{-1}(\sigma+i\omega)\right\} &= 2a\sigma\omega + b\omega, \end{aligned}$$

with $\omega \in \Omega_i$ where the set Ω_i is defined by:

$$\Omega_i := \{\omega \in \mathbb{R} \,|\omega\cot(\tau\omega) + \sigma \neq 0\},$$

where $n \in \mathbb{Z}$. Furthermore, it has a single root in $s = \sigma$ iff $P(\sigma) \neq 0$ and:

$$k_i = -\sigma\left(k_p + G_1^{-1}(\sigma)\right)e^{\tau\sigma}.$$

Furthermore, one presents an additional proposition for computing the stabilizing interval of the delay value given a stabilizing triplet (k_p, k_i, τ).

Proposition 17. *Let (k_p, k_i, τ^*) be a stabilizing triplet, then, the closed-loop system is*

asymptotically stable for any delay value $\tau \in [\tau^*, \tau_c)$*, where:*

$$\tau_c = \min \{\tau \in \mathbb{R} \,|\tau(\omega^*) > 0, \omega^* \in \Omega_p\},$$

in which $\tau(\omega^*)$ *is computed as:*

$$\tau(\omega^*) = \frac{1}{\omega^*}\left[\arg\left\{\frac{k_i}{i\omega^*(k_p + G_1^{-1}(i\omega^*))}\right\} + (2n+1)\pi\right],$$

for $n \in \mathbb{Z}$ *and where the set* Ω_p *is defined as the set of all real roots of the following equation:*

$$|k_i|^2 - {\omega^*}^2 |k_p + G_1^{-1}(i\omega^*)|^2 = 0.$$

3.2.3 $P\delta I$: Numerical Results

All results of this section were obtained by means of the "SimPowerSystems" toolbox in the "Simulink" environment of the software "Matlab". The parameters used in the simulation are summarized in Table 3.1. The tests presented in this section are designed to regulate the output voltage $v_o(t)$ to a nominal value of $V_o := 20V$. Recall that the control scheme has the task to regulate the variations of the output voltage $\tilde{v}_o(t)$ to zero in order to satisfy the following: $v_o(t) \to V_o$. The control law proposed for the achievement of this objectives is given by:

$$u(t) = U + \tilde{u}(t),$$

with:

$$\tilde{u}(t) = k_p e(t) + k_i \int_0^t e(v - \tau) dv,$$

where the error signal is defined as:

$$e(t) = 0 - \tilde{v}_o(t) = V_o - v_o(t),$$

and the nominal value U is obtained directly from (3.6).

Consider a fixed time delay $\tau = 1.6 \times 10^{-3}$ in the $P - \delta I$ controller shown in (1.8) along with the parameters shown in Fig. 3.1. In order to find the set of gains (k_p, k_i) that guaranties the stability of th closed-loop system one partially computes the set $\tilde{\mathcal{T}}^-$ described in Section 2.1.1. First, using Proposition 16 one computes the sets $\mathcal{T}(0)$, which as mentioned before partition the parameters space in regions with a constant number of roots of the characteristic equation (3.8) on the right-half plane of the complex plane. Second, using this proposition, one also computes some of the sets σ with $\sigma > 0$, if a curve of these sets crosses any partitioned region indicates that any choice of parameters inside this implies that the characteristic equation has at least a root in the right-half plane of the complex plane, and therefore, is an unstable region. As can be seen from Fog. 3.11, using this criteria one is able to discriminate the unstable region and finally find a stability region for this fixed delay. An expanded view of this stability region is

shown at the right side of in Fig. 3.11.

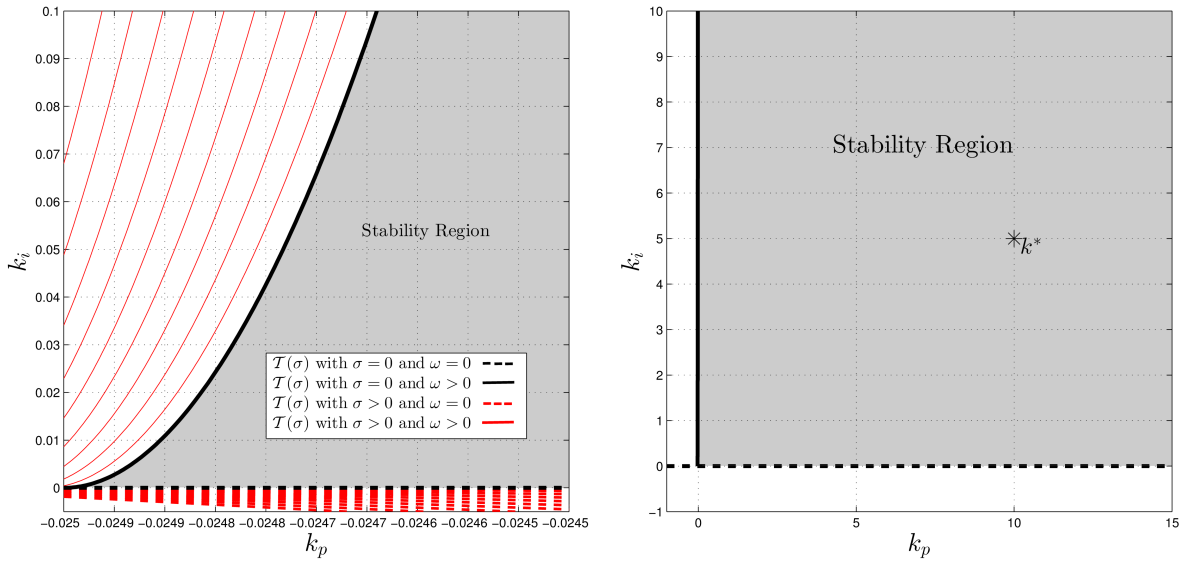

Figure 3.11: Stability Analysis in the (k_p, k_i) Parameters Space

Now, from Fig. 3.11 one chooses the gains pair $k^* = (k_p, k_i) = (10, 5)$, a stabilizing controller for $\tau = 1.6 \times 10^{-3}$. Using Proposition 17 one computes the critical delay value $\tau_c = 3.1494$, which implies that the closed-loop system is stable for any delay value in the interval (τ, τ_c). Furthermore, using Proposition 16 one develops what is known as the σ stability analysis. Using this proposition one computes some curves of the sets $\mathcal{T}(\sigma)$ with $\sigma < 0$, particularly with $\sigma = -1$ and $\sigma = -2$, this results are shown in Fig. 3.12a. Notice that here one enhances three different regions $\mathcal{R}_1$, $\mathcal{R}_2$ and $\mathcal{R}_3$. Consider region $\mathcal{R}_2$ Since this region is bounded by the curves obtained from the sets $\mathcal{T}(-1)$ and $\mathcal{T}(-2)$, this indicates that a variation inside this region implies that no root is crossing through the vertical lines $\Re\{s\} = -1$ and $\Re\{s\} = -2$. Then, the rightmost root is contained in this band and therefore, the maximum exponential decay related to σ is bounded for values of $\sigma \in (-2, -1)$. A similar conclusion can be stated for $\mathcal{R}_1$ with $\sigma \in (-1, 0)$ and for $\mathcal{R}_3$ with $\sigma \in (-2, -3)$.

Finally, using the controllers parameters described above $k^* = (10, 5)$ and $\tau = 1.6 \times 10^{-3}$ one tests the closed-loop control scheme. This result are shown in Fig. 3.12b, in which one depicts a comparison between a normal PI controller ($\tau = 0$) and the delayed control scheme proposed. For this particular set-up it is of interest enhance how the closed-loop response can be manipulated by adding this delayed action. Both responses regulate to $20V$ as expected, however, the addition of the time delay to the control scheme allow us to reduce the ripple of the output of the system.

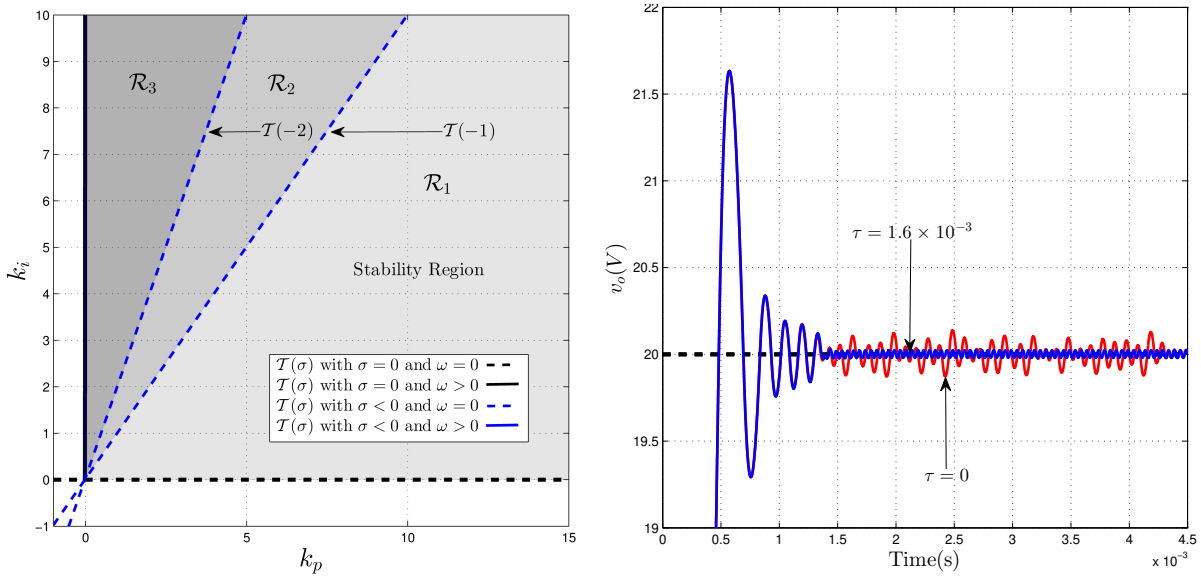

(a) σ Stability Analysis in the (k_p, k_i) Parameters Space

(b) Closed-Loop Response with $\tau = 0$ and $\tau = 1.6 \times 10^{-3}$.

Figure 3.12: Analysis and Closed-Loop Response

3.2.4 $P\delta$: Crossing Roots Analysis

One is interested in finding the stability regions in the (k_p, k_δ) parameters space considering a fixed delay-value τ. To this end, consider the open-loop transfer function $G_1(s)$ (3.7), along with the $P\delta$ controller:

$$C(s) = k_p + k_\delta e^{-\tau s},$$

leading to the closed-loop characteristic equation:

$$\Delta(s) := \frac{LC}{V_s}s^2 + \frac{L}{V_s R}s + \frac{1}{V_s} + k_p + k_\delta e^{-\tau s} = 0.$$

In order to simplify the analysis, in the remaining part of this section one adopt the following notation:

$$a := \frac{LC}{V_s}, \qquad b := \frac{L}{RV_s}, \qquad c := \frac{1}{V_s}.$$

In this way, one can rewrite the characteristic equation as:

$$\Delta(s) = as^2 + bs + c + k_p + k_\delta e^{-\tau s} = 0. \tag{3.13}$$

First, one analyzes the stability of the closed-loop system considering any possible fixed delay value $\tau \in \mathbb{R}_+$, this particular result is shown as follows:

Proposition 18. *Let $a, b, c \in \mathbb{R}_+$, then, the buck dc/dc converter is asymptotically sta-*

ble independent of the delay value $\tau \in \mathbb{R}_+$, if the controller gains satisfy the following conditions:

$$\begin{aligned} k_\delta^2 &< \frac{b^2}{4a^2}\left(4ak_p + 4ac - b^2\right), \\ k_\delta &> -k_p - c, \\ k_p &> \frac{b^2}{4a} - c. \end{aligned}$$

Proof. Consider the characteristic equation of the closed-loop system (3.13) with $s = j\omega$, then:

$$(-a\omega^2 + c + k_p + k_\delta \cos(\tau\omega)) + j(b\omega - k_\delta \sin(\tau\omega)) = 0.$$

Now, (3.13) has at least one root on the imaginary axis, if and only if, there exists some $\omega \in \mathbb{R}_+ \cup \{0\}$ such that the real and imaginary part of the above equation are simultaneously equal to zero, i.e.,

$$\begin{aligned} k_p + k_\delta \cos(\tau\omega) - a\omega^2 + c &= 0, \\ b\omega - k_\delta \sin(\tau\omega) &= 0. \end{aligned}$$

Then, equations (3.17) and (3.18) lead directly to the following expressions:

$$\begin{aligned} k_\delta \cos(\tau\omega) &= -k_p + a\omega^2 - c, \\ k_\delta \sin(\tau\omega) &= b\omega, \end{aligned}$$

Using the fact that $\sin^2(\tau\omega) + \cos^2(\tau\omega) = 1$ provides the following equation:

$$a^2\widetilde{\omega}^2 + (b^2 - 2a(c + k_p))\widetilde{\omega} + (c + k_p)^2 - k_\delta^2 = 0,$$

where $\widetilde{\omega} := \omega^2$. It is clear that there is no real solution of ω if $\widetilde{\omega} \in \widetilde{\Omega}$, where:

$$\widetilde{\Omega} := \mathbb{R}_- \cup \mathbb{C} \setminus \mathbb{R}.$$

First, observe that $\widetilde{\omega} \in \mathbb{C} \setminus \mathbb{R}$, if and only if, the following condition holds:

$$(b^2 - 2a(c + k_p))^2 - 4a^2((c + k_p)^2 - k_\delta^2) < 0, \tag{3.19}$$

which is nothing else than condition (3.14). Second, notice that $\widetilde{\omega} \in \mathbb{R}_-$, if and only if, (3.19) does not hold, and the following conditions hold simultaneously:

$$b^2 - 2a(c + k_p) > 0, \qquad (c + k_p)^2 - k_\delta^2 > 0. \tag{3.20}$$

Now, since the roots of $\Delta(s)$ are continuous with respect to its parameters variations the roots of $\Delta(s)$ cross from the LHP to the RHP (or from the RHP to the LHP) through the

imaginary axis, if and only if, there exists some $\omega \in \mathbb{R}$. Therefore, (3.19) or (3.20) implies that each root of the characteristic equation (3.13) remains in an specific semi-plane of the complex-plane independently of the delay value τ, respectively. In this vein, analyzing the delay-free scenario, i.e., taking $\tau = 0$ in (3.13) leads to a simple second-order polynomial, which is a Hurwitz polynomial, if and only if, (3.15) holds.

Finally, since for the asymptotic stability (3.20) and (3.15) cannot be satisfied simultaneously, one concludes that the closed-loop system will be asymptotically stable, if (3.14) and (3.15) are satisfied. Furthermore, the extra condition (3.16) is addressed in order to obtain a real solution for k_δ in the quadratic inequality (3.14). □

The purpose of this proposition is to give stability conditions independent of the time delay value. This gives a flexibility for choosing the delay value according to the performance required in its application. Also, to have an auxiliary degree of tunning for a further robustness analysis. Furthermore, having selected this parameter is highly recommended to analyze the stability of the closed-loop system for the desired fixed value, this analysis is also presented and is shown in detail in the following lines.

Now, in order to perform a stability analysis for a specific delay value in the controller design, one first needs to construct the *stability crossing boundaries*. Then, it is useful to characterize the behavior of the roots movement as a parameter variation crosses some of these boundaries. This section focuses on analyzing such a behavior.

Proposition 19. *Let $\tau \in \mathbb{R}_+$ be a fixed value and $\sigma, \omega \in \mathbb{R}$. Then, $\Delta(s)$ has a root at $s = \sigma + j\omega$, if and only if the controller gains $k(\sigma, \omega) := [k_p, k_\delta]^T$, are given as:*

$$\begin{cases} k_p(\sigma,\omega) = a(\omega^2 - \sigma) - (2a\sigma + b)\omega\cot(\tau\omega) - b\sigma - c, \\ k_\delta(\sigma,\omega) = (2a\sigma + b)\omega e^{\tau\sigma}\csc(\tau\omega), \ \textit{if } \omega \neq 0, \end{cases}.$$

$$k_\delta = e^{\tau\sigma}\left[-k_p - \left(a\sigma^2 + b\sigma + c\right)\right], \ \textit{if } \omega = 0.$$

Proof. The proof follows straightforwardly by setting $s = \sigma + j\omega$ in (3.13), and solving with respect to k_p and k_δ. □

The *stability crossing curves* are characterized in the following result.

Proposition 20. *Let $\tau \in \mathbb{R}_+$ be a fixed delay value and $\Omega := \bigcup_\ell \Omega_\ell \bigcup \{0\}$ for $\ell \in \mathbb{N}$, where the subsets Ω_ℓ are defined as:*

$$\Omega_\ell := \left\{\omega \in \mathbb{R}_+ \,\middle|\, \omega \in \left(\tfrac{\pi}{\tau}(\ell - 1), \tfrac{\pi}{\tau}\ell\right)\right\}.$$

Then, $\omega \in \Omega \setminus \{0\}$ is a crossing frequency *if and only if $\boldsymbol{k}(\omega) := [k_p(\omega), k_\delta(\omega)]^T$, where:*

$$\begin{aligned} k_p(\omega) =& a\omega^2 - c - b\omega\cot(\tau\omega), \\ k_\delta(\omega) =& b\omega\csc(\tau\omega), \end{aligned}$$

defines a crossing point $\boldsymbol{k}(\omega) \in \mathcal{T}$*. Moreover, the line:*

$$k_\delta = -k_p - c,$$

defines a stability crossing curve at $\omega = 0$*.*

Proof. The proof follows by setting $\sigma = 0$ in Proposition 19. □

Given all stability crossing points $\boldsymbol{k}(\omega)$ and the frequency crossing set Ω, one defines each stability crossing curve through its continuity as follows:

$$\begin{aligned} \mathcal{T}_0 &:= \left\{ \boldsymbol{k} \in \mathbb{R}^2 \,|k_\delta = -k_p - c \right\}, \\ \mathcal{T}_\ell &:= \left\{ \boldsymbol{k}(\omega) \in \mathbb{R}^2 \,|\omega \in \Omega_\ell \text{ for } \ell \in \mathbb{N} \right\}. \end{aligned}$$

Finally, one describes the set $\mathcal{T}$ as:

$$\mathcal{T} = \bigcup_\ell \mathcal{T}_\ell, \quad \ell \in \mathbb{N} \cup \{0\}.$$

It is clear that if $k_\delta(\omega) \neq 0$ for $\omega \in \Omega_\ell$ and $\ell \in \mathbb{N}$, then the *stability crossing curves* $\mathcal{T}_\ell$ does not crosses the k_p-axis. Furthermore, the only curve that crosses the k_p-axis, precisely at $k_p = 0$ is $\mathcal{T}_0$, which is the line defined in (3.21). Now, notice that since the physical parameters L, C and R are positive, then $a, b, c \in \mathbb{R}_+$. Now, observing the sign of $k_\delta(\omega)$, one can conclude that a *stability crossing curve* $\mathcal{T}_\ell$ with ℓ even or ℓ odd is located above or below the k_p-axis, respectively. Finally, bearing in mind the above facts, it is useful to introduce the following sets:

$$\mathcal{B}_\ell := \left\{ \widetilde{k} \in \mathbb{R}^2 \;\middle|\; \begin{array}{lll} \widetilde{k}_\delta < k_\delta; & \forall k \in \mathcal{T}_i & \text{for } \ell \in 2\mathbb{N} \\ \widetilde{k}_\delta > k_\delta; & \forall k \in \mathcal{T}_\ell & \text{for } \ell \in 2\mathbb{N}+1 \\ \widetilde{k}_\delta < -\widetilde{k}_p - c & & \text{for } \ell = 0 \end{array} \right. .$$

Hence, the sets $\mathcal{B}_\ell$ are the collection of all points below and above the curves $\mathcal{T}_\ell$ for ℓ odd and ℓ even, respectively, and the set $\mathcal{B}_0$ is the set of all points below the *stability crossing curve* $\mathcal{T}_0$. Finally, one has the following proposition:

Proposition 21. *Given a fixed delay* $\tau \in \mathbb{R}_+$*, there always exists an open connected* stability region $\mathcal{H}$ *defined by:*

$$\mathcal{H} := \bigcap_{\ell \in \mathbb{N}} \mathcal{B}_\ell \bigcap \mathcal{B}_0.$$

Furthermore, $\mathcal{H}$ *is unbounded.*

Proof. Consider the characteristic equation (3.13). Then, setting $k_\delta = 0$ leads to the following polynomial:

$$as^2 + bs + c + k_p = 0.$$

Thus, clearly the roots of this polynomial will be located in the LHP of the complex plane, if and only if $k_p > -c$. In other words, if $k \in \mathcal{L}$, where

$$\mathcal{L} := \{ k \in \mathbb{R}^2 \big| \; k_\delta = 0 \text{ and } k_p > -c \},$$

then the closed-loop system will be asymptotically stable. Now, from the definition of the set $\mathcal{H}$, it is clear to see that $\mathcal{L} \subset \mathcal{H}$. Hence, from the continuity of the roots of Δ with respect to its parameters $(k_p,\, k_\delta\, \tau)$, and since $\mathcal{L}$ is unbounded, the latter inclusion implies that $\mathcal{H}$ is an open, connected and unbounded stability set. □

In order to compute a *stability index* which is the number of roots in the RHP for a given parametrical region it is of interest to determine the roots tendency as the vector k deviates from the curve $\mathcal{T}$. The following results are the main tools applied in this section to achieve such a task.

Proposition 22. *A pair of roots of the characteristic equation* (3.13) *moves from the LHP to the RHP as k crosses a stability crossing curve $\boldsymbol{k}(\omega)$ with $\omega \neq 0$ in the increasing direction of k_χ for $\chi \in \{p, \delta\}$ if:*

$$C_\chi \triangleq b(\tau\omega \cot(\tau\omega) - 1)\cos(\eta_\chi \tau\omega) + \eta_\chi(b\tau + 2a)\omega \sin(\tau\omega) > 0,$$

where the indicative function η_χ is defined as:

$$\eta_\chi := \begin{cases} 0, & \text{if} \quad \chi = p, \\ 1, & \text{if} \quad \chi = \delta. \end{cases}$$

Furthermore, the crossing is from the RHP to the LHP if the inequality is reversed.

Proof. Let $s \in \mathbb{C}$, be a solution of (3.13), i.e.,

$$\Delta\,(s; k_p, k_\delta, \tau) = 0.$$

Now, according to the *Implicit Function Theorem* (see, for instance, [24]), one knows that:

$$\frac{ds}{dk_p} = -\frac{\frac{\partial \Delta}{\partial k_p}}{\frac{\partial \Delta}{\partial s}}, \qquad \frac{ds}{dk_\delta} = -\frac{\frac{\partial \Delta}{\partial k_\delta}}{\frac{\partial \Delta}{\partial s}},$$

where:

$$\frac{\partial \Delta}{\partial s} = 2as + b - \tau k_\delta e^{-\tau s},$$
$$\frac{\partial \Delta}{\partial k_p} = 1, \qquad \frac{\partial \Delta}{\partial k_\delta} = e^{-\tau s}.$$

In order to characterize the tendency of the roots at the imaginary axis, one considers

$s = j\omega$. Then. considering the k_p-direction, one has:

$$\frac{ds}{dk_p} = -\frac{1}{\tau a s^2 + (b\tau + 2a)s + \tau(c + k_p) + b},$$
$$\Rightarrow \mathcal{R}\left\{\left[\frac{ds}{dk_p}\right]^{-1}\right\} = \tau a\omega^2 - \tau(c + k_p(\omega)) - b,$$
$$\Rightarrow \operatorname{sgn}\left(\mathcal{R}\left\{\frac{ds}{dk_p}\right\}\right) = \operatorname{sgn}(b(\tau\omega\cot(\tau\omega) - 1)),$$

Notice that this latter expression is nothing else than C_p. Finally, similar steps can be applied to derive C_δ. □

Observe that Proposition 9 does not give any information about the crossing when $\omega = 0$. The following result fills this gap.

Proposition 23. *Given a fixed delay $\tau \in \mathbb{R}_+$. Then, one root of* (3.13) *crosses from the LHP to the RHP of the complex plane through the origin as k crosses $\mathcal{T}_0$ from left to right if the intersection of k and $\mathcal{T}_0$ is located at the left of the point $k_0 \in \mathcal{T}_0$, defined by:*

$$k_0 := [k_{p_0}, k_{\delta_0}]^T = \frac{1}{\tau}[-\tau b - c, b]^T.$$

Furthermore, the crossing of the root is from the RHP to the LHP if the intersection is located at the right of k_0.

Proof. The proof follows the same ideas used in proof of Proposition 22 setting $s = 0$. Let $s = 0$ and define

$$\mathcal{S}(k_\delta) := \Re\left[\frac{ds}{dk_p}\Big|_{s=0}\right] \equiv \Re\left[\frac{ds}{dk_\delta}\Big|_{s=0}\right] = \frac{1}{b - \tau k_\delta}.$$

Thus, as k crosses in any direction from left to right of $\mathcal{T}_0$, one root of (3.13) crosses from the LHP to the RHP of the complex plane through the origin if $\mathcal{S}(k_\delta) > 0$, which implies that $k_\delta > k_{\delta_0}$. Furthermore, the crossing is from the RHP to the LHP if $\mathcal{S}(k_\delta) < 0$, equivalent to $k_\delta > k_{\delta_0}$. Finally, by simple algebraic manipulations, one can see that the condition $k_\delta > k_{\delta_0}$ implies that $k_p < k_{p_0}$, as stated in Proposition 23. □

3.2.5 $P\delta$: σ-Stability and Fragility

In this section one proposes two auxiliary results to deal with the problems of σ-stability and fragility of a given controller. These results will be useful in the design of a controller that satisfies a given performance (exponential decay rate) as well as some robustness against parametrical uncertainties.

To this end, let us first state the σ-stability problem: Let $\sigma \in \mathbb{R}_-$, the *σ-stability* problem can be described as the task of determining a controller $\boldsymbol{k}$ such that the real part

of the rightmost roots of the characteristic equation (3.13) is located at the left of σ. Let $\mathcal{T}_\sigma$ denote the set of all $\boldsymbol{k}$ such that (3.13) has at least one root on the vertical line of the complex plane defined as $\boldsymbol{L}_\sigma := \sigma + j\omega$ for all $\omega \in \mathbb{R}$. This vertical line is defined as the *σ-axis*. In order to introduce similar results to those presented in Section 2.1.1 one has the following:

Corollary 1. *Let $\omega \in \Omega$, and let $\tau \in \mathbb{R}_+$, $\sigma \in \mathbb{R}_-$ be fixed values. Then, the set $\mathcal{T}_\sigma$ can be computed as:*

$$\mathcal{T}_\sigma = \mathcal{T}_{\overline{\sigma}} \cup \mathcal{T}_{\sigma,0},$$

with

$$\mathcal{T}_{\sigma,0} = \left\{ \boldsymbol{k} \in \mathbb{R}^2 \,|\boldsymbol{k} = \boldsymbol{k}(\sigma, 0) \right\},$$
$$\mathcal{T}_{\overline{\sigma}} = \left\{ \boldsymbol{k} \in \mathbb{R}^2 \,|\boldsymbol{k} = \boldsymbol{k}(\sigma, \omega) \right\}.$$

Consider now the *fragility problem*, which consists of computing the maximum controller parameters deviation d of a given stabilizing controller $\bar{\boldsymbol{k}} := [\bar{k}_p, \bar{k}_\delta]^T$, such that the closed-loop system remains stable, as long as the controller parameters $\boldsymbol{k}$ satisfy the inequality:

$$\sqrt{(k_p - \bar{k}_p)^2 + (k_\delta - \bar{k}_\delta)^2} < d.$$

In order to address this problem, let $\boldsymbol{k}(\omega) = [k_p(\omega), k_\delta(\omega)]^T$ as given in Proposition 20. Bearing in mind this notation and let us introduce the function $\xi : \mathbb{R}_+ \to \mathbb{R}_+$ defined as:

$$\xi(\omega) := \sqrt{(k_p(\omega) - \bar{k}_p)^2 + (k_\delta(\omega) - \bar{k}_\delta)^2}, \tag{3.24}$$

one introduces the following proposition.

Proposition 24. *Let $\bar{\boldsymbol{k}}$ be a stabilizing controller. Then, the maximum parameter deviation d of $\bar{\boldsymbol{k}}$, such that the closed-loop system remains stable, is given by:*

$$d := \min \left\{ \tilde{d},\ \frac{1}{\sqrt{2}} \left| \bar{k}_p + \bar{k}_\delta + c \right| \right\},$$

with $\tilde{d}$ defined as:

$$\tilde{d} := \min_{\omega \in \Omega_f} \{\xi(\omega)\},$$

where Ω_f denote the set of all roots of $f(\omega)$:

$$f(\omega) := \left\langle \boldsymbol{k}(\omega) - \bar{\boldsymbol{k}}, \frac{d}{d\omega} \boldsymbol{k}(\omega) \right\rangle. \tag{3.25}$$

Proof. By assumption $\bar{\boldsymbol{k}}$ is located inside some stability region delimited by some appropriate stability crossing curves, thus, the closed-loop system is unstable if the controller $\bar{\boldsymbol{k}}$ has a parameter deviation such that it crosses for at least one of its boundaries. Therefore, the goal consists in computing the minimal distances between $\bar{\boldsymbol{k}}$ and the different

boundaries of the stability region. In order to compute the minimal distance between a point $\bar{\boldsymbol{k}}$ and the stability crossing curves with $\omega \neq 0$, one needs to identify the points $\boldsymbol{k}(\omega)$ at which the tangent vectors to the curve are orthogonal to $\boldsymbol{k}(\omega) - \bar{\boldsymbol{k}}$. In other words, to find points at which ω is a root of (3.25). Observe that the boundaries of the stability crossing curve related to $\omega = 0$ are described by the line (3.21). Thus, in order to compute the minimal distance to this line, substitute (3.21) in (3.24), which leads to

$$\xi(0) = \sqrt{(k_p - \bar{k}_p)^2 + \left(k_p + \frac{q_0}{p_0} + \bar{k}_\delta\right)^2}.$$

Hence, the gain k_p at which $\xi(0)$ attains its minimum, is given by the solution of the following equation:

$$\frac{d\xi^2(0)}{dk_p} = 4k_p + 2\left(\bar{k}_p - \bar{k}_\delta + \frac{q_0}{p_0}\right) = 0.$$

Then, straightforward computations reveals that this value is given by $\frac{1}{\sqrt{2}}\left|\bar{k}_p + \bar{k}_\delta + c\right|$, which concludes the proof. □

3.2.6 $P\delta$: Numerical Results

All results of this section were obtained by means of the "SimPowerSystems" toolbox in the "Simulink" environment of the software "Matlab". The parameters used in the simulation are summarized in Table 3.1. The tests presented in this section are designed to regulate the output voltage $v_o(t)$ to a nominal value of $V_o := 20$. Recall that the control scheme has the task to regulate the variations of the output voltage $\tilde{v}_o(t)$ to zero in order to satisfy the following: $v_o(t) \to V_o$. The control law proposed for the achievement of this objectives is given by:

$$u(t) = U + \tilde{u}(t),$$

with:

$$\tilde{u}(t) := k_p e(t) + k_\delta e(t - \tau),$$

where the error signal is defined as:

$$e(t) := 0 - \tilde{v}_o(t) = V_o - v_o(t),$$

and the nominal value U can be obtained directly from (3.6).

Consider the controller's delay value $\tau = 5 \times 10^{-5} s$ for the $P - \delta$ controller (9) along with the parameters given in Table 3.1. Figure 3.13a, first depicts the delay-independent stability region obtained directly from Proposition 18. Second, it illustrates the stability region for the given fixed value τ obtained by means of Proposition 21 and computed by applying Proposition 20.

Making use of these results, the $P - \delta$ controller is set as $k = [50, 1]^T$. Three different values of τ are proposed in order to verify the independent stability condition. The results of the regulation of $v_o(t)$ for this test are depicted in Fig. 3.13b.

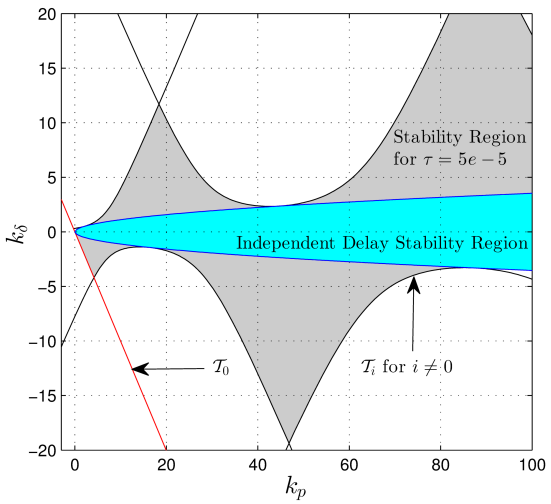

(a) Stability Region for $\tau = 5 \times 10^{-5} s$.

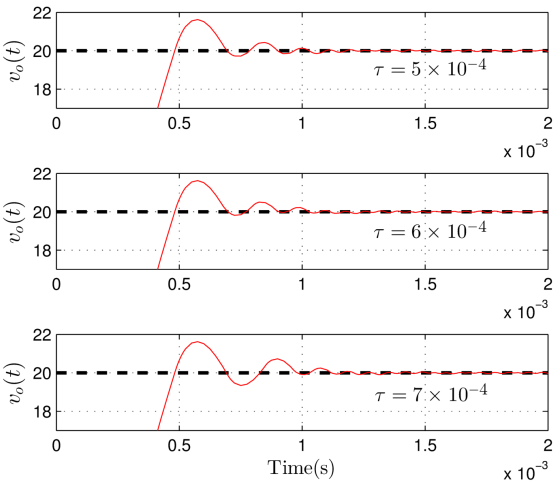

(b) Closed-Loop System Response.

Figure 3.13: Stability Analysis

In order to show how the stability region for the fixed value $\tau = 5 \times 10^{-5}$ behaves, a large view of this region is depicted in Fig. 3.14a.

In the following, let us consider the stability index η (number of roots in the RHP) for different regions delimited by the *stability crossing boundaries*. To this end, Fig. 3.14b presents the results of applying Propositions 22 and 23, where the colors "red", "green", "blue" and "black" stands for $C_p > 0$, $C_\delta > 0$, $C_p C_\delta > 0$ and $(C_p < 0)\&(C_\delta < 0)$ = 'true', respectively.

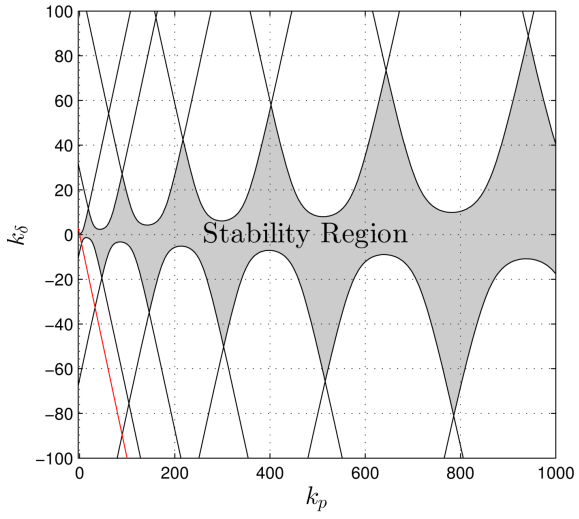

(a) Stability Region for $\tau = 5 \times 10^{-5}$.

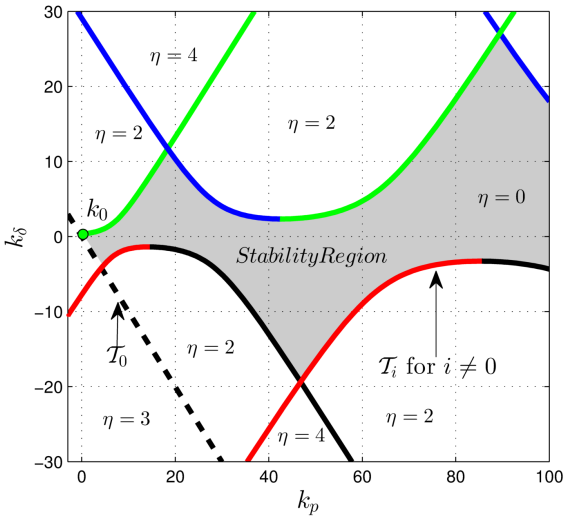

(b) Stability Index Analysis.

Figure 3.14: Stability Index

Finally, one applies the auxiliary results shown in Section 3.2.5. First one uses a σ-

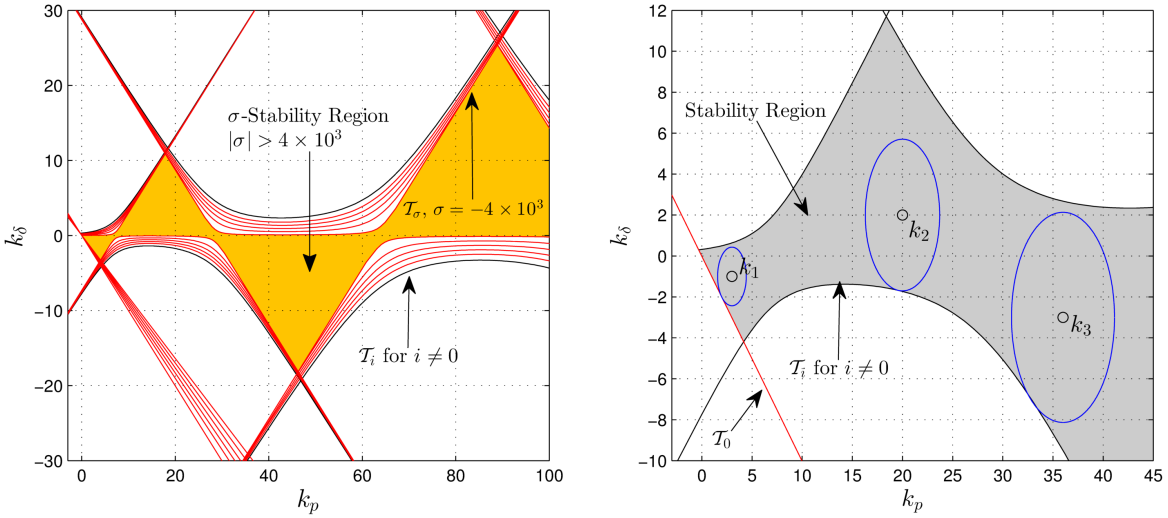

(a) σ-Stability Region. (b) Fragility Analysis.

Figure 3.15: σ Stability

Stability Analysis varying σ from 0 to -4×10^3, the results are summarized in Fig. 3.15a. From this figure, one denotes the finding of a stability region that ensures that all roots of the characteristic equation of the closed-loop system has real part $\sigma < -4\times10^3$. In other words, that the exponential decay rate of the closed-loop system response is smaller than 4×10^3. Second, one tests the fragility for three different controllers, the results are summarized in Table 3.2 and illustrated in Fig. 3.15b.

Table 3.2: Fragility Analysis

k	Ω_f	d_o	d_f	d
k_1	$\{38110, 63023, 252843\}$	1.1431	1.6192	1.4319
k_2	$\{60765, 251703, 314353\}$	15.574	3.7049	3.7049
k_3	$\{120762, 253594, 31548\}$	23.3522	5.1322	5.1322

3.3 Furuta Pendulum: Input Delay

First, one of the most interesting aspects of this study is the manipulation of the closed-loop response by adding a delayed action in the control scheme, experimental tests must be developed to analyze the potential advantages for this converter. Second, one would like to enhance the fact that the stability region shown in Section 3.2.3 appears to be unbounded. In terms of the differential equation related to this system this is perfectly accurate. However, in a real scenario this type of switching circuits have an extra constraint, the control law must be bounded ($u(t) \in [0, 1]$). An open problem for this system is to find the subregion inside the stability region such that this constraint is considered.

In mechanical systems, one of the classical problems of automatic control is the stabilization of the inverted pendulum on its unstable equilibrium point at the upright position. In this work one studies this task in the case of the so-called Furuta pendulum (see Fig. 3.16), also known as the rotatory inverted pendulum. In order to achieve this task, one proposes the use of some standard Linear Quadratic Regulation (LQR) controller. Some insights concerning this control law for three underactuated systems (inverted pendulum on a cart, inverted wedge and ball and beam system) can be found in [59]. Furthermore, one considers a time-delay in the state feedback loop which can be inherent to the system due to data processing, or even designed for performance requirements.

It is worth noticing that even in the simple case of the inverted pendulum, the presence of delays in the input may induce some unexpected properties as, for instance a triple root at the origin (see, for instance [11] and the references therein). In order to consider this scenario in the control scheme design, one uses the results shown in [42] for the inverted pendulum and cart system. This shows a simple method on how to compute the critical delay value in the state feedback loop in which the closed-loop system loses stability. Moreover, one explores the behavior of the stability conditions by considering an auxiliary pair of gains for the position regulation of both angles of the Furuta pendulum. Numerical simulations were conducted in Matlab-Simulink to illustrate how sensitive the tuning of these parameters can be. The main contribution of the section is to construct some appropriate tuning rules able to enlarge the delay margins. Illustrative examples confirm such an approach.

This section is organized as follows. Section 3.3.1 concerns to the Furuta pendulum modelling and the LQR control design for the stabilization in the delay-free scenario. Section 3.3.2 shows a simple method for computing the critical time-delay value in the state feedback loop at which the closed-loop system loses stability. Also, the stability boundaries for two auxiliary gains and the time-delay are characterized. Finally, section 3.3.3 shows some numerical results obtained using"Matlab".

Furthermore, one invites the reader to visit the website refereed in Section 3.3.3, where illustrative support material for the understanding of the results discussed in this section is depicted.

3.3.1 Prerequisites: Pendulum Dynamics and LQR Control

This section includes the basics of the design of an LQR based control scheme in the delay-free scenario for the Furuta pendulum stabilization problem. It covers the Furuta pendulum modelling and the LQR controller gain tuning. As discussed in the sequel, one introduces the Furuta pendulum nonlinear model and a linear representation valid uniquely around an operating point of interest.

Figure 3.16 depicts the representation of the Furuta pendulum, also known as the rotatory inverted pendulum. This mechanical system has two degrees of freedom and two rotatory joints. It consists in three essential components: a motor and two bars known as *arm* and *pendulum*. The motor's shaft is fixed at one end of the arm inducing a rotatory movement of this bar. The pendulum is placed at the opposite end to the motor's shaft with a rotatory joint which provides a free rotatory movement in a normal plane to the

arm. As shown in the schematic representation illustrated in Fig. 3.16, θ_0 and θ_1 are the arm and pendulum angular positions, respectively. θ_0 is measured with respect of the X-axis and θ_1 with respect to the upright position. $\mathcal{T}$ concerns to the torque applied to the arm and it is provided by the motor. I_0 and J_1 stands for the motor-arm and pendulum inertia values and L_0 and l_1 represent the arm length and the pendulum's center of mass location, respectively. Finally, m_1 represents the mass of the pendulum, while g denotes the gravitational acceleration.

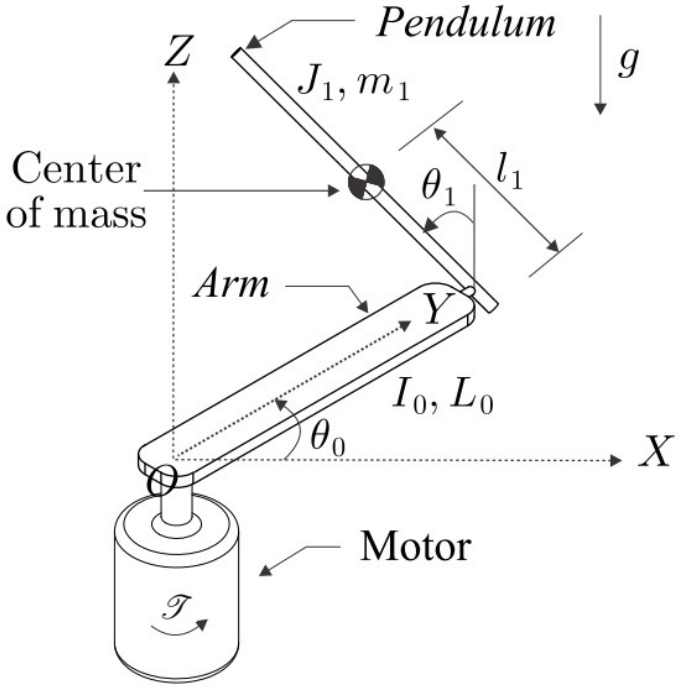

Figure 3.16: Furuta Pendulum Diagram ([30]).

As detailed in [30] (see also, [18] and [19]), the Lagrangian formulation of the Furuta pendulum consists in the following:

$$M(q)\ddot{q} + C(q,\dot{q})\dot{q} + g(q) = F,$$

where:

$$M(q) := \begin{bmatrix} I_0 + m_1(L_0^2 + l_1^2 \sin^2\theta_1) & m_1 l_1 L_0 \cos\theta_1 \\ m_1 l_1 L_0 \cos\theta_1 & J_1 + m_1 l_1^2 \end{bmatrix},$$

$$C(q,\dot{q}) := \begin{bmatrix} c_{11} & c_{12} \\ c_{21} & 0 \end{bmatrix}, \qquad g(q) := \begin{bmatrix} 0 \\ -m_1 l_1 g \sin\theta_1 \end{bmatrix},$$

$$
\begin{aligned}
c_{11} &:= \frac{1}{2} m_1 l_1^2 \dot{q}_2 \sin(2q_2), \\
c_{12} &:= -m_1 l_1 L_0 \dot{q}_2 \sin q_2 + \frac{1}{2} m_1 l_1^2 \dot{q}_1 \sin(2q_2), \\
c_{21} &:= -\frac{1}{2} m_1 l_1^2 \dot{q}_1 \sin(2q_2),
\end{aligned}
$$

$$
F := \begin{bmatrix} \mathcal{T} \\ 0 \end{bmatrix}, \qquad q := \begin{bmatrix} q_1 \\ q_2 \end{bmatrix} = \begin{bmatrix} \theta_0 \\ \theta_1 \end{bmatrix}.
$$

In this work one focuses on the control problem of stabilization and regulation of the solution pair $(\theta_0(t), \theta_1(t))$ around an operating point. Inspired by [30], one considers the corresponding system's linearization:

$$
\dot{x} = Ax + Bu, \tag{3.26}
$$

where the state of the system x and the control variable u are defined as:

$$
x := \begin{bmatrix} x_1 \\ x_2 \\ x_3 \\ x_4 \end{bmatrix} = \begin{bmatrix} \theta_0 \\ \dot{\theta}_0 \\ \theta_1 \\ \dot{\theta}_1 \end{bmatrix}, \qquad u := \mathcal{T}.
$$

The constant matrices A and B are given by:

$$
A = \begin{bmatrix} 0 & 1 & 0 & 0 \\ 0 & 0 & \alpha & 0 \\ 0 & 0 & 0 & 1 \\ 0 & 0 & \beta & 0 \end{bmatrix}, \qquad B = \begin{bmatrix} 0 \\ \gamma \\ 0 \\ \epsilon \end{bmatrix},
$$

where:

$$
\begin{aligned}
\alpha &:= \frac{-g m_1^2 l_1^2 L_0}{I_0(J_1 + m_1 l_1^2) + J_1 m_1 L_0^2}, \quad \beta := \frac{(I_0 + m_1 L_0^2) m_1 l_1 g}{I_0(J_1 + m_1 l_1^2) + J_1 m_1 L_0^2}, \\
\gamma &:= \frac{J_1 + m_1 l_1^2}{I_0(J_1 + m_1 l_1^2) + J_1 m_1 L_0^2}, \quad \epsilon := \frac{-m_1 l_1 L_0}{I_0(J_1 + m_1 l_1^2) + J_1 m_1 L_0^2}.
\end{aligned}
$$

Notice that this system is valid for any operation close to the unstable equilibrium point:

$$
\begin{bmatrix} \theta_0^* & \dot{\theta}_0^* & \theta_1^* & \dot{\theta}_1^* \end{bmatrix}^T = \begin{bmatrix} 0 & 0 & 0 & 0 \end{bmatrix},
$$

(that is, the pendulum is located at the upright position).

As mentioned above, in order to stabilize the linear system (3.26) through a state

feedback control law one uses a similar approach to the one presented in [42]. This is known as the standard LQR control problem. The technique consists in computing the optimal solution for the linear quadratic cost functional:

$$J = \inf_{u(t)\in L_2(0,\infty)} \int_0^\infty \left[x(t)^T Q x(t) + r u(t)^2\right] dt. \tag{3.27}$$

In this expression, the weights $Q \geq 0$ and $r \geq 0$ are chosen with the purpose of reducing the states x and the cost of the control u. Qualitatively, if Q is a diagonal matrix, the position of the greater value of this matrix represents the most important state to be reduced. In the same manner, as r is chosen with a greater value, in such a way that the energy provided by the control law u must be lower.

The solution to the functional (3.27) is the state feedback control law:

$$u(t) = -K^* x(t) = r^{-1} B^T P x(t),$$

where:

$$K^* = [k_a, k_b, k_c, k_d] = -r^{-1} B^T P,$$

and P is the unique symmetric positive-defined solution to the Riccati equation:

$$A^T P + PA - PBr^{-1}B^T P + Q = 0.$$

3.3.2 Controllers Tunning: Delay Margin and Auxiliary Gains

This section contains two stability analysis by considering a time-delay in the state feedback loop. First, one computes the critical delay value in the feedback loop for a proper choice of K^*. Second, one proposes two auxiliary gains which will give us two degrees of freedom (2-DOF), allowing to improve the system's response.

First, it is well known that in a closed-loop system, if the control law is implemented by means of a digital platform, then, there always be present a time-delay due to the computational data processing. In this regard, the delay is a consequence of sensor with built-in data processing. In this section one aims to characterize this behavior by considering a time-delay in the control law.

Having designed the vector gain K^* as shown in the previous section, one proposes the following:

$$u(t) = -K^* x(t - \tau), \tag{3.28}$$

where $\tau > 0$ is a fixed delay value. Furthermore, one may notice that τ can be defined as $\tau := \tau_p + \tau_d$ where the time-delay values τ_p and τ_d refers to the data processing and, to a control design parameter, respectively.

Remark 9. *It is well known that the stability of the closed-loop system is directly related to the location of the roots of the characteristic equation (see, [49], for further details). More precisely, the closed-loop system is stable if and only if all the roots of the characteristic equation are located in the LHP (Left-Half Plane) of the complex plane.*

Since for $\tau = 0$ the closed-loop system is locally asymptotically stable around the origin, therefore, all of the roots of the characteristic equation given by:

$$\Delta_0(s) := \det\{sI - (A - BK^*)\} = 0,$$

have negative real parts. In other words, all of its roots remain in the LHP of the complex plane for a proper choice of K^*. Now, by taking into account the control law (3.28), the characteristic equation of the closed-loop system can be expressed as:

$$\Delta_\tau(s) = \det\left\{sI - (A - BK^* e^{-\tau s})\right\} = 0,$$

or more compactly as:

$$\Delta_\tau(s) = P(s) + Q(s)e^{-\tau s}, \tag{3.29}$$

where:

$$\begin{aligned} P(s) &= s^4 - \beta s^2, \\ Q(s) &= (k_b\gamma + k_d\epsilon)s^3 + (k_a\gamma + k_c\epsilon)s^2 \\ &+ k_b(\alpha\epsilon - \beta\gamma)s + k_a(\alpha\epsilon - \beta\gamma). \end{aligned}$$

Remark 10. *As mentioned by [49], this type of function ($\Delta_\tau(s)$) is known as a quasi-polynomial, one of its main differences with respect to a common polynomial, is that it has an infinite number of roots. Furthermore, the roots of $\Delta_\tau(s)$ move continuously with respect to variations of its parameters (coefficients, delay) and there is always a finite number of roots at the right side of any vertical line of the complex plane.*

The appropriate computation of the critical delay value at which the closed-loop system loses stability is given below:

Proposition 25. *The closed-loop system is asymptotically stable for any delay value $\tau \in [0, \tau_c)$, where:*

$$\tau_c = \min\left\{\tau^* \in \mathbb{R} \,|\tau^*(\omega^*) > 0, \omega^* \in \Omega_p\right\}. \tag{3.30}$$

where:

$$\tau^*(\omega^*) = \frac{1}{\omega^*}\left[\arg\left\{\frac{Q(i\omega^*)}{P(i\omega^*)}\right\} + 2n\pi\right], \qquad n \in \mathbb{Z}, \tag{3.31}$$

and where the set Ω_p is defined as the set of all real roots of the following equation:

$$|Q(i\omega^*)|^2 - |P(i\omega^*)|^2 = 0. \tag{3.32}$$

Proof. By taking into account Remark 10, and the fact that the closed-loop system is stable for $\tau = 0$ implies that for $\tau > 0$ sufficiently small all the roots of (3.29) will remain on the LHP of the complex plane. Moreover, there is a critical value τ such that (3.29) has at least one root on the imaginary axis and hence, such a value induces to the closed-loop system to lose stability.

As can be seen in [50], there exists a value τ such that the quasi-polynomial $\Delta_\tau(s)$ has a root on the imaginary axis in $s = i\omega^*$, if and only if, the following condition:

$$\left|\frac{Q(i\omega^*)}{P(i\omega^*)}\right| = 1, \tag{3.33}$$

holds for some value $\omega^* \in \mathbb{R}_+$. Moreover, the correspondent time-delay value can be computed by (3.31). Furthermore, notice that the condition (3.33) can be rewritten easily as (3.32), which is a polynomial, implying that it has a finite number of solutions. Finally, by defining Ω_p as the set of all real roots of (3.32), the critical delay value can be computed as in (3.30). □

Second, one shows a method for computing the margin delay in order to maintain stability in the closed-loop system. In this section, one proposes a 2-DOF controller, which will be shown to be useful when the inherent delay in the system is larger than the critical delay computed above.

Let K^* be a stabilizing gain for the delay-free scenario, computed using the results shown above. One considers as our new state feedback gain:

$$K = K^* + [k_1, 0, k_2, 0], \tag{3.34}$$

where $k_1, k_2 \in \mathbb{R}$ are compensating gains in both positions (θ_0, θ_1) feedback loop. Considering this extended controller, the characteristic function of the closed-loop system is given by:

$$\Delta_\tau^*(s) = P(s) + \left(Q(s) + (\alpha k_1 + \epsilon k_2)s^2 + k_1(\alpha\epsilon - \beta\gamma)\right) e^{-\tau s}.$$

Remark 11. *It is worth noticing that the proposed state feedback gain* (3.34) *has a particular structure which provides two degrees of freedom in the positions regulation problem. One is interested in such a structure, since the appropriate regulation of position implies the regulation of velocity to the origin.*

Now, one introduces some notation: let $\rho(\omega) := \alpha\epsilon - \gamma(\omega^2 + \beta)$ and, $R(\omega)$ and $I(\omega)$ be the real and imaginary part of $Q(i\omega)$, respectively. Furthermore, it is worth noticing that $P(i\omega) \in \mathbb{R}$, for all real ω. Having explained this approach, the following result characterize the triplet (k_1, k_2, τ) at which the system has at least one root on the imaginary axis.

Proposition 26. *Let K^* be a stabilizing gain of the delay-free scenario and let ρ, I and R be as defined previously. Then, the characteristic function $\Delta_\tau^*(s)$ has at least two roots on the imaginary axis at $s = \pm i\omega$, if and only if:*

$$\tau_\delta = \frac{1}{\omega}\sin^{-1}\left\{-\frac{I(\omega)}{P(i\omega)}\right\}, \qquad \forall\omega \in \Omega_d, \tag{3.35}$$

where:

$$\Omega_d := \left\{\omega \in \mathbb{R} \,\middle|\, \left|\frac{I(\omega)}{P(i\omega)}\right| \leq 1\right\},$$

and the gains k_1 and k_2 belong to the family of lines:

$$k_2 = \frac{1}{\epsilon\omega^2}\left\{\rho(\omega)k_1 + R(\omega) - I(\omega)\cot(\tau\omega)\right\}, \tag{3.36}$$

for any $\omega \in \Omega_d$. Furthermore, it has a single root at the origin, if and only if:

$$k_1 = -k_a. \tag{3.37}$$

Proof. Consider the characteristic function $\Delta_\tau^*(s)$, by setting $s = i\omega$ the following equations system is obtained:

$$\Re\left\{\Delta_\tau^*(s)\right\} = 0, \qquad \Im\left\{\Delta_\tau^*(s)\right\} = 0, \tag{3.38}$$

by trying to solve this system for k_1 and k_2, the following is computed:

$$\begin{bmatrix} \rho(\omega)\cos(\tau\omega) & -\epsilon\omega^2\cos(\tau\omega) \\ -\rho(\omega)\sin(\tau\omega) & \epsilon\omega^2\sin(\tau\omega) \end{bmatrix} \begin{bmatrix} k_1 \\ k_2 \end{bmatrix} = r(\omega), \tag{3.39}$$

where $r(\omega)$ is a vector-valued function which can be easily deduced and for the sake of brevity is omitted. It is clear to see that the determinant of the matrix related to equation (3.39) is equal to zero and, therefore, does not have a unique solution.

However, one can rewrite (3.38) as:

$$\begin{aligned} \ell(\omega)\cos(\tau\omega) + I(\omega)\sin(\tau\omega) + P(i\omega) &= 0, \\ \ell(\omega)\sin(\tau\omega) + I(\omega)\cos(\tau\omega) &= 0, \end{aligned}$$

where:

$$\ell(\omega) = \rho(\omega)k_1 - \epsilon\omega^2 k_2 + R(\omega).$$

By solving the system of equations formed by (3.40) and (3.41) for $\ell(\omega)$, and consequently comparing the obtained expressions the following condition must be fulfilled:

$$P(i\omega)\sin(\tau\omega) + I(\omega) = 0. \tag{3.42}$$

On one hand, any pair $(\tau, \hat{\omega})$ satisfying condition (3.42) also induces to equations (3.40) and (3.41) to be equivalent. On the other hand, for every $\hat{\omega} \in \mathbb{R}$ there exist an infinite set of pairs (k_1, k_2) along the line (3.41), which also solves (3.40).

The proof ends by solving τ and k_2 from (3.42) and (3.41) and obtaining conditions (3.35) and (3.36), respectively. Furthermore, condition (3.37) can be verified simply by solving k_1 from $\Delta_\tau^*(0) = 0$ and the set Ω_d is defined to consider only real solutions of (3.35). □

3.3.3 Numerical Results

For further details on the examples proposed in the sequel, one refers to the website [1]. Such a material is composed by a variety of animations of the Furuta Pendulum system and system response signals behavior. The support material is listed below:

A.1 Free Motion Behavior of the Furuta Pendulum with initial conditions:

$$\Big[\theta_0(0), \dot{\theta}_0(0), \theta_1(0), \dot{\theta}_1(0)\Big]^T = \Big[\frac{\pi}{4}, 0, \frac{\pi}{4}, 0\Big]^T.$$

A.2 Controlled Motion with a delay value $\tau = 0$.

A.3 Controlled Motion with a delay value $\tau = 0.5\tau_c$.

A.4 Controlled Motion with a delay value $\tau = 0.9\tau_c$.

A.5 Unstable Response of the Furuta Pendulum with a delay value $\tau = \tau_c$.

A.6 Smooth Time Delay Variation of the System Transient Response from $\tau = 0$ to $\tau = \tau_c$.

The parameters used in these simulations are taken from the experimental test bench studied in [30] and are summarized in Tab. 3.3. The initial conditions settled for the following numerical results are chosen near the origin as:

$$\Big[\theta_0(0), \dot{\theta}_0(0), \theta_1(0), \dot{\theta}_1(0)\Big]^T = \Big[\frac{\pi}{10}, 0, \frac{\pi}{9}, 0\Big]^T.$$

Table 3.3: Parameters

Symbol	Value	Unit
g	9.81	$\frac{m}{s^2}$
l_1	129×10^{-3}	m
L_0	155×10^{-3}	m
m_1	22.18×10^{-3}	Kg
J_1	184.50×10^{-6}	$Kg.m^2$
I_0	238.49×10^{6}	$Kf.m^2$

As stated in section 3.3.2, in order to compute the state feedback gain K^* one needs

[1] https://furutablind.wixsite.com/furuta

to chose the weights Q and r. One set $r = 1$ and:

$$Q = 1 \times 10^{-4} \begin{bmatrix} 1 & 0 & 0 & 0 \\ 0 & 0.01 & 0 & 0 \\ 0 & 0 & 1 & 0 \\ 0 & 0 & 0 & 0.01 \end{bmatrix},$$

with the purpose of giving more importance to the convergence of the states θ_0 and θ_1 than to the angular velocities or the control effort. More precisely, one sets the position correspondent values in Q one hundred times larger than the ones set for the angular velocities. Given this parameters, the state feedback gain is computed as:

$$K^* = -\left[0.0100, 0.0049, 0.1755, 0.0161\right]^T.$$

Now, the proposed strategy is to find the critical delay in the state feedback loop such that the closed-loop system becomes unstable. Having calculated the gain value K^* and according to Proposition 25, one uses equation (3.32) to compute the set Ω_p. This consists in one element $\omega^* = 30.88$. Second, one calculates the critical delay value $\tau_c = 0.0344s$ from expression (3.30).

One shows the results obtained under these considerations. Fig. 3.17 exhibits the closed-loop system response under different time-delay values below the critical condition: $\tau = 0, 0.5\tau_c, 0.9\tau_c$. The results are illustrated from the nonlinear and linear model point of view. As can be seen in Fig. 3.17, as the time-delay value tends to approximate to the critical value τ_c, the system response tends to have a more oscillatory behavior in both models. This can be explained from the linear model perspective since as $\tau \to \tau_c$, the rightmost root of the characteristic equation (3.29) approaches the imaginary axis. Illustrative animations of the Furuta Pendulum for this particular cases can be found in A.2, A.3 and A.4. Furthermore, A.6 corresponds to the continuous change in the transient response as $\tau \to \tau_c$.

Moreover, in Fig. 3.18, one presents an unstable response of the closed-loop system by setting $\tau = \tau_c$. At this value, the characteristic equation of the closed-loop system has at least one pair of roots on the imaginary axis. One of the main features of this test is that the nonlinear model clearly loses stability against the linear model which behaves more similar to a marginally stable system. The behavior of the Furuta Pendulum in this conditions is illustrated in A-5.

Finally, one uses the result shown in Proposition 26 to compute the stability boundaries for the auxiliary gains k_1 and k_2. The results are depicted in Fig. 3.19 (left), notice that since K^* is a stabilizing gain for the delay-free scenario then, the origin of this figure illustrated by A is a stable point. Moreover, by remark 10 any variation of the parameters (k_1, k_2, τ) around the origin without crossing any stability boundary is stable. Therefore, the region around the origin delimited by the stability boundaries is a stable region. The point B depicts the parameters setting $(0, 0, \tau_c)$ which corresponds to the boundary of the previous analysis. As expected, this point lays on the stability boundaries. Furthermore,

the line from A to B corresponds to the test illustrated in Figs. 3.17 and 3.18.

In order to verify this result, in Fig. 3.19 (right) one explores the region in which $k_1 = 0.005$ illustrating the critical delay τ_c. Furthermore, considering a larger delay $\tau = 0.04$, one tests this regions by setting the (k_2, τ) pair parameters p_1, p_2 and p_3 in the closed-loop system with initial conditions:

$$\left[\theta_0(0), \dot{\theta}_0(0), \theta_1(0), \dot{\theta}_1(0)\right]^T = \left[\frac{\pi}{20}, 0, \frac{\pi}{20}, 0\right]^T.$$

The results are shown in Fig. 3.20, where is clear to see that the system has a stable response when p_1 and p_2 are chosen and an unstable response for p_3.

3.4 Concluding Remarks

In this chapter one studies the control scheme design of a variety of applications by using delay-based controllers. First, experimental results of a virtual and a teleoperated bilateral control schemes using $P\delta$ controllers are presented. Second, a delay-based control scheme design for a power dc/dc converter of type buck is studied. One carries-out the stability analysis for two controllers, the $P\delta$ and $P\delta I$ controller using the results addressed in the last chapter. Finally, one studies a LQR control scheme for the Furuta pendulum by considering input delay. Also, one explores the potential of this delay design for closed-loop response manipulation. Numerical results illustrating the control design and the performance of these delay-based schemes are addressed for all this applications. In the following chapter, similarly at this, one studies a photo-voltaic application, however, the detail and discussion are clearly deeper and one presents a variety of experimental results.

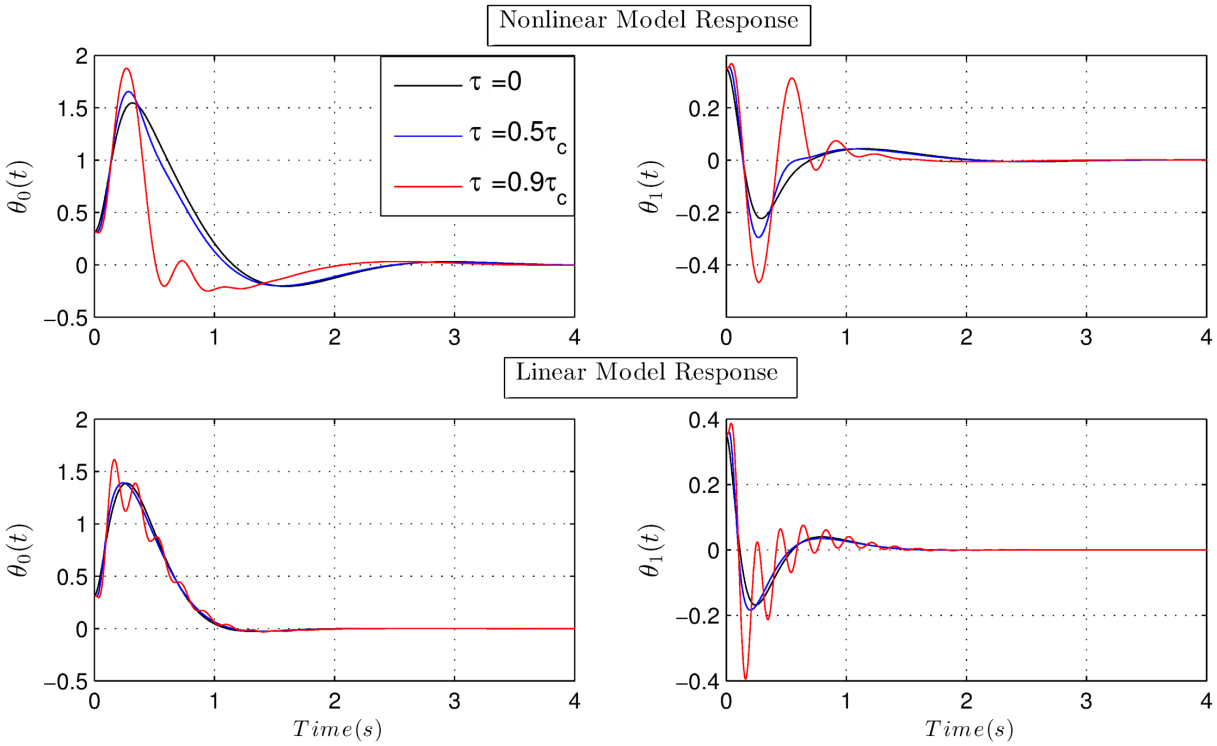

Figure 3.17: Closed-Loop System Response Under Different Delay Values.

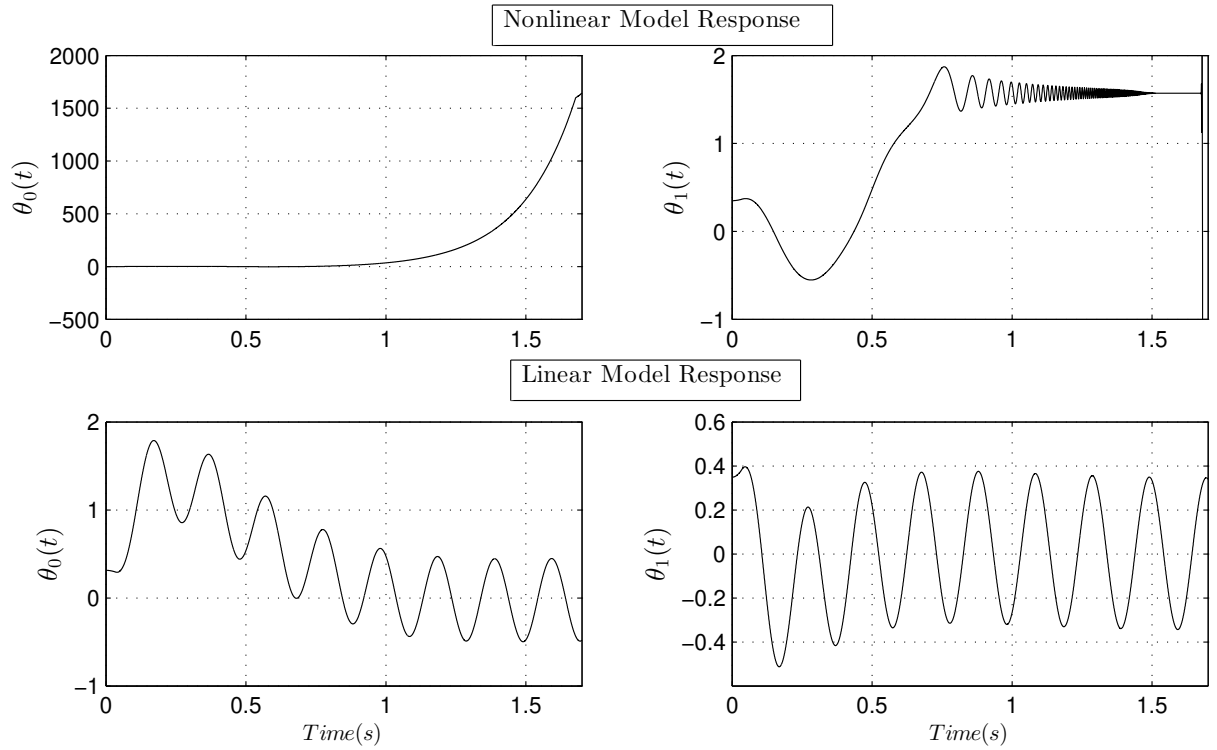

Figure 3.18: Closed-Loop System Unstable Response Under a Critical Delay.

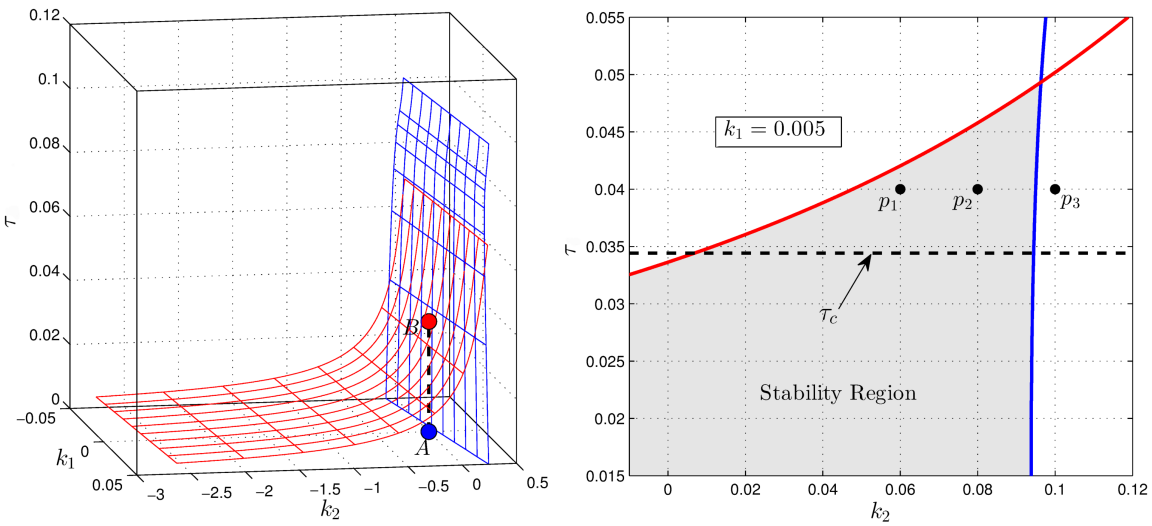

Figure 3.19: Stability Boundaries: (left) (k_1, k_2, τ), (right) $(0.005, k_2, \tau)$.

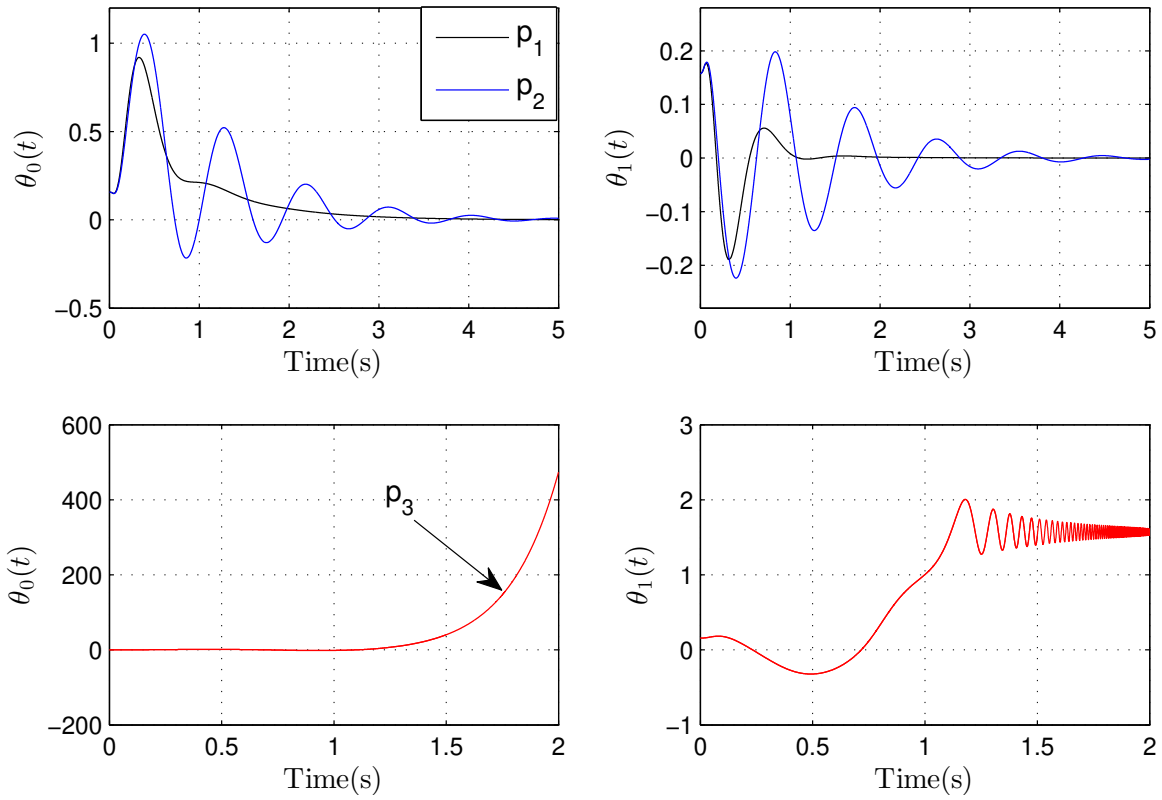

Figure 3.20: Closed-Loop System Response Setting the Tunning Parameters p_1, p_2 and p_3.

Chapter 4

Stabilizing Integrators: Photo-voltaic Application

Renewable energies have been one of the main areas of interest by governments and organizations of almost all countries, since these type of energy sources are considered the cleanest for the environment. As it has been stated in [64], among the alternatives of renewable energies, *photovoltaic (PV) systems has experienced significant growth in recent years, close to 60% in Europe*. In fact, as discussed in [14, 40], these systems are being integrated to the electrical grid more commonly than in past years.

Based on the above observations, it becomes evident that higher precision and safety requirements will be demanded by the power grid companies as this tendency continues to expand. In order to provide such features, power electronics attends directly the high efficiency power conversion problem. In PV systems, it is well known that one of the main solutions to this problem is the application of MPPT techniques [9]. In this sense, the most important task relies on the proper control scheme designed to be applied to a power electronics device.

The main idea behind MPPT techniques consists in finding the Maximum Power Point (MPP) by adjusting the impedance perceived by the PVM (Photovoltaic Module). This process consists in *two dependent tasks*. First, a control scheme is proposed to regulate the PV voltage at the MPP. Second, an algorithm to compute the optimal reference must be designed. In order to solve such control problems, this work uses a topology based on a boost dc/dc converter. As a first approach to the development of an MPPT strategy, our main contribution is focused on the *PV voltage regulation problem*. As discussed in [37, 67], a variety of benefits can be achieved by using MPPT techniques in conjunction with closed–loop control strategies, such as *efficiency improvement* and *low frequency disturbances rejection* in the load terminals.

It is worth mentioning that there exist several works that have considered a similar topology but using different control methods. Some of these works are summarized in Table 4.1. From this table, one can note a variety of control techniques with different needs for its implementation. One may notice the following observations: (i) all solutions require at least two sensors; (ii) moreover, at least a current sensor is needed; (iii) not all

solutions are evaluated under transient conditions. By contrast, the *delay-based control scheme* proposed in this work requires: (i') only one voltage sensor and consequently, (ii') no current sensors are needed; (iii') also, experimental results considering abrupt irradiance disturbances are presented.

We would like briefly to emphasize some of the advantages of not requiring a current measurement. One of the main benefits is that current sensors are often large and of expensive implementation in the control system. By contrast, we are aware that current measurement is commonly available on MPPT systems since MPPT algorithms such as P&O regularly need it. However, this can be avoided by using the fractional method (see, for instance, [44]) and moreover, it can be also estimated; such is the case in [47], in which a model-based predictive control principle is used to predict the states of the PV system.

The method proposed in the sequel is inspired by the ideas developed by the authors in [17, 53] and [72]. On one hand, the work made in [17] proposes the use of a buck dc/dc converter using feedback linearization and a low-order controller of PID type. Among low-order controllers, those of PID-type have shown a well-known suitable performance coping with parametrical uncertainties and undesired disturbances, also, to achieve elimination of steady-state errors and transient response manipulation (see, for instance, [7, 61]). However, as reported in [7, 4], one of the main drawbacks of PID controllers is related to the tuning of the derivative action which may amplify additive high-frequency noise in measurements.

As seen in the sequel, the feedback linearized system using a boost dc/dc converter has a relative degree two, that roughly speaking, consists in a chain of two integrators. Thus, one of the main contributions of this chapter is to propose a delay–based control scheme in conjunction with explicit analytical tools that allows designing non-fragile stabilizing controller for these types of systems. In the remaining part of the chapter, this scheme will be called Pδ controller.

In this vein, a more complex behavior is proposed through the delay–based feedback loop. In contrast with the obtained second-order open-loop transfer function, a delayed system has an infinite number of characteristic roots. On one hand, due to the fact that these roots are deeply related to the behavior of the output of the system, we are dealing with a more diverse system in terms of dynamical behavior. On the other hand, this mere fact complicates the overall stability analysis, since the classical Routh-Hurwitz criterion of linear systems is no longer applicable. Nevertheless, as stated in [29], besides the fact that including a delay will induce a more complex behavior, it is important to point out that the delay phenomenon can also promote the system's stability, where classical PID controllers fail to stabilize the closed-loop system.

Encouraged by the previous observations, in this work we propose the use of $PI\delta$ controllers instead of standard of PID type in order to achieve two technical objectives. First, as seen in the experimental results section, to decrease the number of sensors needed for the implementation to only one voltage sensor. Second, as mentioned in [32] and references therein, to reduce the processing effort in the application of such a controller in comparison to one of PID type. This is due to the fact that delaying a signal is numerically simpler than derivating it, in which some numerical procedure or algorithm is required. Moreover, we propose the adding of an integral action by designing a $PI\delta$ controller to

Table 4.1: Comparative Table of Control Techniques for PV MPPT Systems Using a Boost dc/dc Converter

References	Number of Sensors	Control Strategy	Settling Time	Evaluation Under Transient Conditions
[10]	2–(v_{pv}, i_{pv})	Sliding Mode	$0.2ms$	✓
[71]	2–(v_{pv}, i_L)	Adaptive	$14.3ms$	×
[60]	3–(v_{pv}, i_{pv}, i_L)	Double Integral Sliding Mode	$150ms$	×
[22]	2–(v_{pv}, i_{pv})	Sliding Mode	$0.5ms$	✓
[63]	3–(v_{pv}, i_{pv}, i_L)	Adaptive Passivity	$300ms$	×
[13]	4–$(v_{pv}, i_{pv}, i_L, v_o)$	Backstepping Sliding Mode	$50ms$	✓
[39]	4–$(v_{pv}, i_{pv}, i_L, v_o)$	Sliding Mode	$1ms$	✓

achieve steady state error equal to zero in its experimental application and to cope with parametric uncertainties.

The main contributions of this section can be summarized as follows:

C1: We present a control scheme for the proper regulation of the PV voltage of a PVM by using a boost dc/dc converter and a delay–based controller guaranteeing internal stability;

C2: A tunning methodology for a PIδ controller is described. In fact, this methodology provides necessary and sufficient conditions for the stabilization of the closed-loop system;

C3: Experimental tests for this delay–based control scheme are addressed using a 350 W boost dc/dc prototype and a solar array simulator. Particularly, we test the closed-loop scheme under set-point changes and solar irradiation disturbances.

The experimental test bench used for the validation of this control scheme consists in a standalone PV system with a battery bank as load. The main goal is to validate a scenario with a fixed dc bus, in this case emulated by a battery bank. Such a scenario can be found also on grid-connected PV power systems. Moreover, this can be applied in the same manner to an MPPT distributed system in which such a voltage output is not fixed. Also, notice that even without a constant output voltage only voltage sensors are required, and still no current sensors are needed.

The remaining chapter is organized as follows: Section 4.1 discusses the modeling of the boost dc/dc converter on an MPPT system. Section 4.2 describes the control scheme proposed and some important remarks are addressed, such as the stability of the zero dynamics. Section 4.3 concerns to the presentation of the necessary results to develop a stability analysis of such delayed control scheme through a frequency-based approach (see also the ideas proposed by Neimark [51], related to $\mathcal{D}$-partition curves). Section 4.4 shows an illustrative example on how such results can be applied in order to tune the PIδ controller. Finally, several experimental tests using a solar array simulator in order to verify the performance of the control strategy are proposed.

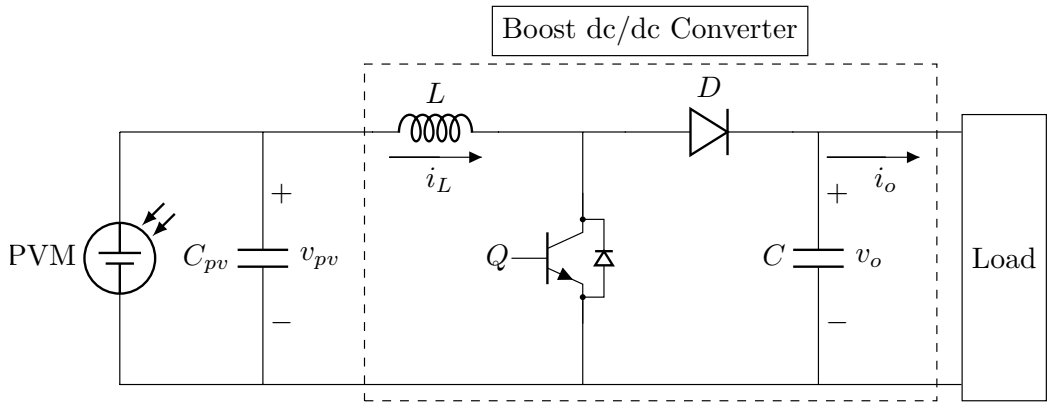

Figure 4.1: MPPT System Considering a Boost DC/DC Converter

4.1 PV Boost DC/DC Converter Dynamics

This section describes the open-loop system considered along this work, as well as some assumptions that will be taken into account in order to perform its closed–loop stability analysis. The methodology presented in the sequel follows similar steps to those proposed in [17], but applied to the analysis of a boost dc/dc converter and using a delay-based controller.

The topology consisting of the equivalent electrical circuit of the boost dc/dc power converter, a PV module and a load element is illustrated in Fig. 4.1.

From this figure, we derive the average model, which is described by the following equation:

$$\dot{\boldsymbol{x}} = \boldsymbol{f}(\boldsymbol{x}) + \boldsymbol{g}(\boldsymbol{x})u, \quad y = h(\boldsymbol{x}) = x_1, \tag{4.1}$$

with

$$\boldsymbol{f}(\boldsymbol{x}) := \begin{bmatrix} -\frac{1}{C_{pv}}x_2 + \frac{1}{C_{pv}}i_{pv} \\ \frac{1}{L}x_1 - \frac{1}{L}x_3 \\ \frac{1}{C}x_2 - \frac{1}{C}i_o \end{bmatrix}, \quad \boldsymbol{g}(\boldsymbol{x}) := \begin{bmatrix} 0 \\ \frac{1}{L}x_3 \\ -\frac{1}{C}x_2 \end{bmatrix},$$

where the state vector is defined by $x = [x_1, x_2, x_3]^T := [v_{pv}, i_L, v_o]^T$, v_{pv} represents the input voltage in the terminals of the capacitor C_{pv}, i_L denotes the current through the inductor L and v_o is the output voltage in terminals of the capacitor C. In addition, i_{pv} denotes the PV current generated by the PV module, i_o is the load current and $u \in [0, 1]$ defines the limited control variable (duty cycle for the switch Q).

Remark 12. *It is worth recalling that our main goal in the closed–loop scheme, is the proper regulation of the PVM voltage v_{pv}. This constant reference defined as v_{pv}^* is obtained by an external MPP tracking algorithm. However, we are focusing on the regulation problem.*

In the remaining part of the chapter, we consider the following assumptions:

Assumption 2. *The voltage reference v_{pv}^* is considered as a piecewise constant signal.*

Assumption 3. *The current i_{pv} is considered as a very low–frequency signal.*

Assumption 4. *The inductance value of the boost converter is as low as possible, i.e.,* $0 < L \ll 1$.

The ideal voltage reference v_{pv}^* is located at the maximum power point v_{mpp}. We consider Assumption 2 since the MPP is a slow time–varying signal which mainly changes by effects of the ambient temperature. In a similar manner, we consider Assumption 3 since, ideally, i_{pv} must be of a direct current type and it changes with respect to solar irradiation disturbances. Finally, as can be seen in the sequel, Assumption 4 is nothing else than a design consideration helpful for the control scheme design. Furthermore, as can be seen from (4.1), the input capacitor voltage v_{pv} is chosen as the output of the system. It is worth mentioning that similar assumptions have been considered in [17] and [72].

4.2 Global Control Scheme

This section presents the proposed control scheme for the regulation problem of the PV system. The procedure consists in two basic steps. First, a feedback linearization control scheme is designed to obtain an input-output linear mapping. Second, we propose a delayed controller in order to stabilize the resulting dynamics.

By computing the derivatives of the output $y = x_1$, one gets:

$$\begin{aligned} C_{pv}\dot{y} &= -x_2 + i_{pv}, \\ LC_{pv}\ddot{y} &= -x_1 + x_3 - x_3 u + L\frac{d}{dt}\left(i_{pv}\right). \end{aligned}$$

Since the control signal u appears up to the second derivative, the system has a relative degree $\rho = 2$ in an open and not connected set $\boldsymbol{\beta} = \{\boldsymbol{x} \in \mathbb{R}^3 \,|x_3 \neq 0\}$. Thus, by considering Assumptions 3 and 4 into (4.3) one neglects the photo-voltaic current derivative related term. And, by simply substitution one can corroborate that:

$$u = \left(1 - \frac{x_1}{x_3}\right) - \frac{1}{x_3} v, \tag{4.4}$$

reduces the input-output mapping to:

$$LC_{pv}\ddot{y} = v, \tag{4.5}$$

where v is considered as an auxiliary control law.

4.2.1 PIδ Control Strategy

As mentioned in the Introduction, the main focus of this work concerns the design of a PIδ controller for the regulation of the output of system (4.5). In this vein, considering

the constant voltage reference v_{pv}^*, we propose the following auxiliary control law as:

$$v(t) = k_p\left(v_{pv}^* - y(t)\right) + k_\delta\left(v_{pv}^* - y(t-\tau)\right) + k_i\int_0^t \left(v_{pv} - y(w)\right)dw. \tag{4.6}$$

Hence, we can rewrite the system (4.5) in terms of the output error $e(t) := y(t) - v_{pv}^*$, as follows:

$$LC_{pv}\ddot{e}(t) + k_i\int_0^t e(u)du + k_p e(t) + k_\delta e(t-\tau) = 0,$$

where τ is a fixed delay value. It is worth mentioning that the form of the system (4.5) suggests the use of a proportional-derivative controller to achieve asymptotic stabilization. Nevertheless, as we will detail in Section 4.3, the delay-based controller can asymptotically stabilize the closed-loop system by a proper choice of the controller parameters (k_p, k_δ, τ). This implies that as $t \to \infty$, then, $e(t) \to 0$ and therefore $y \to v_{pv}^*$. In addition, in order to improve the system's performance, we have included the integral term in (4.6) with the aim to cope with the parametric uncertainties. The analytical procedure to tuning such a $PI\delta-$controller $(k_p, k_i, k_\delta, \tau)$ will be explained in detail in the Section 4.3.

4.2.2 Zero Dynamics

As mentioned previously, the system (4.1) has a relative degree $\rho = 2$. As it is well known in the literature (see, for instance [65]), there exists a zero dynamics which has to be properly analyzed in order to be able to consider the linear mapping (4.5). This section covers in detail the characterization of such dynamics.

First, as mentioned in [65], we need to find a diffeomorfism, also described as the change of coordinates:

$$\boldsymbol{z} = \begin{bmatrix}\epsilon_1\\ \epsilon_2\\ \eta\end{bmatrix} = \boldsymbol{T}(\boldsymbol{x}) = \begin{bmatrix} h(\boldsymbol{x})\\ \left\langle \nabla h, \boldsymbol{f}\right\rangle \\ \varphi(\boldsymbol{x})\end{bmatrix}, \tag{4.7}$$

with inverse:

$$\boldsymbol{x} = \boldsymbol{T}^{-1}(\boldsymbol{z}).$$

Next, in order to express the dynamics of the change of coordinates (4.7) in the normal form, the function $\varphi(\boldsymbol{x})$ must satisfy the following condition:

$$\left\langle \nabla\varphi, \boldsymbol{g}\right\rangle = 0. \tag{4.8}$$

Hence, following (4.8) we get:

$$Cx_3\frac{\partial\varphi}{\partial x_2} = Lx_2\frac{\partial\varphi}{\partial x_3}. \tag{4.9}$$

It is clear to see, that a solution of the partial differential equation (4.9) can be easily

computed by assuming a solution φ satisfying:

$$\frac{\partial \varphi}{\partial x_2} = 2Lx_2, \quad \frac{\partial \varphi}{\partial x_3} = 2Cx_3.$$

The above consideration leads to the solution:

$$\varphi(\boldsymbol{x}) = Lx_2^2 + Cx_3^2. \tag{4.10}$$

Hence, this diffeomorfism and its inverse are given by:

$$\boldsymbol{z} = \boldsymbol{T}(\boldsymbol{x}) = \begin{bmatrix} x_1 \\ -\frac{1}{C_{pv}} x_2 + \frac{1}{C_{pv}} i_{pv} \\ Lx_2^2 + Cx_3^2 \end{bmatrix}, \tag{4.11}$$

$$\boldsymbol{x} = \boldsymbol{T}^{-1}(\boldsymbol{z}) = \begin{bmatrix} \epsilon_1 \\ -C_{pv}\epsilon_2 + i_{pv} \\ \sqrt{\frac{1}{C}\left(\eta - L\left(C_{pv}\epsilon_2 - i_{pv}\right)^2\right)} \end{bmatrix}.$$

Now, in order to model a battery bank as load, let us consider $i_o = \gamma(x_3)$, where γ has the property that $\operatorname{sgn}(\gamma) = \operatorname{sgn}(x_3)$ for all $x_3 \in \mathbb{R}$. Let $\boldsymbol{\epsilon} := [\epsilon_1, \epsilon_2]^T$, by computing the time derivative of $\boldsymbol{z}$ and considering (4.5) and (4.11), the dynamics of $\boldsymbol{z}$ can be split into a linear system:

$$\dot{\boldsymbol{\epsilon}} = \begin{bmatrix} 0 & 1 \\ 0 & 0 \end{bmatrix} \boldsymbol{\epsilon} + \begin{bmatrix} 0 \\ 1 \end{bmatrix} \frac{1}{LC_{pv}} v \tag{4.12}$$

in conjunction with a nonlinear one:

$$\dot{\eta} = -2\gamma(x_3(\eta))x_3(\eta) + 2\epsilon_1(C_{pv}\epsilon_2 - i_{pv}).$$

Finally, in order to characterize the zero dynamics of the system we assume that as $t \to \infty$, then $\boldsymbol{\epsilon} \to [0, 0]^T$ and:

$$x_3(\eta) \to \sqrt{\frac{1}{C}\eta - \frac{L}{C} i_{pv}^2}. \tag{4.13}$$

Considering the above results, the zero dynamics of the system is given as:

$$\dot{\eta} = -2\gamma(x_3(\eta))x_3(\eta).$$

In order to verify the stability of such dynamics, we propose the classical Lyapunov function:

$$\mathcal{V}(\eta) := \frac{1}{2}\eta^2.$$

Computing its time derivative yields:

$$\dot{\mathcal{V}} = -2\gamma(x_3(\eta))x_3(\eta)\eta.$$

Now, according to (4.10) and (4.13) we observe that $\eta \geq 0$ and $x_3(\eta) \geq 0$, respectively. Hence, $\gamma \geq 0$ implying that $\dot{\mathcal{V}} \leq 0$. This last condition allows concluding the stability of the zero dynamics.

4.3 PIδ Controller Design

As mentioned above, the proposed auxiliary control law consists in the use of a $PI\delta$ controller. The most important contribution of this section lies in the development of the necessary tools to implement an appropriate tunning of the controller parameters (k_p, k_i, k_δ) with a delay value τ.

The proposed approach relies in two steps. First, assuming $k_i = 0$ we aim to find at least one stability region in the parameters space (k_p, k_δ) with a fixed delay value τ. Second, in order to tune the integral gain k_i, we take into account a stabilizing controller pair (k_p^*, k_δ^*), and we establish a similar method to find a stability region on the parameters space (k_δ, k_i). Such a procedure will be explained in detail in the sequel.

Consider the system (4.5) together with the proposed control law (4.6). Hence, the closed–loop transfer function of the linearized system is given as:

$$G_{cl}(s) = \frac{(k_p + k_\delta e^{-\tau s})s + k_i}{LC_{pv}s^3 + (k_p + k_\delta e^{-\tau s})s + k_i}. \tag{4.14}$$

Thus, the closed–loop characteristic equation is given by the following quasi-polynomial:

$$\tilde{\Delta}\left(s; k_p, k_\delta, k_i, \tau\right) = LC_{pv}s^3 + (k_p + k_\delta e^{-\tau s})s + k_i = 0. \tag{4.15}$$

Notice that by considering only a proportional-delay controller (i.e., $k_i = 0$) in (4.14) the characteristic equation behaves as:

$$\Delta\left(s; k_p, k_\delta\tau\right) = LC_{pv}s^2 + k_p + k_\delta e^{-\tau s} = 0. \tag{4.16}$$

Remark 13. *It is well known that the stability of a linear system free of delay, is directly related to the location of the roots of its characteristic equation. More precisely, the system is asymptotically stable, if and only if, all roots of its characteristic equation lie on the left-half plane of the complex plane. This argument is also true for delayed linear systems (see, for instance, [49]). However, unlike the free delay case, in time-delay systems, it is well known that the quasi-polynomial* (4.16) *(or* (4.15)*) has an infinite number of roots that depend continuously on the parameter* (k_p, k_δ, τ) *(or* $(k_p, k_\delta, k_i, \tau)$*). Hence, the corresponding closed-loop system will be asymptotically stable if and only if the rightmost characteristic root is located in* $\mathbb{C}_-$.

4.3.1 Crossing Roots Existence

Now, with the purpose of developing a stability analysis, we first derive the *stability crossing boundaries*. In other words, we characterize the controller parameters choice (k_p, k_δ, k_i) such that the quasi-polynomial (4.16) has at least one root on the imaginary axis (at $s = \pm i\omega$) of the complex plane.

Proposition 27. *Let $\tau \in \mathbb{R}_+$ be a fixed delay value. Then, the characteristic equation (4.16) of the closed–loop system Δ has at least one pair of roots on the imaginary axis (at $s = \pm i\omega$), if and only if, the controller gains $\boldsymbol{k}(\omega) := [k_p, k_\delta]^T$, are given as:*

$$k_\delta = (-1)^n \left(-k_p + \frac{LC_{pv}\pi^2}{\tau^2} n^2 \right), \quad \text{for } \omega = \frac{n\pi}{\tau},$$
$$k_p = LC_{pv}\omega^2 \quad \& \quad k_\delta = 0, \quad \text{for } \omega \in \left(\frac{(n-1)\pi}{\tau}, \frac{n\pi}{\tau} \right),$$

for all $n \in \mathbb{Z}_+$. Furthermore, it has a single root at the origin ($\omega = 0$) if and only if:

$$k_\delta = -k_p \quad \text{and} \quad k_p \neq 0. \tag{4.19}$$

Proof. As a first step let us consider the characteristic equation (4.16) at $s = i\omega$, yielding to

$$-LC_{pv}\omega^2 + k_p + k_\delta \cos(\tau\omega) - ik_\delta \sin(\tau\omega) = 0. \tag{4.20}$$

Clearly (4.20) holds whenever $n \in \mathbb{Z}$ and $\omega = \frac{n\pi}{\tau}$, or when $k_\delta \equiv 0$. Thus, considering such situations in (4.20) we derive (4.17) and (4.18), respectively. Finally, by setting $s = 0$ in (4.20) and following similar arguments than those presented above, leads to (4.19). □

Remark 14. *It is clear to see from the structure of Δ or $\tilde{\Delta}$, that in the absence of the delay term, the closed-loop system will be oscillatory (if $k_p > 0$) or even unstable (if $k_p < 0$). Such an observation is congruent with the derived experimental results (see, for instance, the behavior of controller c_3, in section 4.4.2).*

Proposition 28. *Let $\tau \in \mathbb{R}_+$ and $k_p^* \in \mathbb{R}$ be fixed values. The characteristic equation of the closed–loop system has a pair of roots on the imaginary axis ($s = i\omega$), if and only if the controller gains $\tilde{k}(\omega) = [\tilde{k}_\delta(\omega), \tilde{k}_i(\omega)]^T$, are given as:*

$$\begin{aligned} \tilde{k}_\delta(\omega) &= \frac{LC_{pv}\omega^2 - k_p^*}{\cos(\tau\omega)}, \\ \tilde{k}_i(\omega) &= -\omega \tan(\tau\omega)(LC_{pv}\omega^2 - k_p^*), \end{aligned}$$

for all $\omega \in \mathbb{R}_+$ such that $\omega \neq \frac{(2n+1)\pi}{2\tau}$ with $n \in \mathbb{Z}_+ \cup \{0\}$. Furthermore, it has a single root at the origin ($\omega = 0$) iff:

$$k_i = 0 \quad \text{and} \quad k_\delta \neq -k_p^*. \tag{4.23}$$

Proof. Consider the characteristic equation (4.15) with $s = i\omega$,

$$(k_\delta \omega \sin(\tau\omega) + k_i) + i\left(k_\delta \omega \cos(\tau\omega) + k_p^*\omega - LC_{pv}\omega^3\right) = 0. \tag{4.24}$$

It is clear to see that (4.24) is fulfilled, as long as the following equation holds:

$$\begin{bmatrix} \omega \sin(\tau\omega) & 1 \\ \omega \cos(\tau\omega) & 0 \end{bmatrix} \begin{bmatrix} k_\delta \\ k_i \end{bmatrix} = \begin{bmatrix} 0 \\ LC_{pv}\omega^3 - k_p^*\omega \end{bmatrix}.$$

Thus, assuming that $\omega \neq \frac{(2n+1)\pi}{2\tau}$, $\forall n \in \mathbb{Z}_+ \cup \{0\}$ we derive (4.21) and (4.22). In a similar way, by setting $s = 0$ in $\tilde{\Delta}$ leads to (4.23). □

Based on the previous results, for a fixed delay value $\tau^* \in \mathbb{R}_+$ the *stability crossing curves* for a $P\delta$ controller $\boldsymbol{k} = [k_p, k_\delta]^T$ are characterized by means of the following manifolds:

$$\mathcal{T}_n^\ell := \left\{ \boldsymbol{k} \in \mathbb{R}^2 \,\middle|\, k_\delta = (-1)^n \left(-k_p + \frac{LC_{pv}\pi^2}{\tau^2} n^2 \right) \right\},$$
$$\mathcal{T}_n^p := \left\{ \boldsymbol{k} \in \mathbb{R}^2 \,\middle|\, \boldsymbol{k} = \left[LC_{pv}\omega^2, 0\right]^T, \omega \in \left(\frac{\pi}{\tau}(n-1), \frac{\pi}{\tau} n \right) \right\},$$

where $n \in \mathbb{Z}_+$. The curve characterizing a real simple crossing is given by:

$$\mathcal{T}_o := \left\{ \boldsymbol{k} \in \mathbb{R}^2 \,|k_\delta + k_p = 0 \text{ and } k_p \neq 0 \right\}.$$

For the $PI\delta$ controller, consider $\tilde{\boldsymbol{k}} := [k_\delta, k_i]^T$ and let $\tau^* \in \mathbb{R}_+$ and $k_p^* \in \mathbb{R}$ be fixed values. Then, *the stability crossing curves* are defined as:

$$\widetilde{\mathcal{T}}_n^m := \left\{ \tilde{\boldsymbol{k}} \in \mathbb{R}^2 \,\middle|\, \tilde{\boldsymbol{k}} = \tilde{\boldsymbol{k}}(\omega), \omega \in \left(\frac{(\operatorname{sgn} n)(2n-1)\pi}{2\tau}, \frac{(2n+1)\pi}{2\tau} \right) \right\},$$

for $n \in \mathbb{Z}_+ \cup \{0\}$, and the curve characterizing a real simple crossing is given by

$$\widetilde{\mathcal{T}}_o := \left\{ \tilde{\boldsymbol{k}} \in \mathbb{R}^2 \,\middle|\, k_i = 0 \text{ and } k_\delta \neq -k_p^* \right\}.$$

Thus, the *stability crossing curves* can be described as

$$\mathcal{T} = \bigcup_n \mathcal{T}_n^\ell \bigcup_n \mathcal{T}_n^p \bigcup \mathcal{T}_o,$$

$$\widetilde{\mathcal{T}} = \bigcup_n \widetilde{\mathcal{T}}_n^m \bigcup \widetilde{\mathcal{T}}_o,$$

for the Pδ and PIδ controllers, respectively.

4.3.2 Crossing Roots Directions

In order to compute a *stability index*, which is the number of roots in the RHP for a given parametrical region, it is of interest to characterize the behavior of the roots as a function of the corresponding parameter, when a parameter deviates from any boundary. The following results are the main tools to achieve such a task.

Proposition 29. *Let $\tau \in \mathbb{R}_+$ be a fixed delay value. Then, as $\boldsymbol{k}$ crosses in any direction from left to right of: $\mathcal{T}_n^\ell$, $n \in \mathbb{Z}_+$ traversing the point $\hat{\boldsymbol{k}} = [\hat{k}_p, \hat{k}_\delta]^T \in \mathcal{T}_n^\ell$, one pair of roots of the characteristic equation* (4.16) *moves from the LHP to the RHP of the complex plane if $\hat{\boldsymbol{k}}$ satisfies the following conditions:*

$$\hat{k}_\delta > 0 \text{ for } n \text{ even}, \quad \hat{k}_\delta < 0 \text{ for } n \text{ odd}. \tag{4.25}$$

Furthermore, the crossing of the roots is from the RHP to the LHP if these inequalities are reversed.

Proof. Consider the characteristic equation (4.16). Now, by the Implicit Function Theorem (see, for instance, [24]), we have:

$$\frac{ds}{dk_p} = -\frac{\frac{\partial \Delta}{\partial k_p}}{\frac{\partial \Delta}{\partial s}}, \qquad \frac{ds}{dk_\delta} = -\frac{\frac{\partial \Delta}{\partial k_\delta}}{\frac{\partial \Delta}{\partial s}},$$

where:

$$\frac{\partial \Delta}{\partial s} = 2LC_{pv}s - \tau k_\delta e^{-\tau s},$$
$$\frac{\partial \Delta}{\partial k_p} = 1, \quad \frac{\partial \Delta}{\partial k_\delta} = e^{-\tau s}.$$

Then, by taking $s = in\frac{\pi}{\tau}$, for $n \in \mathbb{Z}_+$ yields

$$\left[\frac{ds}{dk_p}\right]^{-1}\Bigg|_{s=i\frac{n\pi}{\tau}} = \tau k_\delta (-1)^n - i\frac{2\pi n LC_{pv}}{\tau}.$$

Since, $\tau \in \mathbb{R}_+$ and $\frac{ds}{dk_\delta} = \frac{ds}{dk_p}e^{-\tau s}$, we can conclude:

$$\begin{aligned} \operatorname{sgn}\left\{\Re\left\{\left.\frac{ds}{dk_p}\right|_{s=i\frac{n\pi}{\tau}}\right\}\right\} &= \operatorname{sgn}\left\{(-1)^n k_\delta\right\}. \\ \operatorname{sgn}\left\{\Re\left\{\left.\frac{ds}{dk_\delta}\right|_{s=i\frac{n\pi}{\tau}}\right\}\right\} &= \operatorname{sgn}\left\{k_\delta\right\}. \end{aligned}$$

Therefore, the proof follows straightforwardly by simply observing that (4.28)-(4.29) imply (4.25). □

Proposition 30. *Let $\tau \in \mathbb{R}_+$ be a fixed delay value. Then, one pair of roots of the characteristic equation* (4.16) *moves from the LHP to the RHP of the complex plane as $\boldsymbol{k}$ crosses the curve $\mathcal{T}_n^p$ in the increasing direction of k_δ if n is odd. Furthermore, the crossing is from the RHP to the LHP if n is even.*

Proof. Consider the characteristic equation (4.16). Making use of the Implicit Function Theorem and following similar arguments than those presented in the proof of Proposition 29, one gets:

$$\left[\frac{ds}{dk_\delta}\right]^{-1} = \tau k_\delta - 2LC_{pv}se^{\tau s}.$$

Now, by considering the set of *stability crossing curves* $\mathcal{T}_n^p$, $s = i\omega$ for $\omega \in \mathcal{I}_n := \left(\frac{\pi}{\tau}(n-1), \frac{\pi}{\tau}n\right)$ and $k = [LC_{pv}\omega^2, 0]^T$, yields

$$\mathcal{D}(\omega) := \Re\left\{\left[\frac{ds}{dk_\delta}\right]^{-1}\right\} = 2LC_{pv}\omega\sin(\tau\omega).$$

The proof ends by noting that $\mathcal{D} > 0$ for all $\omega \in \mathcal{I}_n$ with n odd and $\mathcal{D} < 0$ for all $\omega \in \mathcal{I}_n$ with n even. □

Proposition 31. *Let $\tau \in \mathbb{R}_+$. Then, a simple root of the characteristic equation* (4.16) *moves from the LHP to the RHP through the origin as $\boldsymbol{k}$ crosses from left to right the stability crossing curve $\mathcal{T}_o$ if $k_\delta > 0$. Furthermore, the crossing is from the RHP to the LHP if the inequality is reversed.*

Proof. By setting $s = 0$, the proof follows the same lines as the proof of Proposition 29. □

Proposition 32. *Let $\tau \in \mathbb{R}_+$ and k_p^* be fixed values. Then, a simple root of the characteristic equation* (4.15) *moves from the LHP to the RHP through the origin as $\tilde{\boldsymbol{k}}$ crosses the k_δ-axis in the increasing direction of k_i if $k_\delta < -k_p^*$. Furthermore, the crossing is from the RHP to the LHP if the inequality is reversed.*

Proof. The proof follows similar ideas to those presented in the proof of Proposition 29 but setting $s = 0$ and computing $\frac{ds}{dk_i}$. □

4.4 Experimental Implementation

In this section, we illustrate the application of the previously discussed results. More precisely, the design of a stabilizing controller for the PV boost dc/dc converter system. First, by means of the stability crossing curves, we present the tuning methodology of the $PI\delta$ controller. Second, we consider some experimental results in order to evaluate the performance of the control strategy. The standalone PV system consists of a boost dc/dc converter, five 12 V lead-acid batteries with a capacity of 80 Ah as load and a solar array simulator as PVM. A series connection has been considered for the battery

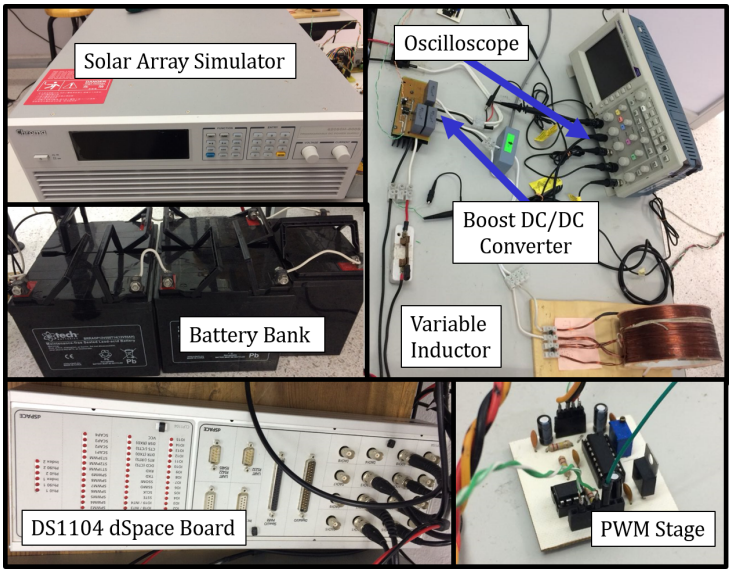

Figure 4.2: Experimental Test Bench - Main Components

Table 4.2: Passive Elements of the Boost dc/dc Converter

Parameters	Value	Unity
C_{pv}	352×10^{-6}	F
L	4.77×10^{-3}	H
C	144×10^{-6}	F

bank which establishes a dc bus voltage of 60 V. The parameters values of the passive elements of the boost dc/dc converter are summarized in Table 4.2. These values were chosen by considering a continuous mode operation at a rated power of 350 W and the power converter PWM stage operating at a switching frequency of $f_c = 10$ KHz (see, for instance, [62]). The control algorithm was implemented on a DS1104 dSpace board at sampling frequency $f_s = 40$ KHz. However, the measurements presented in this section were obtained using the following Tektronix equipment: an ac/dc current probe (A622), a high voltage differential probe (P5200) and a digital signal oscilloscope TDS2024B. Finally, the active elements, the power diode D and the power switch Q are STTH30R04W and IRFP250N, respectively. The main components are illustrated in Fig. 4.2.

4.4.1 PIδ Controller Tuning

Let us consider the system (4.12) in closed-loop with the $P\delta-$controller, where the fixed delay value has been chosen equal to $\tau = 2 \times 10^{-3}s$. By means of Proposition 27, we construct the stability crossing curves depicted in Fig. 4.3a. In addition, also in this figure for each stability boundary, the crossing directions for which at least a root moves from the LHP to the RHP are indicated by arrows. These crossing directions are derived by applying Propositions 29, 30 and 31.

Using the crossing directions of $\mathcal{T}_n^p$ presented in Proposition 29, we can find easily the

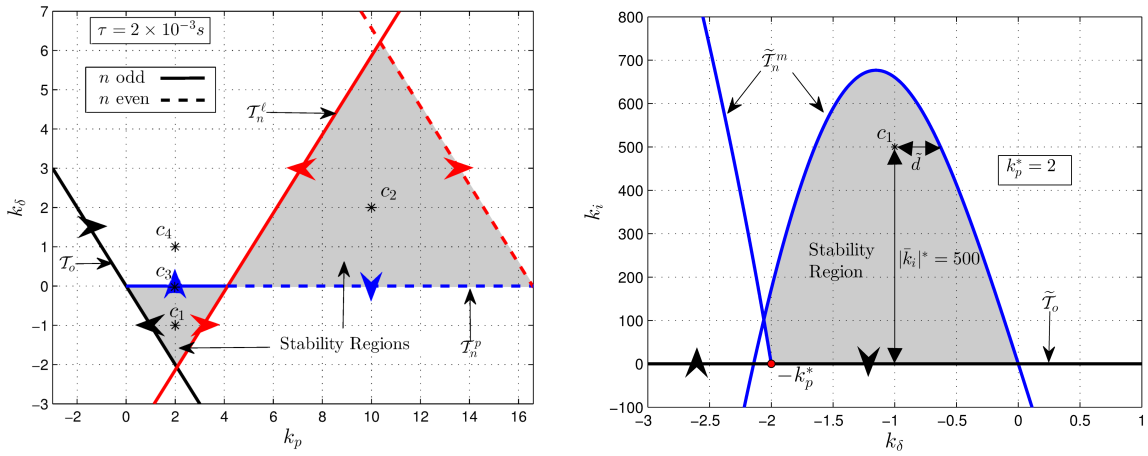

(a) $k_p - k_\delta$ Parameters Space Analysis

(b) $k_\delta - k_i$ Parameters Space Analysis

Figure 4.3: Stability Regions.

segments at which the roots will cross to the LHP. Giving as a result the two stability regions illustrated in Fig. 4.3b.

As a next step, let us consider the tuning of the k_i term. To this end, let us consider first the stabilizing P$\delta-$controller c_1, where $(k_p, k_\delta) = (2, -1)$. Then, taking $k_p^* = 2$ in Proposition 28 yields the stability crossing curves depicted in Fig.4.3b. As in the previous step, by means of Proposition 32 we compute the crossing directions, allowing us to derive the stability region illustrated in Fig. 4.3b. Based in the stability regions presented in Fig. 4.3, we consider the four different controllers summarized in Table 4.3 and illustrated in Fig. 4.3a. From this figure, it is easy to see that two of these controllers are stabilizing controllers (c_1, c_2), whereas the others not (c_3, c_4). It is worth to mention that the integral term of each stabilizing controller is designed individually following the procedure presented above. Furthermore, the unstable ones are just a variation of c_1 in which the gain related to the delayed action is perturbed.

Remark 15. *One must notice that the methodology for tunning the PIδ controller presented in this chapter requires two individual processes. First, one looks for a stability region for the Pδ controller given a fixed delay value (two parameters gains variations (k_p, k_δ) are taken into account). After, one choses from this region a particular proportional gain value $k_p = k_p^*$. Second, one looks for a stability region for the PIδ controller given fixed delay and proportional gain values (two parameters gains variations (k_δ, k_i) are taken into account). It is evident that fixing such delay and gain values in each process enables a two-dimensional parametric analysis which as demonstrated in this chapter is easy to carry-out and to interpret. However, one must highlight that each time that one fixes a parameter, one is compromising all other possibilities for it. Which even could end-up in not finding any stability regions, or not those with a better control performance. This is directly a limitation of this method, and to diminish it, one should repeat recursively this two step process using different parametric choices.*

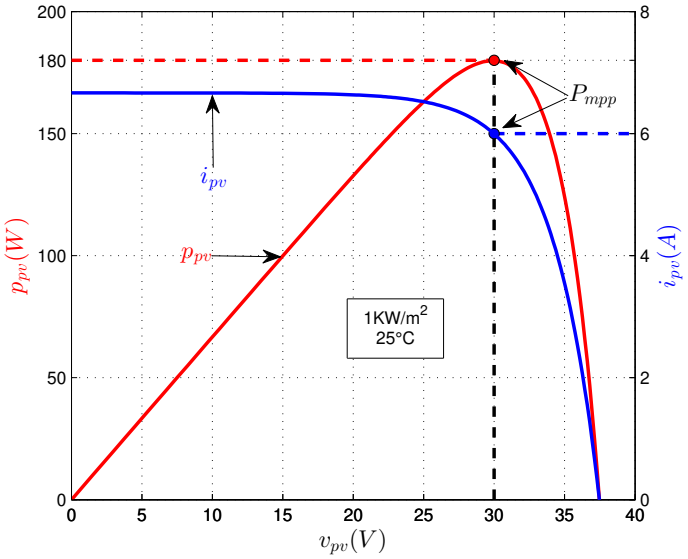

Figure 4.4: Characteristic Current-Voltage Curve Set in the Solar Array Simulator

Table 4.3: $PI\delta$ Controllers Parameters

c_i	k_p	k_i	k_δ	$\tau\,[s]$
c_1	2	500	-1	2×10^{-3}
c_2	10	600	2	2×10^{-3}
c_3	2	500	0	2×10^{-3}
c_4	2	500	1	2×10^{-3}

4.4.2 Experimental Tests

For the experimental tests, the characteristic current-voltage curve set in the solar array simulator was programmed with 180 W in standard conditions as shown in Fig. 4.4. From this figure, it is worth to notice that the MPP is located at $v_{mpp} = 30\,\text{V}$, $i_{mpp} = 6\,\text{A}$ and $P_{mpp} = 180\,\text{W}$. As mentioned in the test bench description, we consider a battery bank as load of the MPPT system. This common scenario is known as an isolated PV system, at which the main goal is to keep the battery bank completely charged using the energy gathered by the PV modules. Observe that since the auxiliary control la v only needs the PV voltage $x_1 = v_{pv}$, one may notice that the total control law (4.4) will also require the output voltage $x_3 = v_o$. However, in this experimental results we consider this as a constant voltage of $60V$ since in general this will be the common case. It is worth mentioning that even though this voltage is varying slowly as batteries are being charged, for control purposes, such a voltage can be considered as constant. This, since the numerical uncertainties will be coped by means of the integral action. In conclusion, for the experiments shown in this section only the PV voltage v_{pv} sensor was needed.

Experiment 1 (1 V and 5 V set-point changes)**.** *For the stabilizing controllers c_1 and c_2, let us test their behavior in two different scenarios: 1 V and 5 V set-point changes. One*

of the most common MPPT techniques "perturb and observe" (P&O) consists in varying the PV voltage reference in consistent steps changes, by observing the PV power in order to locate the MPP. These tests are designed to test the closed-loop system reliance on an online MPPT tracking system which attends such behavior. The results are summarized in Figs. 4.5, where from these figures we can notice that there always exists an abrupt transitory state in which the settling time measured goes from $9\,ms$ *to* $10.9\,ms$*, where these experiments have been implemented for* $1\ V$ *and* $5\ V$ *set-point changes. Furthermore, it is shown in every test that the control effort remains in the operation interval* $u \in [0, 1]$ *with this delayed strategy, even for the* $5\ V$ *set-point changes. This is the ideal scenario in which the closed-loop system must remain. Now, from the comparative table shown in the introduction (Table 4.1), we can observe that the settling times documented for these experiments goes from* $0.2\,ms$ *to* $300\,ms$*. In addition, we would like to highlight the fact that all these strategies need at least two sensors, while as discussed above, in the experimental test bench shown in this work, only the PV voltage sensor is required.*

Experiment 2 (Irradiance disturbances)**.** *As a second experimental test, let us evaluate the system under transient conditions. To this end, the test consists in setting a constant voltage reference* $v_{pv}^* = 30\ V$*, while an irradiance disturbance which oscillates from* $100\ W/m^2$ *to* $1000\ W/m^2$ *is applied by the solar array simulator. We consider this as an abrupt scenario, irradiance variation through the day or even shading caused by clouds movement can be considered as slower scenarios which would be easier to handle for the control system. The obtained results are shown in Fig. 4.7 for the controllers* c_1 *and* c_2*. Moreover, from these figures, we can observe a stable regulation with expected transient scenarios enhanced. Hence, despite any disturbance, the PV voltage tends to the voltage reference* $v_{pv}^* = 30\ V$*.*

Experiment 3 (Unstable controllers)**.** *Finally, to complete the tests we consider the two unstable controllers for a constant regulation with* $v_{pv}^* = 30\ V$ *and without any transient condition. In this vein, as expected, Fig. 4.7 illustrates the unstable responses. One may notice from Table 4.3 that the experiment shown in Fig. 4.7a has a lack of the delayed action, illustrating that the proposed controller needs the "gain-delay block" in order to have an asymptotically stable behavior. In a similar fashion, it is interesting to observe how the design analysis suggests the use of a negative gain* k_δ *(for* c_1*), in which if we switch the sign to this gain, results in an unstable behavior, as can be appreciated from Fig. 4.7b.*

4.5 Concluding Remarks

In this chapter we describe in detail the control scheme design of a MPPT-PV system using a power dc/dc boost converter and a $P\delta I$ controller. The system is controlled by applying an input-output linearization technique obtaining a linear system. This last one is composed by a double integrator and is controlled by using the $P\delta I$ controller. One uses crossing roots theory to develop a methodology for designing the controller's parameters in the same spirit as the second chapter of this thesis. Experimental results concerning

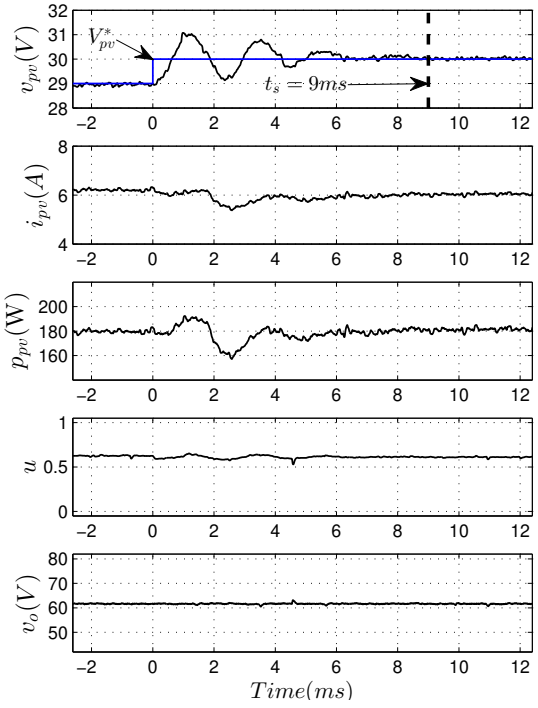

(a) 1 V Variation - Controller c_1

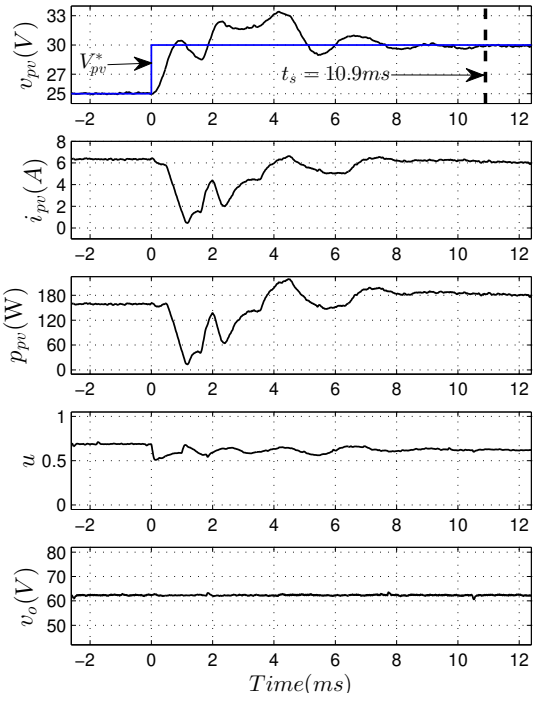

(b) 5 V Variation - Controller c_1

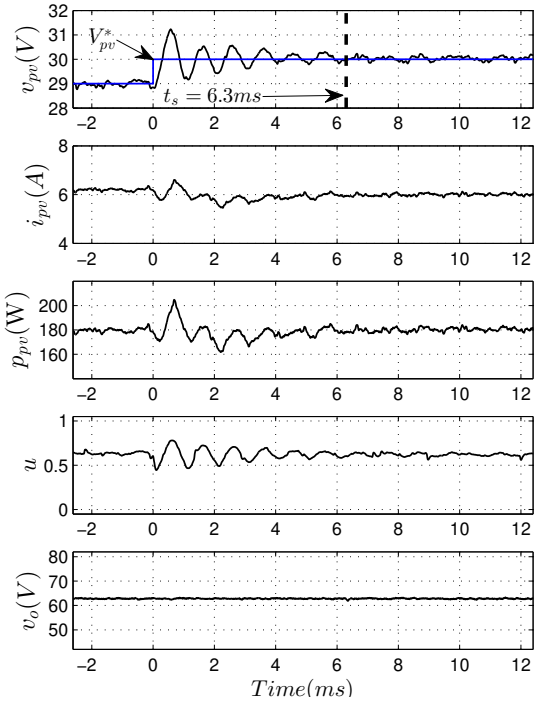

(c) 1 V Variation - Controller c_2

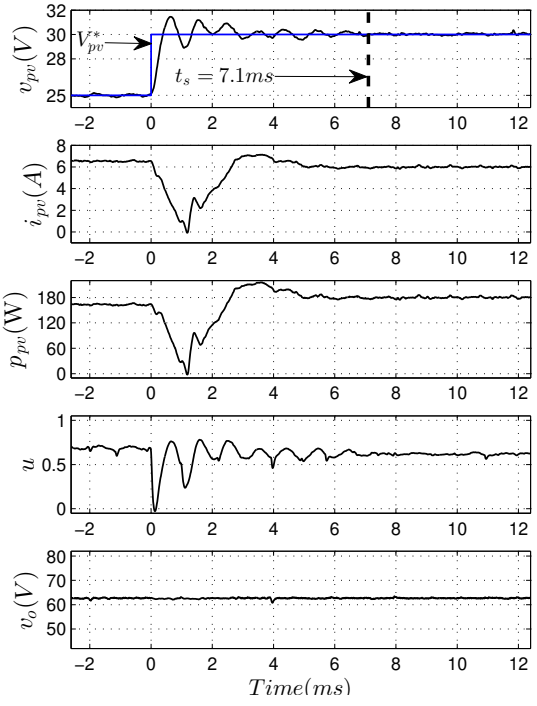

(d) 5 V Variation - Controller c_2

Figure 4.5: Experiment 1. Set-Point Variations

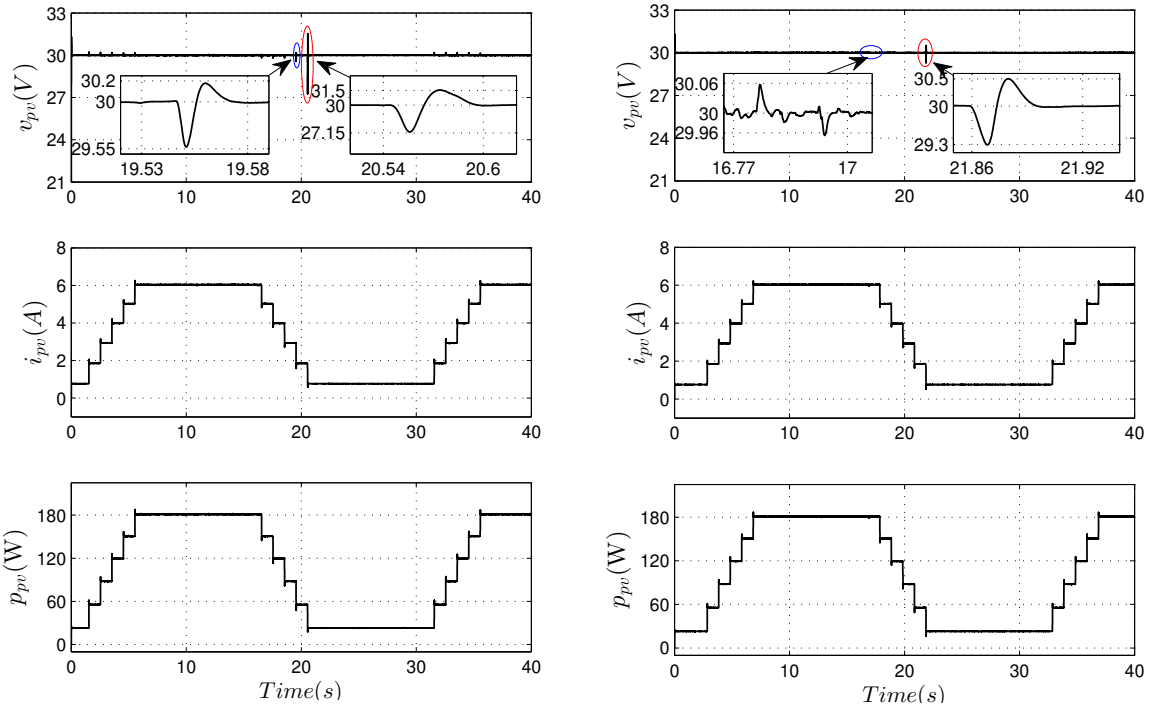

(a) Controller c_1 (b) Controller c_2

Figure 4.6: Experiment 2. Irradiance Disturbances

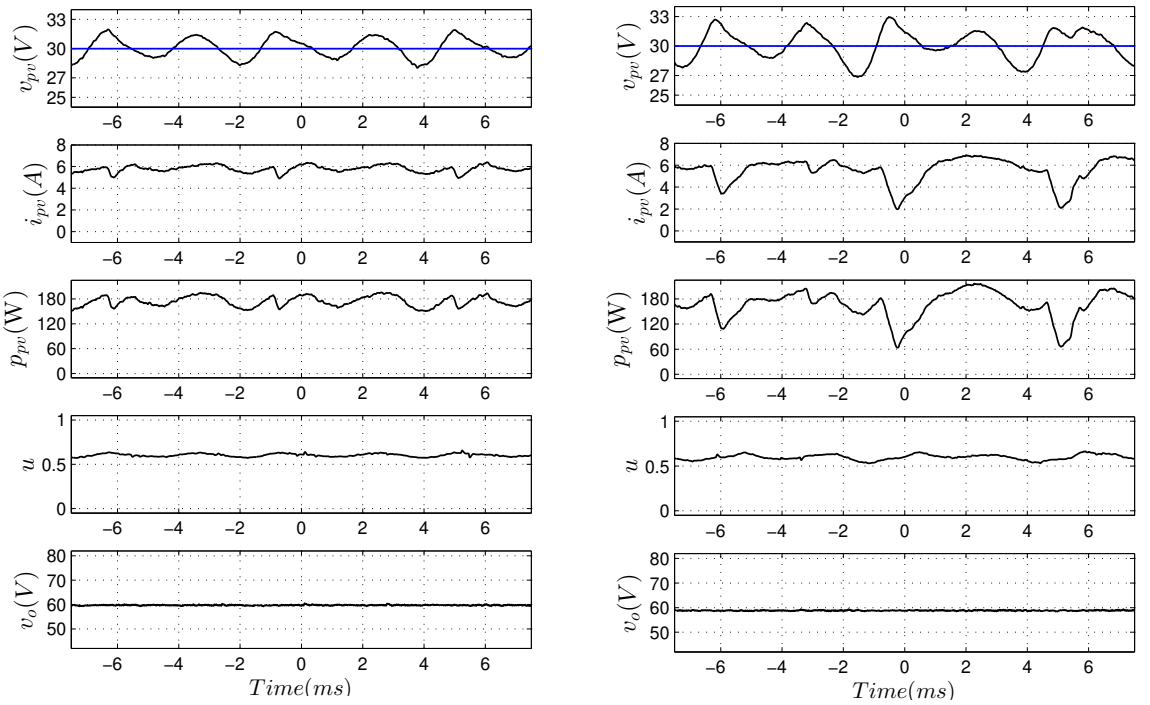

(a) Unstable Controller c_3 (b) Unstable Controller c_4

Figure 4.7: Experiment 3. Unstable Controllers

set-point changes simulating a P&O method and irradiance disturbances are presented and discussed. In this chapter one shows how a chain of two integrators can be stabilized using delays. In the next one, one studies the potential of delays for stabilizing chains of oscillators.

Chapter 5

Stabilizing Oscillators: Remarks on the Solution of the General Case

The content of this chapter is a deep study of what one the classical problems in linear delay-based control: the stabilization of a chain of any number of oscillators by a single delay "block" (gain,delay) as controller. Considering a classical feedback control scheme, this is nothing else than using as control law a delayed error signal multiplied by a proportional gain. Being this proportional scaling factor and the time the error signal is delayed the only tunable controller parameters. According with the analysis shown further in this chapter, the proper and subtle selection of this gain-delay pair values can stabilize any chain of oscillators. The mere fact that such a simple control scheme can always make the enough impact to achieve such a task, makes this problem not only a really elegant one, but one worthy to study. In fact, one would say that it is an interesting puzzle piece to better understand the particular advantages that linear delay-based control can brought up to classical control theory.

Deeply inspired by the remarks presented in these works, this chapter presents an "in detail" analysis of the characteristic quasi-polynomial of the closed-loop system. Such being focused on the behavior of its roots by means of variations of the controller parameters (gain, delay). More precisely, this chapter develops first a similar analysis concerning stability crossing conditions and the roots further deviations from the imaginary axis. Giving as a result necessary conditions for the time-delay value. Later, such insights are used in conjunction with the so-called Mikhailov criterion to further compute stabilizing explicit conditions on the delay block parameters. Such a criterion is directly related to the well-known Cauchy's argument principle.

5.1 Open-Loop System and Controller Nature

Consider the class of strictly proper single-input single-output (SISO) open-loop systems given by the transfer function:

$$G(s) = \frac{Y(s)}{U(s)} = \frac{1}{Q(s)}, \tag{5.1}$$

which characteristic polynomial $Q(s)$ is defined by:

$$Q(s) := (s^2 + \omega_1^2)(s^2 + \omega_2^2)\dots(s^2 + \omega_N^2) = \prod_{m=1}^{N}(s^2 + \omega_m^2), \tag{5.2}$$

where all values $\omega_m > 0$ for all $m \in M := \{1, 2, \dots, N\}$ and are defined accordingly to an ascending distribution as shown below:

$$0 < \omega_1 < \omega_2 < \cdots < \omega_N.$$

Such a system is one that has no zeros and whose open-loop poles are located exactly on the imaginary axis. More precisely, $Q(s) = 0$ iff $s = \pm i\omega_m$ for some $m \in M$. In other words, this depicts a class of the so-called marginally stable systems. One can easily observe from the characteristic equation (5.2) that each term of this product is a second-order polynomial with no linear term. From a mechanical interpretation, one can understand each of these as an "undamped" characteristic polynomial. One would expect an undamped response from each of those, and for total response a combination of these due to its cascade configuration. Such a behavior is partially discussed in the following remark.

Remark 16. *In order to better understand such an open-loop system one may study its impulse response. To such end, consider $U(s) = 1$ (the Laplace transform of an impulse), the output of the system is given directly by:*

$$Y(s) = \frac{1}{(s^2 + \omega_1^2)(s^2 + \omega_2^2)\dots(s^2 + \omega_N^2)}.$$

Using well-known partial fractions decomposition one can rewrite such an expression as:

$$Y(s) = \frac{A_1 s + B_1}{(s^2 + \omega_1^2)} + \frac{A_2 s + B_2}{(s^2 + \omega_2^2)} + \cdots + \frac{A_N s + B_N}{(s^2 + \omega_N^2)},$$

where all coefficients (A_m, B_m) are real ordered pairs for all $m \in M$. This can be easily

rewritten as follows:

$$Y(s) = \left[A_1 \frac{s}{(s^2+\omega_1^2)} + \frac{B_1}{\omega_1}\frac{\omega_1}{(s^2+\omega_1^2)}\right] + \left[A_2 \frac{s}{(s^2+\omega_2^2)} + \frac{B_2}{\omega_2}\frac{\omega_2}{(s^2+\omega_2^2)}\right] + \dots \\ \dots + \left[A_N \frac{s}{(s^2+\omega_N^2)} + \frac{B_N}{\omega_N}\frac{\omega_N}{(s^2+\omega_N^2)}\right],$$

which structure is easily associated to the well-known Laplace transformations:

$$\mathcal{L}\{cos(\omega t)\} = \frac{s}{s^2+\omega^2}, \quad \mathcal{L}\{sin(\omega t)\} = \frac{\omega}{s^2+\omega^2}, \quad , \ for\ \omega \in \mathbb{R}.$$

Then, it is evidently that the output response of the system $y(t) = \mathcal{L}^{-1}\{Y(s)\}$ *is computed directly as:*

$$y(t) = A_1 \cos(\omega_1 t) + \frac{B_1}{\omega_1}\sin(\omega_1 t) + A_2 \cos(\omega_2 t) + \frac{B_2}{\omega_2}\sin(\omega_2 t) + \dots \\ \dots + A_N \cos(\omega_N t) + \frac{B_N}{\omega_N}\sin(\omega_N t).$$

Such response is a purely oscillating one. More precisely, it is a linear combination of pure oscillations at each frequency value ω_m*, directly related to each pair of pure imaginary open-loop poles. In a way, a dynamical that starts vibrating indefinitely in response at the slightest contact.*

Having discussed in detail the chain of oscillators dynamical nature, it is now introduced the proposed delay-based control scheme. The one delay "block" controller:

$$C(s) = Ke^{-\tau s}, \tag{5.7}$$

where $K \in \mathbb{R}$ and τ is a positive fixed delay value. In the classical feedback control scheme considered in this study this is nothing else than the application of the control law:

$$u(t) = Ke(t-\tau),$$

where $e(t)$ is an error signal. Recall that the main task to achieve by this chapter is to study the potential of this delay-based controller to guarantee closed-loop stability. This is stated formally in the following lines.

Problem 4. *Consider the open-loop system showed in* (5.1) *and the linear controller depicted in* (5.7)*. These are the so-called chain of any oscillators and the one delay "block" controller, respectively. One aims to find explicit conditions on the controller parameters pair* (K, τ) *such that the closed-loop system is asymptotically stable. In other words, to find the proper parametric setting such that the characteristic equation of the*

closed-loop system $C(s)G(s)+1=0$, computed explicitly as:

$$\Delta(s) = Ke^{-\tau s} + Q(s) = 0, \tag{5.8}$$

has all of its zeros on the left-half plane (LHP) of the complex plane.

5.2 Time-Delay Stabilizing Conditions

This section derives useful conditions on the time delay value to study the stability of quasi-polynomial (5.8). Such an analysis is based in a simple idea brought up by studying the quasi-polynomial roots movement due to variations of K around its origin. More precisely, consider equation (5.8) with $K = 0$, then, $\Delta(s) = Q(s)$ is a fixed degree polynomial with exactly $2N$ purely imaginary roots. One could say that such roots are at the edge of stability, since the slight movement of one of them passing to the RHP of the complex plane implies directly instability. In the same lines, one could think that it may exists a particular continuous path of the ordered pair (K, τ) (starting from $K = 0$ and some value τ) which my imply a movement of all $2N$ purely imaginary roots to the LHP of the complex plane. Such an idea is taken into consideration in the sequel.

In general, the analysis presented in this section studies the particular controller parametric settings in which at least one root of the characteristic quasi-polynomial (5.8) is located on the imaginary axis. Subsequently, its behavior as such choices of parameters variate continuously. Both analysis are presented in the following sections. However, for a better understanding of the results shown it is important to bare in mind that $Q(i\omega)$ is a real valued function and $Q'(i\omega)$ is a purely imaginary function with null real part. This is explained in the following remark:

Remark 17. *If $s = i\omega$ then:*

$$Q(i\omega) = \prod_{m=1}^{N} (\omega_m^2 - \omega^2),$$

from this expression it is evident that $Q(i\omega)$ is a real valued function of ω. Second, the derivative $Q'(s)$ can be computed as:

$$Q'(s) = 2s \sum_{m=1}^{N} \prod_{\ell \neq m} (s^2 + \omega_\ell^2), \quad \ell \in \{1, 2, \ldots, N\},$$

straightforwardly:

$$Q'(i\omega) = i2\omega \sum_{m=1}^{N} \prod_{\ell \neq m} (\omega_\ell^2 - \omega^2), \;\; \ell \in \{1, 2, \ldots, N\}, \tag{5.9}$$

from this, it can be observed that $Q'(i\omega)$ is a purely complex function of ω with null real part.

5.2.1 Crossing Roots Existence

Consider $s = i\omega$ in (5.8) and solve for K as follows:

$$K = -Q(i\omega)\Big[\cos(\tau\omega) + i\sin(\tau\omega)\Big], \tag{5.10}$$

there exists a real solution of K for this last expression only in two different approaches. On one hand, if $\omega = \omega_m$ then $Q(i\omega) = 0$, and therefore $K = 0$. This is nothing else than the open-loop crossing roots. In fact, it is evident that if $K = 0$ then $\Delta(s) = Q(s)$, and therefore the characteristic equation has only these N roots. On the other hand, given that $Q(i\omega)$ is a real valued function of ω, a real solution of $K \neq 0$ exists, iff $\omega = \tilde{\omega}_n(\tau) := n\frac{\pi}{\tau}$ for some $n \in \mathbb{Z}$. We defined these as the closed-loop crossing roots. Such arguments are formalized in the following proposition:

Proposition 33. *Let τ be a positive fixed delay value. Then, the characteristic equation of the closed-loop system* (5.8) *has at least a root on the imaginary axis $s = i\omega$, iff:*

- *$K = 0$, being $\omega = \omega_m$ for any $m \in \{1, 2, \ldots, N\}$,*
- *$K = K(\tau, n)$, being $\omega = n\frac{\pi}{\tau}$ for some $n \in \mathbb{Z}$,*

where:

$$K(\tau, n) = (-1)^{n+1} Q\left(n\frac{\pi}{\tau}\right). \tag{5.11}$$

Proof. The proof is straightforward noting that if $\omega = \tilde{\omega}_n(\tau)$ in equation (5.10) then (5.11) follows directly. □

From this last proposition, it is important to emphasize the fact that there are two different scenarios concerning root crossing ($s = i\omega$) in the characteristic equation (5.8). Particularly, the roots cross the imaginary axis through $\omega = \omega_m$ or $\omega = \tilde{\omega}_n$. Being this notation referring to the open- and closed-loop crossing roots frequencies, respectively. Considering this observation, its most important aspect is described in the following remark.

Remark 18. *As being well documented in the literature (see for instance [52]), the roots of a quasi-polynomial move continuously against continuous variation of its parameters (gain, coefficients). Let $\tau > 0$ be a fixed delay value, and since $K = 0$ or $K = K(\tau, n)$ implies root crossing, then, these values partition the number line of K in intervals in which no roots crossing is possible. Therefore, in intervals of K in which the characteristic equation has a constant number of roots at the right-half plane (RHP) of the complex plane (unstable roots).*

5.2.2 Crossing Roots Directions

In this section we aim to characterize the crossing roots deviation tendency of characteristic equation (5.8). To such an end, we compute the following derivative using the *implicit function theorem*:

$$\left[\frac{ds}{dK}\right]^{-1} = \tau K - Q'(s)e^{\tau s}. \tag{5.12}$$

In the following two propositions we describe both scenarios described above regarding the close- and open-loop crossing roots, respectively.

Proposition 34. *Let τ be a fixed delay value and $n \in Z$. If K variates increasingly (decreasingly) around $K = K(\tau, n)$, then, at least a root moves to the RHP of the complex plane iff $K(\tau, n) > 0 (< 0)$.*

Proof. Consider the closed-loop crossing roots, that is $s = i\tilde{\omega}_n(\tau)$ and $K = K(\tau, n)$. Let us analyze such a scenario in the derivative presented in (5.12), also notice that $e^{i\tau\tilde{\omega}_n(\tau)} = (-1)^n$, the following is obtained:

$$\left[\frac{ds}{dK}\right]^{-1}\Bigg|_{s=i\tilde{\omega}_n} = \tau K(\tau, n) + (-1)^{n+1}Q'(i\tilde{\omega}_n).$$

Recall that $Q'(i\omega)$ is a purely complex function of ω with null real part, then its crossing direction is computed as:

$$\tilde{R}(\tau, n) := \Re\left\{\left[\frac{ds}{dK}\right]^{-1}\Bigg|_{s=i\tilde{\omega}_n}\right\} = \tau K(\tau, n).$$

It is important to state that since $\tau > 0$, then, $\operatorname{sgn}\left\{\tilde{R}(\tau, n)\right\} = \operatorname{sgn}\{K(\tau, n)\}$. This expression implies directly the arguments stated in this proposition. □

It is important to enhance the implications of the proposition shown above with respect to Remark 18. Compute all values of $K(\tau, n)$ for all $n \in Z$ arranged in such a way that:

$$\cdots < K_2^- < K_1^- < 0 < K_1^+ < K_2^+ < \ldots,$$

where the super-index is used to observe the sign of such values on the number line of K. As mentioned in Remark 18, these values partition the number line of K in intervals in which the characteristic equation has a constant numbers of roots located on the RHP of the complex plane. Assume now that for $K \in (0, K_1^+)$ the characteristic equation has r roots on the RHP. By applying Proposition 34, we can state that as K crosses increasingly through any value K_j^+ at least a root crosses to the RHP. Therefore, no stabilizing interval exists for $K > K_1^+$. A similar argument implying the same for $K < K^-1$ can be easily deduced. In general, using this approach, it appears that the only possible stabilizing

intervals are those concerning the behavior of the open-loop crossing roots ($K = 0$). In order to have a clear understanding of these we present the following Proposition.

Proposition 35. *Let τ be a fixed delay value and $m \in \{1, 2, \ldots, \mathbb{N}\}$. If K variates increasingly around $K = 0$, then, the pair of open-loop crossing roots $s = \pm i\omega_m$ move to the LHP (RHP) of the complex plane iff:*

$$(-1)^{m-1} \sin(\tau\omega_m) < 0 \quad (> 0).$$

Proof. Consider the open-loop crossing roots, that is $s = i\omega_m$ when $K = 0$. Let us analyze such a scenario in the derivative presented in (5.12), the following is obtained:

$$\left[\frac{ds}{dK}\right]^{-1}\Bigg|_{s=i\omega_m} = -Q'(i\omega_m)\Big[\cos(\tau\omega_m) + i\sin(\tau\omega_m)\Big].$$

Since $Q'(i\omega)$ is a purely complex function with null real part, then its crossing direction can be computed as:

$$R_m := \Re\left\{\left[\frac{ds}{dK}\right]^{-1}\Bigg|_{s=i\omega_m}\right\} = -iQ(i\omega_m)\sin(\tau\omega_m),$$

which by recalling (5.9) can be rewritten as:

$$R_m = 2\omega_m \sin(\tau\omega_m) \prod_{\ell \neq m} (\omega_\ell^2 - \omega_m^2),$$

where $\ell \in \{1, 2, \ldots, N\}$. At this point, it is important to notice the following:

$$\prod_{\ell \neq m} (\omega_\ell^2 - \omega_m^2) = (\omega_1^2 - \omega_m^2)(\omega_2^2 - \omega_m^2)\ldots$$
$$\ldots(\omega_{m-1}^2 - \omega_m^2)(\omega_{m+1}^2 - \omega_m^2)\ldots(\omega_N^2 - \omega_m^2),$$

also recall that $\omega_{m+1} > \omega_m$, then:

$$\operatorname{sgn}\left\{\prod_{\ell \neq m} (\omega_\ell^2 - \omega_m^2)\right\} = (-1)^{m-1}.$$

Therefore, the sign of R_m can be expressed as:

$$\operatorname{sgn}\{R_m\} = (-1)^{m-1} \operatorname{sgn}\{\sin(\tau\omega_m)\},$$

this last expression implies directly the arguments stated in this Proposition. □

Bearing in mind Proposition 35 shown above, it is clear that if there exists a fixed value τ such that:

$$(-1)^{m-1}\sin(\tau\omega_m) < 0, \quad \forall m \in M, \tag{5.13}$$

then, all open-loop crossing roots cross to the LHP of the complex plane as K is varied increasingly from zero. Such conditions may imply closed-loop asymptotic stability for a positive interval of K. In the next section we assume such conditions on the parameter τ to develop a vectorial analysis in the sense of the criterion presented in [53]. It is worthy to mention that since the parameter τ is assumed to be chosen in advance and for the sake of clarity, we drop its notation on the closed-roots frequencies $\tilde{\omega}_n(\tau)$.

5.3 Vectorial Interpretation and Main Results

The results shown in this section are based in an argument based stability criterion (similar to the well-known Nyquist criterion and Cauchy's argument principle). To such an end, it is important to consider the following result concerning the Mikhailov stability criterion (see for instance [58, 23]) for retarded quasi-polynomials. In the following one presents a simpler version of such a result by considering one delay only.

Theorem 2. *Mikhailov Stability Criterion. Consider the retarded quasi-polynomial with single delay:*

$$\Delta_r(s) = P(s) + Q(s)e^{-\tau s},$$

where $\tau > 0$ and $k := \deg\{P(s)\} > \deg\{Q(s)\}$. The characteristic quasi-polynomial has all of its zeros located on the LHP of the complex plane (i.e. the corresponding system is asymptotically stable) iff:

$$\underset{\omega\in[0,\infty)}{\theta \arg}\{\Delta_r(i\omega)\} = k\frac{\pi}{2}.$$

In this notation, $\underset{\omega\in I}{\theta} \arg\{F(\omega)\}$ stands for the accumulative argument of complex function $F(\omega)$ while ω varies increasingly inside interval I.

In particular, the following remark states the case studied in this chapter.

Remark 19. *Consider the particular retarded quasi-polynomial* (5.8) *studied in this work. It is evident that Theorem 2 implies that the closed-loop systems achieves asymptotic stability iff:*

$$\underset{\omega\in[0,\infty)}{\theta \arg}\{\Delta(i\omega)\} = N\pi.$$

Before going into deep detail of the main results of this chapter it is important to observe the behavior of $\Delta(i\omega)$ in its complex vector form. As show in Fig. 5.1a the vectorial interpretation of $\Delta(i\omega)$ consists in the addition of a purely real vector $Q(i\omega)$ with the complex vector $Ke^{-i\tau\omega}$. One one hand, $Ke^{-i\tau\omega}$ is a rotatory vector which describes a path on a circle with radium K centered on $Q(i\omega)$ with a clockwise direction. More precisely, let $n \in \mathbb{Z}$ and $K > 0$, as illustrated in Fig. 5.1b, $Ke^{-i\tau\omega}$ has the following behavior:

- It rests on the real axis with positive direction for any value $\omega = \tilde{\omega}_{2n}$ (even closed-loop cross frequencies).
- It moves in a clockwise direction through the lower half-plane of the complex plane for $\omega \in (\tilde{\omega}_{2n}, \tilde{\omega}_{2n+1})$.
- It rests on the real axis with negative direction for any value $\omega = \tilde{\omega}_{2n+1}$ (odd closed-loop cross frequencies).
- It moves in a clockwise direction through the upper half plane of the complex plane for $\omega \in (\tilde{\omega}_{2n+1}, \tilde{\omega}_{2n+2})$.

On the other hand, notice that $Q(i\omega)$ is a polynomial on ω of degree $2N$ which changes sign as ω variates through the open-loop crossing frequencies ω_m. More precisely, let $\omega_0 := 0$, if $\omega \in (\omega_m, \omega_{m+1})$, then $\operatorname{sgn}\{Q(i\omega)\} = (-1)^m$ and let $\omega \geq \omega_N$ then $\operatorname{sgn}\{Q(i\omega)\} = (-1)^N$.

5.3.1 General Case

In this section, we establish stabilizing conditions on the gain K such that τ satisfies conditions shown in (5.13). In other words, such a value of τ implies that the following inequalities hold simultaneously:

$$\sin(\tau\omega_m) < 0, \text{ for odd } m, \quad \sin(\tau\omega_m) > 0, \text{ for even } m.$$

Subsequently, there exist natural numbers n_m odd (even) if m is odd (even) such that:

$$n_m\pi < \tau\omega_m < (n_m + 1)\pi, \quad n_m = \left\lfloor \omega_m \frac{\tau}{\pi} \right\rfloor,$$

straightforwardly, it is clear that:

$$n_m \frac{\pi}{\tau} < \omega_m < (n_m + 1)\frac{\pi}{\tau} \rightarrow \tilde{\omega}_{n_m} < \omega_m < \tilde{\omega}_{n_m+1}. \tag{5.14}$$

It is worthy to notice that this last arguments show a particular interlacing condition between the open- and closed-loop crossing roots frequencies. Such an observation is heavily used in the proof of the following Proposition. Also notice that (5.14) can be rewritten as follows:

$$n_m < \omega_m \frac{\tau}{\pi} < (n_m + 1),$$

then, by means of the definition of the floor and ceiling functions, it is clear that the computation of such bounding integers can be done as:

$$n_m = \left\lfloor \omega_m \frac{\tau}{\pi} \right\rfloor, \quad n_m + 1 = \left\lceil \omega_m \frac{\tau}{\pi} \right\rceil. \tag{5.15}$$

Proposition 36. *Consider the open-loop system* (5.1) *with* N *distinct single roots on the imaginary axis and the one delay block controller* (5.7)*. Let* $\tau > 0$ *be a fixed delay value such that:*

$$(-1)^{m-1}\sin(\tau\omega_m) < 0, \quad \forall m\,\{1,2,\ldots,N\}\,, \tag{5.16}$$

and K *be a positive real gain. Then, the closed-loop system is asymptotically stable iff:*

$$K < \left|Q\left(i\left\lfloor\omega_m\frac{\tau}{\pi}\right\rfloor\frac{\pi}{\tau}\right)\right|, \text{ and } K < \left|Q\left(i\left\lceil\omega_m\frac{\tau}{\pi}\right\rceil\frac{\pi}{\tau}\right)\right|,$$

for all m*.*

Proof. The proof of this proposition is based in the geometric vectorial analysis presented in Fig. 5.1 by means of the Mikhailov stability criterion. As stated in Theorem 2, this result establish that asymptotic stability is achieved iff the complex vector $\Delta(i\omega)$ has an accumulative phase of $N\pi$ as $\omega \in [0,\infty)$. For the sake of clarity, in this proof we focus on the sufficiency of the conditions presented in this proposition. To such an end, assume that $K < |Q(i\tilde{\omega}_n)|$ for all $n \in \mathbb{Z}$.

Consider the intervals $\omega \in (\omega_m, \omega_{m+1})$ for any $m \in \{0,1,\ldots,N-1\}$, recall that $\omega_0 := 0$. Consider first m even, then $\operatorname{sgn}\{Q(i\omega)\} = 1$ and $Q(i\omega)$ is a positive real vector. As illustrated in Fig. 5.1c, since $Ke^{-i\tau\omega}$ is a rotatory vector with a clockwise direction, $\Delta(i\omega)$ has a tendency to encircle the origin with a clockwise direction (negative accumulated phase). More precisely, it achieves it if $K > |Q(i\tilde{\omega}_n)|$ for some odd n. Second, consider m odd, then $\operatorname{sgn}\{Q(i\omega)\} = -1$ and $Q(i\omega)$ is a negative real vector. Similarly, as illustrated in Fig. 5.1e, $\Delta(i\omega)$ encircles the origin with a clockwise direction (negative accumulated phase) if $K > |Q(i\tilde{\omega}_n)|$ for some even n. Finally, consider $\omega \in (\omega_N, \infty)$ then $\operatorname{sgn}\{Q(i\omega)\} = (-1^N)$, depending on the number N this match any of the two scenarios presented above. In general, since $K < |Q(i\tilde{\omega}_n)|$ for any n then $\Delta(i\omega)$ does not encircle the origin if $\omega \in (\omega_m, \omega_{m+1})$ for $m \in \{0,1,\ldots,N-1\}$ or $\omega \in (\omega_N, \infty)$.

We now study the behavior of $\Delta(i\omega)$ as ω varies through the open-loop crossing frequencies ω_m. To such an end, we analyze the intervals $\omega \in [\tilde{\omega}_{n_m}, \tilde{\omega}_{n_m+1}]$. First consider m odd, for this case n_m is an odd number and as illustrated in Fig. 5.1e, $Q(i\omega)$ changes sign from positive to negative and $Ke^{-i\tau\omega}$ rotates in a clockwise direction through the upper half-plane. Since $K < |Q(i\tilde{\omega}_{n_m})|$ and $K < |Q(i\tilde{\omega}_{n_m+1})|$, this behavior starts in the positive real axis and traverses the upper half-plane describing a path accumulating its phase in π radians. Second, consider m even, for this case n_m is an even number and as illustrated in Fig. 5.1f, $Q(i\omega)$ changes sign from negative to positive and $Ke^{-i\tau\omega}$ rotates in a clockwise direction through the lower half-plane. Similarly, this behavior starts in the negative real axis and traverses the lower half-plane describing a path accumulating its phase in π radians. In general, we can state that:

$$\underset{\omega\in[\tilde{\omega}_{n_m},\tilde{\omega}_{n_m+1}]}{\theta\arg\Delta(i\omega)} = \pi,$$

and bearing in mind the above observations, then:

$$\underset{\omega\in[0,\infty)}{\theta \arg \Delta(i\omega)} = \sum_{m=1}^{N} \left[\underset{\omega\in[\tilde{\omega}_{n_m},\tilde{\omega}_{n_m+1}]}{\theta \arg \Delta(i\omega)} \right] = N\pi,$$

if $K < |Q(i\tilde{\omega}_n)|$ for all $n \in \mathbb{N} \cup \{0\}$, which implies asymptotic stability according to the Mikhailov Theorem.

The following section of this proof describes how conditions assumed on K can be simplified through a deeper analysis of the real valued function $Q(i\omega)$. Notice that $Q(i\omega)$ is a polynomial with N distinct real roots. Using Rolle's theorem it is easy to deduct that its derivative with respect to ω has only real roots, precisely $2N-1$. Also, each of these are distributed in such a way that there is only one between every pair of consecutive roots of $Q(i\omega)$. More precisely, in each interval (ω_m, ω_{m+1}), $(-\omega_{m+1}, -\omega_m)$ for $m \in \{1, 2, \ldots, N-1\}$ and $(-\omega_1, \omega_1)$, this last one is precisely $\omega = 0$.

First, given that the derivative of $Q(i\omega)$ does not have roots for $\omega \geq \omega_N$ and since $\tilde{\omega}_{n_N+1} > \omega_N$ then, its modulus $|Q(i\omega)|$ is a strictly increasing function for $\omega \geq \tilde{\omega}_{n_N+1}$. Therefore $|Q(i\tilde{\omega}_{n_N+1})| < |Q(i\tilde{\omega}_n)|$ for any $n > n_N + 1$. Second, consider the interval $[0, \omega_1]$, in this case $Q(i\omega)$ has a root in $\omega = \omega_1$ and its derivative has only one root in $\omega = 0$ in which achieves its maximum. Then, over this interval its modulus is a strictly decreasing function. Therefore, given that $\omega_{n_1} \in (0, \omega_1)$, $|Q(i\tilde{\omega}_{n_1})| < |Q(i\tilde{\omega}_n)|$ for any positive $n < n_1$.

Third, consider any interval $[\tilde{\omega}_{n_m+1}, \tilde{\omega}_{n_{m+1}}]$ which is a subset of (ω_m, ω_{m+1}). In other words, such an interval contains all closed-loop crossing frequencies between any two consecutive open-loop crossing frequencies. As mentioned before, the derivative of $Q(i\omega)$ has only one root in (ω_m, ω_{m+1}), and subsequently it has at least one in $[\tilde{\omega}_{n_m+1}, \tilde{\omega}_{n_{m+1}}]$. It can be easily deducted that its modulus achieves its minimum at some of its extreme points. Therefore, $|Q(i\tilde{\omega}_{n_m+1})| < |Q(i\tilde{\omega}_n)|$ or $\left|Q(i\tilde{\omega}_{n_{m+1}})\right| < |Q(i\tilde{\omega}_n)|$ for any integer $n \in (n_m + 1, n_{m+1})$.

Bearing in mind the above observations, we can simplify our stabilizing conditions on K as $K < |Q(i\tilde{\omega}_n)|$ for all $n \in n_1, n_2, \ldots, n_N$ and $n \in n_1 + 1, n_2 + 1, \ldots, n_N + 1$. Finally, such numbers can be computed straightforwardly using the floor and ceiling functions as described in (5.15) and as proposed in this proposition.

□

5.3.2 Equidistant Distribution

Consider the particular case of an equidistant distribution of the open-loop crossing roots. More precisely, such a case implies that $\omega_m = m\omega_b$ for some base frequency $\omega_b \in \mathbb{R}$. For such a scenario its characteristic polynomial $Q(s)$ can be explicitly described as:

$$Q(s) = \prod_{m=1}^{N} \left(s^2 + m^2\omega_b^2\right).$$

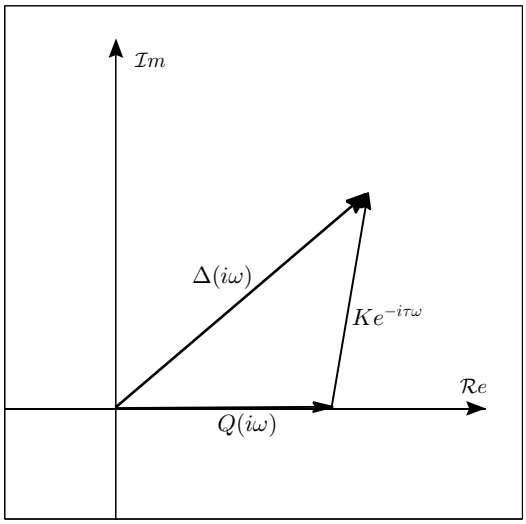

(a) Vector Interpretation of $\Delta(i\omega)$.

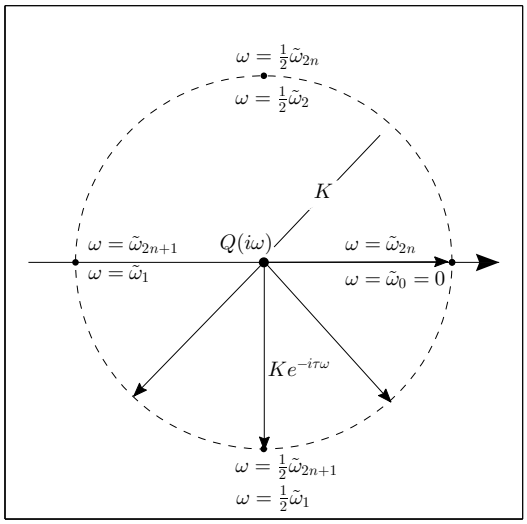

(b) Vector Interpretation of $Ke^{-\tau\omega}$.

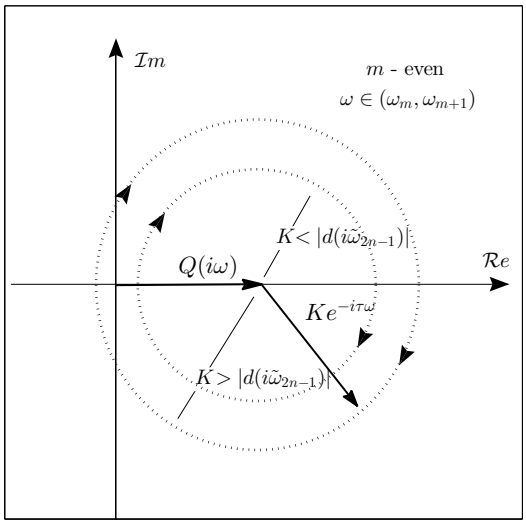

(c) $\omega \in (\omega_m, \omega_{m+1})$ for m even.

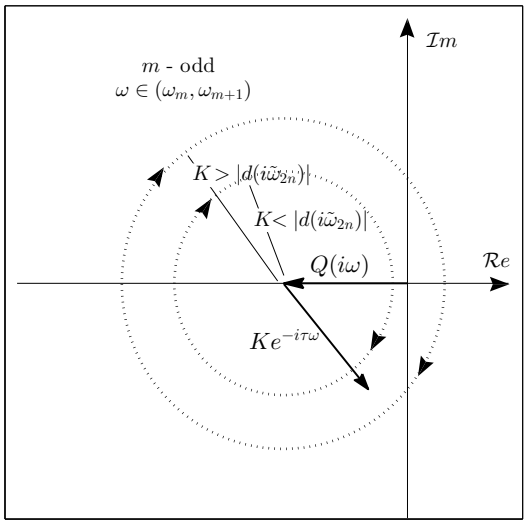

(d) $\omega \in (\omega_m, \omega_{m+1})$ for m odd.

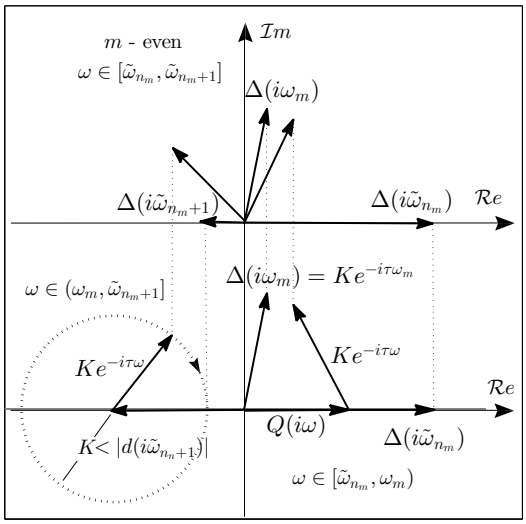

(e) $\omega \in [\tilde{\omega}_{n_m}, \tilde{\omega}_{n_m+1}]$ for m even.

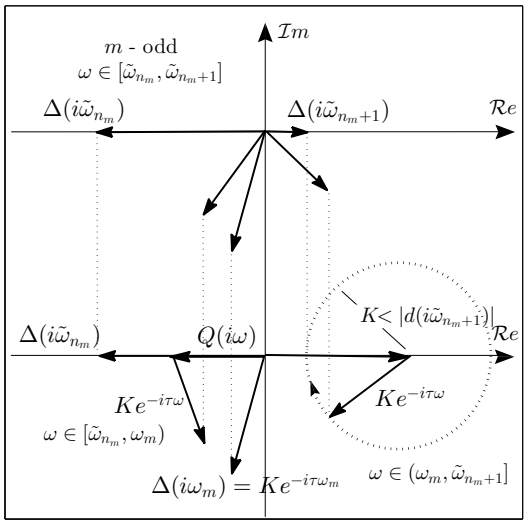

(f) $\omega \in [\tilde{\omega}_{n_m}, \tilde{\omega}_{n_m+1}]$ for m odd.

Figure 5.1: Accumulative Argument Analysis of the Complex Vector $\Delta(i\omega)$.

In the following proposition we state stabilizing conditions on the controller parameters.

Proposition 37. *Consider the open-loop system* (5.1) *with* N *distinct single roots on the imaginary axis such that* $\omega_m = m\omega_b$*, where* $\omega_b > 0$*. Also, the one delay block controller* (5.7)*. Let* τ *be a fixed delay value:*

$$\tau \in \left((2j-1)\frac{\pi}{\omega_b}, \frac{(2j-1)N+1}{N}\frac{\pi}{\omega_b} \right),$$

for some $j \in \mathbb{N}$*, and* K *be a positive real gain. Then, the closed-loop system is asymptotically stable iff:*

$$K < \left| d\left(in\frac{\pi}{\tau} \right) \right|, \text{ and } K < \left| d\left(i\,(n+1)\,\frac{\pi}{\tau} \right) \right|,$$

where $n = m(2j-1)$ *for all* $m \in \{1, 2, \ldots, N\}$

Proof. The proof of this result makes use of Proposition 36. First, in order to construct a solution τ for conditions (5.16) we propose the following distribution of the values $\omega_m{=}m\omega_b$:

$$m\pi < \tau m\omega_b < (m+1)\pi, \quad \forall m \in \{1, 2, \ldots, N\} \tag{5.17}$$

It is clear that a solution τ for these inequalities can be computed as:

$$\frac{\pi}{\omega_b} < \tau < \frac{m+1}{m}\frac{\pi}{\omega_b}, \quad \forall m \in \{1, 2, \ldots, N\}, \tag{5.18}$$

since $m \leq N$ it follows directly:

$$\frac{1}{m} \geq \frac{1}{N} \to 1 + \frac{1}{m} \geq 1 + \frac{1}{N} \to \frac{m+1}{m} \geq \frac{N+1}{N},$$

then, the intersection of all intervals solving (5.18) can be computed explicitly as:

$$\frac{\pi}{\omega_b} < \tau < \frac{N+1}{N}\frac{\pi}{\omega_b}.$$

Similarly, multiplying inequalities (5.17) by any odd number yields the following

$$(2j-1)m\pi < \tau m\omega_b < ((2j-1)m+1)\,\pi, \quad j \in \mathbb{N}, \tag{5.19}$$

which are also valid conditions for (5.16). Using the same steps as before we compute the stabilizing τ intervals:

$$\frac{\pi}{\omega_b}(2j-1) < \tau < \frac{(2j-1)N+1}{N}\frac{\pi}{\omega_b}. \tag{5.20}$$

The following step is to compute the proper stabilizing value of K defined through Proposition 36. To such end, first notice that if τ is chosen from (5.20), then inequality

(5.19) holds and can be rewritten as:

$$(2j-1)m < \frac{\tau m \omega_b}{\pi} < (2j-1)m + 1, \quad j \in \mathbb{N},$$

where $m \in \{1, 2, \ldots, N\}$. Bearing in mind this inequality it is evident that:

$$\begin{aligned} \left\lfloor \omega_m \frac{\tau}{\pi} \right\rfloor &= \left\lfloor \frac{m\omega_b \tau}{\pi} \right\rfloor = (2j-1)m, \\ \left\lceil \omega_m \frac{\tau}{\pi} \right\rceil &= \left\lceil \frac{m\omega_b \tau}{\pi} \right\rceil = (2j-1)m + 1, \end{aligned}$$

which in according Proposition 36 implies conditions stated in this proposition. □

5.4 Illustrative Example - Equidistant Distribution

In this section, we present an illustrative example concerning the result shown in Proposition 37 regarding an equidistant distribution of the open-loop crossing roots. For the sake of clarity, consider $\omega_b = \pi$ and $N = 3$, in other words, a sixth-order open-loop system with poles located exactly in $s = \pm i\pi, \pm i2\pi, \pm i3\pi$. Using this proposition, we construct the stability regions shown in Fig 5.2a, particularly for $j = 1, 2, 3, 4$. Let us take a look at the case $j = 2$ correspondent to the stability region shown in Fig. 5.2b. According to Proposition 37, its stabilizing interval of τ is directly computed as $\tau \in (3, \frac{3N+1}{N}) = (3, \frac{10}{3})$. Consider now a value of such an interval $\tau = 3.31 \in (3, 3.333)$, this is enough information for computing the stabilizing gain interval $K \in (0, 4460)$. In order to test this numerical result, one considers a parametrical variation concerning this information. We test this scenario using the MatLab package DDEBifTools which allows us to find a numerical solution of the roots of the characteristic quasipolynomial. The results are presented in Fig. 5.2c which illustrates the movement of the characteristic roots as the controller parameters are varied. In this figure, it is shown how starting in $K = 0$ the roots lie on the imaginary axis, and as K increases, they move to the LHP of the complex plane (implying stability) tending to cross again through the imaginary axis at the end of such a variation. In conclusion, such parameters choices shows that the characteristic roots remain in the LHP of the complex plane implying asymptotic stability of the closed-loop system.

5.5 Concluding Remarks

In this chapter one studies the classical problem of stabilizing a chain of oscillators using a single delay block. In other words, such an open-loop system has only poles that are purely imaginary. First, one studies deeply this problem by using crossing roots theory. Second, using some insights from this first stage, one complements the analysis using the Mikhailov criterion. This is an analysis based on the well-known argument principal. Explicit conditions for the delay and gain are derived. Finally, numerical results concerning the case in which the open-loop roots are evenly distributed are addressed.

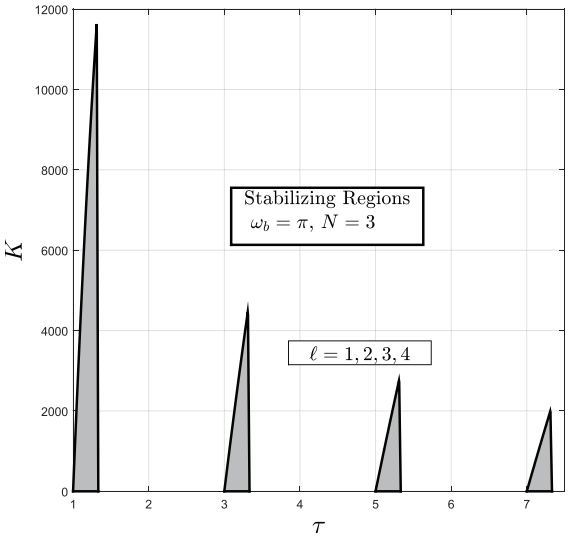

(a) Stability Regions

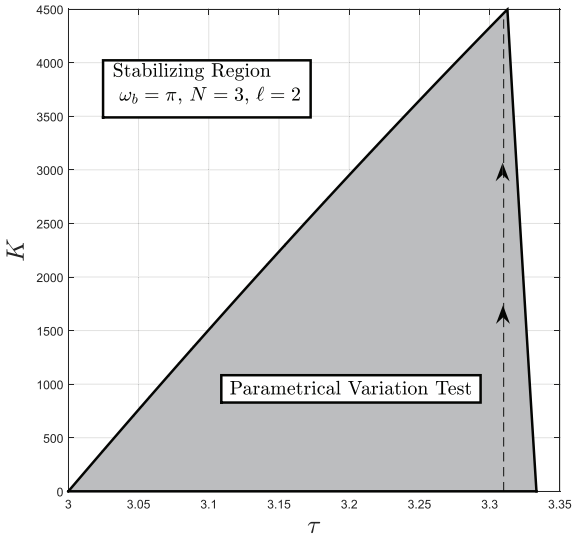

(b) Parametrical Variation

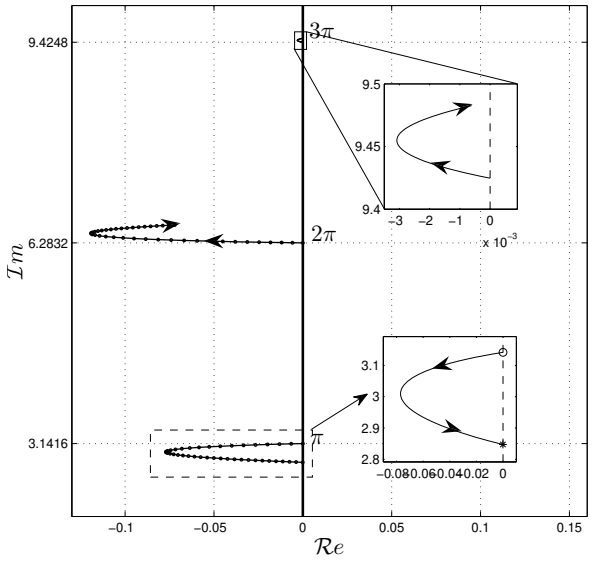

(c) Roots Behavior.

Figure 5.2: Illustrative Example.

Chapter 6

Concluding Remarks

This thesis considers the use of delay-based controllers to stabilize closed-loop control schemes applied to SISO-LTI systems. In this regard, we could say that every aspect of this thesis revolves towards one single task: the proper selection of the controllers' parameters of delay-based control schemes to achieve asymptotic stability.This fact is directly related to the location of the characteristic roots of the closed-system. As a consequence, this document is also a detailed study of some classes and particular examples of the so-called quasi-polynomial functions (linear DDE's characteristic functions). More precisely, we study the location of the roots of these functions with respect to its parameters (coefficients, delay). In the following we address some concluding remarks and future work ideas for each chapter.

In Chapter 2 we introduce two different methods to find stability conditions on the controller's parameters of three delay-based controllers: the $P\delta$, PD^{δ} and $P\delta I$ controllers. To such end, two methods based on crossing roots stability theory are used: stability index computation through direct crossing roots counting and the σ-instability analysis, first presented in this research. Some future work ideas are presented below:

- σ-stability analysis: to find the minimum number of curves needed to discriminate all possible unstable regions. And therefore, to achieve necessary and sufficient conditions.
- To develop a deeper understanding in the role of the delay in these delay-based controllers. For example, computing performance indicators in terms of the delay and gain related values, at least for first and second-order transfer functions.
- To include at least partially the modulus and phase information together with the founded stability regions for Bode-alike frequential analysis.
- Delay-based control design: to develop a user friendly toolbox containing all methods studied in this chapter to design control schemes based on the $P\delta$, PD^{δ} and $P\delta I$ controllers.

In Chapter 3 we present a variety of applications using delay-based control schemes designed by using similar approaches to the ones introduced in Chapter 2. Particularly,

the experimentation results of some bilateral teleoperation (and virtual) haptic systems. The design of a voltage regulation control scheme for a buck dc/dc converter using two delay-based controllers: $P\delta I$ and $P\delta$ controllers. Finally, the study of a classical control problem, the stabilization of the Furuta pendulum, done by a LQR strategy considering input-delay. Some future work ideas are presented below:

- Power electronics applications: to study the implications of having a delay nature in the control scheme on commutation frequency related phenomena. More precisely, how does it affect the voltage and current ripples.
- Furuta pendulum: to extend the control law from different gains and one single delay to using different delays for each variable in the state feedback.

In Chapter 4 we explore a real engineering application using a delay-based controller. More precisely, this chapter studies the design of a MPPT-PV system using a buck dc/dc converter and a $P\delta I$ controller (with an output/input linearization technique). A methodology for computing the controller's parameters stability regions and the zero dynamics analysis are addressed. Furthermore, and most importantly, experimental results with such delay-based setup are shown and discussed. Some future work ideas are presented below:

- MPPT system: To include an algorithm for the computation of the MPP (control reference) directly on the controller scheme's dynamics.
- Power electronics: To develop a methodology for computing stability regions implying not only stability, but also a bounded control effort (duty cycle $d(t) \in [0, 1]$)) given initial conditions. In other words, to considered the bounded input nature of these PWM controlled system.

Lastly, in Chapter 5 we aim to solve the classical delay-based control problem of stabilizing a chain of oscillators using one single delay-block. To such end, we make use of crossing roots stability theory with the Mikhailov criterion (stretchy based on the principle argument theorem) to find explicit conditions on the gain and delay values assuring closed-loop asymptotic stability. Also, a simple corollary for the case in which the oscillators's frequencies are multiples of a single base frequency value is presented with numerical examples. Some future work ideas are presented below:

- To study the necessity property for such stabilizing conditions.
- To consider negative gain values.

Finally, in our personal opinion, we would like to say that the strongest feature of this thesis is its diversity. Throughout this document one is introduced to the presentation and development of analytical statements, numeric methods, applications examples, real engineering problematics, control design methodologies and experimentation. In general, we allow us to believe that this thesis is successful in building a motivation for the serious study of delay-based control schemes.

Bibliography

[1] C. Abdallah, P. Dorato, J. Benitez-Read, and R. Byrne. Delayed positive feedback can stabilize oscillatory systems. In *Proc. American Contr. Conf.*, pages 3106–3107, 1993.

[2] J. Ackerman. *Robust control: systems with uncertain physical parameters*. Springer, 1993.

[3] W. Aggoune, D. Şendrescu, and S.-I. Niculescu. Some remarks on vehicle following control systems with delays. *IFAC Proceedings Volumes*, 40(23):103–110, 2007. ISSN 1474-6670. 7th IFAC Workshop on Time Delay Systems TDS 2007, Nantes, France, 17–19 September, 2007.

[4] W. Altmann and D. Macdonald. *Practical process control for engineers and technicians*. Elsevier/Newnes, 2005.

[5] H. Arioui, A. Kheddar, and S. Mammar. A predictive wave-based approach for time delayed virtual environments haptics systems. In *Proceedings. 11th IEEE international workshop on robot and human interactive communication*, pages 134–139, 2002. doi: 10.1109/ROMAN.2002.1045611.

[6] H. Arioui, S. Mammar, and T. Hamel. A smith-prediction based haptic feedback controller for time delayed virtual environments systems. In *Proceedings of the 2002 American Control Conference (IEEE Cat. No.CH37301)*, volume 5, pages 4303–4308 vol.5, 2002. doi: 10.1109/ACC.2002.1024609.

[7] K. J. Aström and T. Hägglund. *PID controllers: theory, design, and tuning*. Instrument Society of America, Research Triangle Park, NC, 2 edition, 1995.

[8] K. J. Aström and T. Hägglund. The future of pid control. *Chem. Eng. Progress*, 9 (11):1163–1175, 2001.

[9] E. I. Batzelis, G. E. Kampitsis, S. A. Papathanassiou, and S. N. Manias. Direct mpp calculation in terms of the single-diode pv model parameters. *IEEE Transactions on Power Electronics*, 30(1):226–2336, 2015.

[10] E. Bianconi, J. Calvente, R. Giral, E. Mamarelis, G. Petrone, C. A. Ramos-Paja, G. Spagnuolo, and M. Vitelli. A fast current-based mppt technique employing sliding mode control. *IEEE Transactions on Industrial Electronics*, 60(3):1168–1178, 2013.

[11] I. Boussaada, C.-I. Morărescu, and S.-I. Niculescu. Inverted pendulum stabilization: Characterization of codimension-three triple zero bifurcation via multiple delayed proportional gains. *System & Control Letters*, 82:1–9, 2015.

[12] C. G. Cullen. *Matrices and Linear Transformations: Second Edition*. Dover Books on Mathematics. Dover Publications, 2nd edition, 1990. ISBN 0486663280,9780486663289.

[13] K. Dahech, M. Allouche, T. Damak, and F. Tadeo. Backstepping sliding mode control for maximum power point tracking of a photovoltaic system. *Electric Power Systems Research*, 143:182–188, 2017.

[14] E. Dallago, A. Liberale, D. Miotti, and G. Venchi. Direct mppt algorithm for pv sources with only voltage measurements. *IEEE Transactions on Power Electronics*, 30(12):6742–6750, 2015.

[15] R. Datko. A Procedure for Determination of the Exponential Stability of Certain Differential-Difference Equations. *Quarterly of Applied Mathematics*, 1978.

[16] T. Erneux, J. Javaloyes, M. Wolfrum, and S. Yanchuk. Introduction to Focus Issue: Time-Delay Dynamics . *Chaos: An interdisciplinary Journal of Nonlinear Science*, 27(11), 2017.

[17] D. R. Espinoza-Trejo, E. Bárcenas-Bárcenas, D. U. Campos-Delgado, and C. De Angelo. Voltage-oriented input-output linearization controller as maximum power point tracking technique for photovoltaic systems. *IEEE Transactions on Industrial Electronics*, 2014.

[18] I. Fantoni and R. Lozano. Stabilization of the futura pendulum around its homoclinic orbit. *International Journal of Control*, 75(6):390–398, 2002.

[19] I. Fantoni and R. Lozano. *Non-linear control for underactuated mechanical systems*. Springer-Verlag, 2002.

[20] A. Fattouh and O. Sename. H_∞-based impedance control of teleoperation systems with time delay. *IFAC Proceedings Volumes*, 36(19):141 – 146, 2003. ISSN 1474-6670. doi: https://doi.org/10.1016/S1474-6670(17)33316-5. 4th IFAC Workshop on Time Delay Systems (TDS 2003), Rocquencourt, France, 8-10 September 2003.

[21] C. Foias, H. Özbay, and A. Tannenbaum. *Robust control of Infinite dimensional systems: frequency domain methods*. Springer-Verlag Berlin Heidelberg, 1996.

[22] D. González-Montoya, C. A. Ramos-Paja, and R. Giral. Improved design of sliding mode controllers based on the requirements of mppt techniques. *IEEE Transactions on Power Electronics*, 31(1):235–247, 2016.

[23] H. Gorecki, P. Fuksa, S. Grabowsky, and K. A. *Analysis and synthesis of time-delay systems*. New York: John Wiley & Sons, 1989.

[24] H. Guggenheimer. *Differential Geometry*. Dover, New York, NY, 1977.

[25] J. K. Hale and S. M. Verduyn Lunel. *Introduction to functional differential equations*, volume 99 of *Applied Math. Sciences*. Springer-Verlag, New York, 1993.

[26] K. Hashtrudi-Zaad and S. E. Salcudean. Transparency in time-delayed systems and the effect of local force feedback for transparent teleoperation. *IEEE Transactions on Robotics ans Automation*, 18(1):31–38, 2002.

[27] J. E. Hernández-Díez, E. J. González-Galván, C. F. Méndez-Barrios, S. I. Niculescu, A. Loredo-Flores, and R. I. Hernández-Molinar. A bilateral control scheme of a haptic-virtual system using proportional-delayed controllers. *AMRob Journal, Robotics: Theory and Applications*, 49(2):1–7, 2016.

[28] J.-E. Hernández-Díez, C.-F. Méndez-Barrios, S. Monday, and S.-I. Niculescu. Proportional-delayed controllers design for lti-systems: A geometric approach. *International Journal of Control*, 91(4):907–925, 2018.

[29] J.-E. Hernández-Díez, C.-F. Méndez-Barrios, and S.-I. Niculescu. Practical guidelines for tuning pd and pi delay-based controllers. In *15th IFAC Workshop on Time Delay Systems*, Sinaia, Romania, 2019. IFAC.

[30] V. M. Hernández-Guzmán, M. Antonio-Cruz, and R. Silva-Ortigoza. Linear state feedback regulation of a furuta pendulum: Design bases on differential flatness and root locus. *IEEE Access*, 4:8721–8736, 2016.

[31] J.-E. Hernández. *Proportional-Delayed Controllers for Teleoperated Systems*. Universidad Autónoma de San Luis Potosí, México, 2016.

[32] J.-E. Hernández-Díez, S.-I. Niculescu, C. Méndez-Barrios, E. J. González-Galván, and R. Hernández-Molinar. A transparent bilateral control scheme for a local teleoperation system using proportional-delayed controllers. In *2016 12th IEEE International Conference on Control and Automation*, pages 473–478, 2016. doi: 10.1109/ICCA.2016.7505322.

[33] J.-E. Hernández-Díez, C.-F.Méndez-Barrios, S.-I. Niculescu, E.-J. González-Galván, G. Mejía-Rodríguez, and V. Ramírez-Rivera. Closed-loop stability analysis of voltage mode buck using a proportional-delayed controller. In *2017 25th Mediterranean Conference on Control and Automation (MED)*, pages 490–495, 2017. doi: 10.1109/MED.2017.7984165.

[34] J.-E. Hernández-Díez, C.-F. Méndez-Barrios, S.-I. Niculescu, E.-J. González-Galván, and A. Loredo. Delay margin in controlling a furuta pendulum. In *XIX Congreso Mexicano de Robótica*, Mazatlán, Sinaloa, Mexico, 2017.

[35] J.-E. Hernández-Díez, C.-F. Méndez-Barrios, and S.-I. Niculescu. Some insights on the asymptotic stabilization of a class of siso marginally stable systems using one delay block. In *IFAC World Congress*, Berlin, Germany, 2020.

[36] J.-E. Hernández-Díez, C.-F. Méndez-Barrios, S.-I. Niculescu, and E. Bárcenas-Bárcenas. A current sensorless delay–based control scheme for mppt–boost converters in photovoltaic systems. *IEEE Access*, 8:174449–174462, 2020. doi: 10.1109/ACCESS.2020.3024566.

[37] R. Khanna, Q. Zhang, W. E. Stanchina, G. F. Reed, and Z.-H. Mao. Maximum power point tracking using model reference adaptive control. *IEEE Transactions on Power Electronics*, 29(3):1490–1499, 2014.

[38] V. Kharitonov, S.-I. Niculescu, J. Moreno, and W. Michiels. Static output feedback stabilization: Necessary conditions for multiple delay controllers. *IEEE Transactions On Automatic Control*, 50(1):82–86, 2005.

[39] A. Kihal, F. Krim, A. Laib, B. Talbi, and H. Afghoul. An improved mppt scheme employing adaptive integral derivative sliding mode control for photovoltaic systems under fast irradiation changes. *ISA Transactions*, 1(87):297–306, 2019.

[40] M. Killi and S. Samanta. Modified perturb and observe mppt algorithm for drift avoidance in photovoltaic systems. *IEEE Transactions on Industrial Electronics*, 62 (9):5549–5559, 2015.

[41] A. M. Krall. On the real parts of zeros of exponential polynomials. *Bulletin of the American Mathematical Society*, 70(2):291–292, 1964.

[42] M. Landry, S. A. Campbell, M. Morris, and A. C. O. Dynamics of an inverted pendulum with delayed feedback control. *SIAM Journal on Applied Dynamical Systems*, 4(2):333–351, 2005.

[43] B. Liacu, A. T. Koru, H. Ozbay, S.-I. Niculescu, and C. Andriot. Optimizing low-order controllers for haptic systems under delayed feedback. *Control Engineering Practice*, 21:655–668, 2013.

[44] S. Lyden and M. E. Haque. Maximum power tracking techniques for photovoltaic systems: A comprehensive review and comparative analysis. *Renewable & Sustainable Energy Reviews*, 52:1504–1518, 2015.

[45] M. Marden. *Geometry of polynomials*. American Mathematical Society, 1949.

[46] C.-F. Méndez-Barrios, S.-I. Niculescu, I.-C. Morărescu, and K. Gu. On the fragility of pi controllers for time-delay siso systems. In *16th Mediterranean Conference on Control and Automation*, pages 529–534, Ajaccio, France, 2008. IEEE.

[47] M. Metry, M. B. Shadmand, R. S. Balog, and H. Abu-Rub. Mppt of photovoltaic systems using sensorless current-based model predictive control. *IEEE Transactions on Industry Applications*, 2017.

[48] W. Michiels and S.-I. Niculescu. *Stability and stabilization of time-delay systems: an eigenvalue-based approach*. Advances in Design and Control, 2007.

[49] W. Michiels and S.-I. Niculescu. *Stability, control, and computation for time-delay systems. An eigenvalue-based approach.* SIAM, Philadelphia, 2014. ISBN 978-1-611973-62-4.

[50] C.-I. Morărescu and S.-I. Niculescu. Stability crossing curves of siso systems controlled by delayed output feedback. *Dynamics of Continuous, Discrete and Impulsive Systems*, 2007.

[51] J. Neimark. D-subdivisions and spaces of quasi-polynomials. *Prikl. Math. Mech.*, 10: 349–380, 1949.

[52] S.-I. Niculescu. *Delay effects on stability: a robust control approach.* Heidelberg: Springer, 2001.

[53] S.-I. Niculescu and W. Michiels. Stabilizing a chain of integrators using multiple delays. *IEEE Trans. Aut. Control*, 49(5):802–807, 2004.

[54] S.-I. Niculescu, W. Michiels, K. Gu, and C. Abdallah. Delay effects on output feedback control of dynamical systems. In F. Atay, editor, *Complex Time-Delay Systems*, pages 63–84. Berlin: Springer-Verlag, 2010.

[55] A. O'Dwyer. *Handbook of PI and PID controller tuning rules.* Imperial College Press (ICP), London, 3rd edition, 2009.

[56] A. Otto, W. Just, and G. Radons. Nonlinear dynamics of delay systems: An overview. *Philosophical Transactions Royal Society A*, 377, 2019.

[57] Y. Pan, C. Canudas-de-Wit, and O. Sename. A new predictive approach for bilateral teleoperation with applications to drive-by-wire systems. *IEEE Transactions on Robotics*, 22(6):1146–1162, 2006. doi: 10.1109/TRO.2006.886279.

[58] L. Pekar, P. R., and R. Matusu. Stability conditions for a retarded quasipolynomial and their applications. *International Journal of Mathematics and Computers in Simulation*, 2010.

[59] J. Petrić and Z. Situm. Pneumatic balancing mechanisms in control education. *International Journal of Engineering Education*, 9(4):309–314, 2006.

[60] R. Pradhan and B. Subudhi. Double integral sliding mode mppt control of a photovoltaic system. *IEEE Transactions on Control Systems Technology*, 24(1):285–292, 2016.

[61] A. Ramírez, S. Mondié, R. Garrido, and R. Sipahi. Design of proportional-integral-retarded (pir) controllers for second-order lti systems. *IEEE Transactions On Automatic Control*, 61(6):1688–1693, 2016.

[62] M. H. Rashid. *Power electronics: devides, circuits and applications.* Pearson, 2013.

[63] M. Rassol and Ali-Badamchizadeh. Adaptative passivity-based control of a photovoltaic system. *IEEE Journal of Photovoltaics*, 6(2):532–539l, 2016.

[64] E. Romero-Cadaval, B. Francois, M. Malinowsky, and Q. C. Zhong. Grid-connected photovoltaic plants: An alternative energy source, replacing conventional sources. *IEEE Industrial Electronics Magazine*, 9(1):18–32, 2009.

[65] S. S. Sastry. *Nonlinear Systems: Analysis, Stability and Control*. Springer, 1999.

[66] K. Schmidt. *Delay and functional differential equations and their applications*. Academic Press, 1972.

[67] J. M. Shen, H. L. Jou, and J. C. Wu. Transformers-less three-port grid-connected power converter for distribution power generation system with dual renewavle energy sources. *IET Power Electronics*, 5(3):501–509, 2011.

[68] R. Sipahi, S.-I. Niculescu, C. T. Abdallah, W. Michiels, and K. Gu. Stability and stabilization of systems with time delay. *IEEE Control Systems Magazine*, 31(1): 38–65, 2011.

[69] M. W. Spong and M. Vidyasagar. *Robot dynamics and control*. John Wiley & Sons, Inc, 1989.

[70] M. Tavakoli, R. V. Patel, M. Moallem, and A. Aziminejad. *Haptics for teleoperated surgical robotic systems*. World Scientific Publishing Company, 2003.

[71] A. Urtasun, P. Sanchis, and L. Marroyo. Adaptive voltage control of the dc/dc boost stage in pv converter with small input capacitor. *IEEE Transactions on Power Electronics*, 28(11):5038–5048, 2015.

[72] P. Vázquez, A. Alviso, V.-M. Tovar, and D.-R. Espinoza-Trejo. High-performance controller for a boost dc/dc converter in photovoltaic mppt systems by using a pic32mz microcontroller. *Currently Submitted to Energies*, 2018.

[73] T. Vyhlidal and P. Zitek. Mapping based algorithm for large-scale computation of quasi-polynomial zeros. *IEEE Transactions on Automatic Control*, 54(1):171–177, 2009. doi: 10.1109/TAC.2008.2008345.

[74] T. Vyhlídal and P. Zítek. Qpmr - quasi-polynomial root-finder: algorithm update and examples. 2014.

université PARIS-SACLAY

ÉCOLE DOCTORALE
Sciences et technologies de l'information et de la communication (STIC)

Titre: Conception de Contrôleurs à retards pour Systèmes Dynamiques

Mots clés: Systèmes à Retards, Systèmes Linéaires, Contrôle à Retards

Résumé: Dans ce mémoire, on considère l'analyse de plusieurs classes de contrôleurs à complexité réduite en dimension infinie. Ces contrôleurs généralisent les contrôleurs PID "classiques" en incluant des retards dans leur représentation mathématique. Les apports principaux de la thèse concernent la caractérisation du comportement des systèmes en boucle fermée par rapport aux paramètres du contrôleur (gains et retards) dans plusieurs configurations. De plus, les résultats obtenus permettent d'avoir une meilleure compréhension des effets induits par la présence des retards sur la stabilité (asymptotique) des dynamiques. Ces résultats sont appliqués à plusieurs cas d'étude couvrant un spectre thématique large: mécanique et robotique, électronique de puissance et systèmes photovoltaïques.

Title: Delay-Based Controllers Design for Dynamical Systems

Keywords: Delayed Systems, Linear Systems, Delay-Based Control

Abstract: In this thesis, we consider the analysis of several classes of infinite-dimensional controllers with reduced complexity. These controllers generalize the "classic" PID controllers by including delays in their mathematical representation. The main contributions of the thesis concern the characterization of the behavior of the closed-loop systems with respect to the controller's parameters (gains and delays) in several configurations. In addition, the derived results allow a better understanding of the effects induced by the delays on the dynamics (asymptotic) stability. The results are applied at several case studies covering a broad thematic spectrum: mechanics and robotics, power electronic and photovoltaic systems.